ANALYSIS OF BENDING STIFFNESS VARIATION AT CRACKS IN CONTINUOUS PAVEMENTS

by

Adnan Abou-Ayyash
W. Ronald Hudson

Research Report Number 56-22

Development of Methods for Computer Simulation of Beam-Columns and Grid-Beam and Slab Systems

Research Project 3-5-63-56

conducted for

The Texas Highway Department

in cooperation with the
U. S. Department of Transportation
Federal Highway Administration

by the

CENTER FOR HIGHWAY RESEARCH
THE UNIVERSITY OF TEXAS AT AUSTIN

April 1972

The opinions, findings, and conclusions expressed in this publication are those of the authors and not necessarily those of the Federal Highway Administration.

PREFACE

This report describes an analytical evaluation of the effect of transverse cracks on the longitudinal bending rigidity of continuously reinforced concrete pavements. It also presents a sensitivity study of the variables affecting the design of such pavements by the use of the discrete-element method of slab analysis.

This is the twenty-second in a series of reports that describes the work done in Research Project 3-5-63-56, entitled "Development of Methods for Computer Simulation of Beam-Columns and Grid-Beam and Slab Systems." The project is divided into two parts, one concerned primarily with bridge structures and the other with pavement slabs. This is the seventh report in the series that deals directly with pavement slabs. The crack analysis is also useful in structures.

Our thanks are extended to Professor Hudson Matlock, Dr. B. F. McCullough, and Messrs. John J. Panak and Harvey J. Treybig for their suggestions and help at various stages of the work.

We are grateful to the entire staff of the Center for Highway Research, who provided support during the preparation of this report. Particular thanks are due to Mrs. Rose Mary Sturges, Mrs. Jean Merritt, and Miss Darlene Neva for typing the drafts of the manuscript, and Mr. Art Frakes for his great efforts in editing and coordinating the report preparation.

This project is sponsored by the Texas Highway Department in cooperation with the U. S. Department of Transportation Federal Highway Administration.

Adnan Abou-Ayyash

W. Ronald Hudson

August 1971

LIST OF REPORTS

Report No. 56-1, "A Finite-Element Method of Solution for Linearly Elastic Beam-Columns" by Hudson Matlock and T. Allan Haliburton, presents a solution for beam-columns that is a basic tool in subsequent reports. September 1966.

Report No. 56-2, "A Computer Program to Analyze Bending of Bent Caps" by Hudson Matlock and Wayne B. Ingram, describes the application of the beam-column solution to the particular problem of bridge bent caps. October 1966.

Report No. 56-3, "A Finite-Element Method of Solution for Structural Frames" by Hudson Matlock and Berry Ray Grubbs, describes a solution for frames with no sway. May 1967.

Report No. 56-4, "A Computer Program to Analyze Beam-Columns under Movable Loads" by Hudson Matlcok and Thomas P. Taylor, describes the application of the beam-column solution to problems with any configuration of movable non-dynamic loads. June 1968.

Report No. 56-5, "A Finite-Element Method for Bending Analysis of Layered Structural Systems" by Wayne B. Ingram and Hudson Matlock, describes an alternating-direction iteration method for solving two-dimensional systems of layered grids-over-beams and plates-over-beams. June 1967.

Report No. 56-6, "Discontinuous Orthotropic Plates and Pavement Slabs" by W. Ronald Hudson and Hudson Matlock, describes an alternating-direction iteration method for solving complex two-dimensional plate and slab problems with emphasis on pavement slabs. May 1966.

Report No. 56-7, "A Finite-Element Analysis of Structural Frames" by T. Allan Haliburton and Hudson Matlock, describes a method of analysis for rectangular plane frames with three degrees of freedom at each joint. July 1967.

Report No. 56-8, "A Finite-Element Method for Transverse Vibrations of Beams and Plates" by Harold Salani and Hudson Matlock, describes an implicit procedure for determining the transient and steady-state vibrations of beams and plates, including pavement slabs. June 1968.

Report No. 56-9, "A Direct Computer Solution for Plates and Pavement Slabs" by C. Fred Stelzer, Jr., and W. Ronald Hudson, describes a direct method for solving complex two-dimensional plate and slab problems. October 1967.

Report No. 56-10, "A Finite-Element Method of Analysis for Composite Beams" by Thomas P. Taylor and Hudson Matlock, describes a method of analysis for composite beams with any degree of horizontal shear interaction. January 1968.

Report No. 56-11, "A Discrete-Element Solution of Plates and Pavement Slabs Using a Variable-Increment-Length Model" by Charles M. Pearre, III, and W. Ronald Hudson, presents a method for solving freely discontinuous plates and pavement slabs subjected to a variety of loads. April 1969.

Report No. 56-12, "A Discrete-Element Method of Analysis for Combined Bending and Shear Deformations of a Beam" by David F. Tankersley and William P. Dawkins, presents a method of analysis for the combined effects of bending and shear deformations. December 1969.

Report No. 56-13, "A Discrete-Element Method of Multiple-Loading Analysis for Two-Way Bridge Floor Slabs" by John J. Panak and Hudson Matlock, includes a procedure for analysis of two-way bridge floor slabs continuous over many supports. January 1970.

Report No. 56-14, "A Direct Computer Solution for Plane Frames" by William P. Dawkins and John R. Ruser, Jr., presents a direct method of solution for the computer analysis of plane frame structures. May 1969.

Report No. 56-15, "Experimental Verification of Discrete-Element Solutions for Plates and Slabs" by Sohan L. Agarwal and W. Ronald Hudson, presents a comparison of discrete-element solutions with small-dimension test results for plates and slabs, including some cyclic data. April 1970.

Report No. 56-16, "Experimental Evaluation of Subgrade Modulus and Its Application in Model Slab Studies" by Qaiser S. Siddiqi and W. Ronald Hudson, describes a series of laboratory experiments to evaluate layered foundation coefficients of subgrade reaction for use in the discrete-element method. January 1970.

Report No. 56-17, "Dynamic Analysis of Discrete-Element Plates on Nonlinear Foundations" by Allen E. Kelly and Hudson Matlock, presents a numerical method for the dynamic analysis of plates on nonlinear foundations. July 1970.

Report No. 56-18, "A Discrete-Element Analysis for Anisotropic Skew Plates and Grids" by Mahendrakumar R. Vora and Hudson Matlock, describes a tridirectional model and a computer program for the analysis of anisotropic skew plates or slabs with grid-beams. August 1970.

Report No. 56-19, "An Algebraic Equation Solution Process Formulated in Anticipation of Banded Linear Equations" by Frank L. Endres and Hudson Matlock, describes a system of equation-solving routines that may be applied to a wide variety of problems by using them within appropriate programs. January 1971.

Report No. 56-20, "Finite-Element Method of Analysis for Plane Curved Girders" by William P. Dawkins, presents a method of analysis that may be applied to plane-curved highway bridge girders and other structural members composed of straight and curved sections. June 1971.

Report No. 56-21, "Linearly Elastic Analysis of Plane Frames Subjected to Complex Loading Conditions" by Clifford O. Hays and Hudson Matlock, presents a design-oriented computer solution for plane frames structures and trusses that can analyze with a large number of loading conditions. June 1971.

Report No. 56-22, "Analysis of Bending Stiffness Variation at Cracks in Continuous Pavements," by Adnan Abou-Ayyash and W. Ronald Hudson, describes an evaluation of the effect of transverse cracks on the longitudinal bending rigidity of continuously reinforced concrete pavements. April 1972 (P).

(P) indicates Preliminary Report.

ABSTRACT

Discontinuities exert significant influence on the bending rigidity of structural members. This study reports an analytical look at the effect of transverse cracks on the behavior of continuously reinforced concrete pavements. Results show that the percent reduction in bending stiffness at crack locations ranges between 80 and 90 percent of the original uncracked value.

By simulating this effect on the discrete-element model, a sensitivity study was performed on the parameters considered in the design of continuously reinforced concrete pavements. These covered the practical range of each of the following variables: slab bending stiffness, modulus of subgrade reaction, and crack spacing.

From the analysis of variance, the most significant variables, which explained around 90 percent of the variation in deflection and principal moment (stress) responses, were slab bending stiffness and modulus of subgrade reaction. While the latter variable showed a higher contribution to deflections than to principal moments, slab bending stiffness possessed a contracting effect. Crack spacing showed a minor effect on slab behavior.

The orthogonal polynomial breakdown indicated that in a logarithmic model, the linear effect of both subgrade modulus and slab bending stiffness is highly significant. Furthermore, interactions between these two design variables do occur, indicating that variations in deflections and principal moments are not defined by the main effect of design variables alone.

The influence of the width of the crack on the behavior and performance of continuously reinforced concrete pavements is highly significant. Slab deflections increase drastically as crack width increases, while no significant change in principal moments is encountered.

KEY WORDS: discrete-element analysis, cracks, pavement slab, continuously reinforced concrete pavements, sensitivity analysis, deflection, principal moment, boundary, restraints, program SLAB.

SUMMARY

The problem of transverse cracking in continuously reinforced concrete pavements and its influence on the bending rigidity of the slab in the longitudinal direction was studied using basic moment-curvature relationships. Results showed that a significant drop is encountered in the bending rigidity (80 to 90 percent of the original full value) at the crack locations. A procedure to simulate this effect using the discrete-element method is outlined. Besides the crack effect, other slab characteristics were investigated for use in modeling the real problem. These included slab partitioning with the corresponding boundary restraints, tension in the longitudinal reinforcement, and Poisson's ratio effect.

A sensitivity study was performed on the design variables used in the design of such pavements, namely slab bending stiffness, subgrade modulus, and crack spacing. Principal moment and deflection responses for the factorial combination of the design variables were obtained by the discrete-element slab method.

For the range of variables studied in this experiment, the analysis of variance indicated that the main effects of slab bending stiffness and subgrade modulus, as well as their interactions, explained most of the variations in the deflections and principal moments. Crack spacing showed minor influence on slab behavior.

The comparison between the 90 and 100 percent reduction in bending stiffness at crack locations indicated the importance of crack width on the behavior of continuously reinforced concrete pavements. Slab deflections increase at a high rate as crack width increases, while no significant drop is experienced in the principal moments.

IMPLEMENTATION STATEMENT

The influence of transverse cracking on the behavior of continuously reinforced concrete pavements (CRCP) has been studied by use of the discrete-element analysis method (SLAB). In the past it has been extremely difficult to evaluate the effect of these transverse cracks on the load carrying capacity of the pavement. The results of this investigation provided additional information on the effect of these discontinuities on the structural behavior of such pavements.

The sensitivity analysis performed on the factorial combination of slab bending stiffness, subgrade modulus, and crack spacing yielded information which is quite useful for evaluating the importance of CRC pavement parameters, and should ultimately lead to improved design methods. The results of the study can be made even more useful by correlating them with work from Research Project 1-8-69-123, entitled "A System Analysis of Pavement Design and Research Implementation." Regression equations can be developed to predict the maximum deflections and principal moments or stresses. These equations may be a part of a pavement system analysis model that requires stress or deflection values for certain design parameters.

TABLE OF CONTENTS

NOMENCLATURE

Symbol	Typical Units	Definition
A_s	in^2	Area of steel
b	ft	Width of slab
C	$lb\text{-}in^2/in/rad$	Plate twisting stiffness
CS	ft	Crack spacing
d	in	Distance from top of compression fiber to the centroid of the steel
D^x , D^y	$(lb\text{-}in^2)/in$	Plate bending stiffness
$\bar{e}_s$	in/in	Average strain in steel
E	lb/in^2	Modulus of elasticity of concrete
ϵ	per ^oF	Thermal coefficient of steel and concrete
E_s	lb/in^2	Modulus of elasticity of steel
$\bar{f}_s$	lb/in^2	Average stress in steel
f'_c	lb/in^2	Compressive stress of concrete
f_r	lb/in^2	Flexural stress of concrete
$\bar{f}_t$	lb/in^2	Average tensile stress of concrete
f'_s	lb/in^2	Stress in reinforcement corresponding to M'
f_s	lb/in^2	Steel stress at the crack

Symbol	Typical Units	Definition
f_y	lb/in^2	Yield stress of the steel
F	----	Friction factor
h_x , h_y	----	Discrete-element widths
i	----	Numbering associated with x-direction
$\bar{I}$	in^4	Average moment of inertia
j	----	Numbering associated with y-direction
k	$lb/in^2/in$	Modulus of subgrade reaction
k_1 , k_2 , k_3	----	Reduction factors
K	----	Fraction when multiplied by d gives the distance to the neutral axis of the transformed cracked section (Eq 3.4)
L	in	Length affected by the discontinuity
M_w	lb-in	Working moment
M'	lb-in	Portion of the resisting moment corresponding to the average tensile stress of concrete
n	----	Ratio of modulus of elasticity of steel to that of concrete
P	----	Percentage of longitudinal reinforcement
p	in	Perimeter of bar(s)
q	lb/in^2	Distributed lateral load
$\bar{\rho}$	----	Average radius of curvature
R_x , R_y	(lb-in)/radian	Rotational restraint in the x and y directions
S_t	lb/in^2	Allowable tensile strength of concrete

Symbol	Typical Units	Definition
S_z	lb/in	Spring value in z direction
t	in	Plate or slab thickness
T_c	lb	Tension in concrete
T_s	lb	Tension in steel
$\bar{\theta}$	radians/in	Average curvature
μ	----	Poisson's ratio
u	lb/in^2	Nominal bond stress
U	lb/in	Bond force per unit length
w	inch	Deflection
ΔT	^oF	Temperature range
ϕ	in	Bar diameter
x	----	Coordinate in the short slab direction
y	----	Coordinate in the long slab direction

CHAPTER 1. INTRODUCTION

A general discrete-element method for solution of discontinuous plates and slabs has been developed by Hudson and Matlock (Ref 1) and Stelzer and Hudson (Ref 4). The method is based on a physical model representation of the plate or slab by bars, springs, and torsion bars which are grouped in a system of orthogonal beams. The initial development utilized an alternating-direction iterative technique to solve for the deflections of the plate or slab, and a subsequent development utilized a direct matrix manipulation technique. The direct solution method has been shown to be more efficient computationally. Subsequent modification of the method for more precise modeling of orthotropic plates was done by Panak (Ref 7).

The discrete-element method has been thoroughly checked by comparing its solutions with closed-form solutions of certain problems. Verification of the discrete-element model as a satisfactory tool for two-dimensional problems such as elastic plates under transverse loads was obtained by Agarwal and Hudson (Ref 11) through an experimental study of plates and slabs. Comparison of the experimental results with the analytical solution (Ref 11) showed that the discrete-element techniques provide extremely good results in predicting plate and slab stresses and deflections and can be a useful tool in the analysis of bridge slabs and pavements. Computer programs developed for the above discrete-element method are designated by the acronym SLAB.

Extensive use of SLAB programs has been made in solution of two-way floor slabs continuous over many supports (Ref 7) and subjected to different concentrated load patterns and in the analysis of rigid pavements (Refs 22 and 15). This report describes the application of SLAB methods in a study of continuously reinforced concrete pavements (CRCP). The design variables usually considered in this pavement type are concrete flexural strength, elastic modulus, slab thickness, percentage reinforcement, modulus of subgrade reaction, Poisson's ratio, environmental conditions, expected traffic loading, and crack spacing. In addition, in CRCP there are very fine cracks, which develop due to volume-change stresses. In previous analyses of such pavements, it has been

extremely difficult to evaluate the effect of these cracks on the load carrying capacity and consequent performance of the slab.

Objectives

The objectives of this research are

(1) to analyze the effect of cracks on bending stiffness of concrete pavement slabs and

(2) to investigate the importance of various rigid pavement variables on design, as shown by predicted changes in deflections and principal moments.

Scope

This report describes the use of discrete-element SLAB methods to study the behavior of continuously reinforced concrete pavement, including modeling cracks and joints. The effect of cracks on slab bending stiffness was investigated in this study using basic moment-curvature relationships, which consequently made discrete-element modeling of the crack feasible. Other slab characteristics were involved in modeling the real problem, including slab partitioning and the corresponding boundary restraints to represent continuity, tension in the longitudinal steel, position of the loads, and Poisson's ratio.

For the second objective, the following design variables were considered:

(1) pavement thickness,
(2) modulus of elasticity of concrete,
(3) modulus of subgrade reaction,
(4) loading position,
(5) crack spacing, and
(6) Poisson's ratio.

The relative importance of each of these variables was based on changes in principal moments and deflections due to external wheel loads only. This study does not include temperature and warping stresses or their effects on slab performance.

Report

This report describes the analysis carried out to accomplish the study objectives. Chapter 2 discusses the influence of cracks on bending rigidity

and the use of moment curvature relationships as an approach to the problem. It also presents the factorial design experiment of CRCP design variables for the sensitivity analysis.

Chapter 3 presents the analysis and modeling of real effects encountered in the cracked slab problem and their influence on changes in deflections and stresses.

Chapter 4 is a brief presentation of SLAB results and a discussion on the analysis of variance performed on the maximum deflections and principal moments. Furthermore, different stiffness reductions at crack locations were studied to investigate its influence on slab behavior.

Chapter 5 presents conclusions and some recommendations suggested for further study.

CHAPTER 2. THE PROBLEM AND APPROACH

Continuously reinforced concrete pavement (CRCP) may be defined as a concrete pavement in which the longitudinal reinforcing steel acts continuously for its length and no transverse joints other than occasional construction joints, which do not interrupt the continuity, are installed. In actual practice, the continuity is sometimes interrupted by expansion joints at structures. Except for these, there is technically no limit to the possible length of CRCP.

Transverse contraction joints were long considered essential to preventing pavement damage from volume-change stresses. CRCP takes care of these stresses in another way. It allows the pavement to develop a random pattern of very fine transverse cracks (Fig 1). The design concept for this pavement type is to provide sufficient reinforcement to keep the cracks tightly closed and to provide adequate pavement thickness to carry the wheel loads across these tightly closed cracks (Ref 2).

Because of volume-change stresses, crack formation in the continuously reinforced pavement slab is inevitable until expansive cements are better perfected. Therefore, a thorough understanding of the behavior of a pavement structure with such discontinuities is needed. The real pavement system including the cracks must be analyzed. This can be approximated with reasonable confidence using the SLAB programs.

Figure 2(a) shows a cracked portion of CRCP and Fig 2(b) shows a schematic variation in the moment of inertia in the cracked region. The exact shape of this curve is not clearly known due to the complexity of the problem. To apply the discrete-element method to the discretized continuously reinforced concrete pavement, a method was developed using basic moment-curvature relationships in which an average moment of inertia to simulate the effect of cracks on slab bending stiffness was determined. Furthermore, the development length bond idea (Ref 35) was used to specify the slab portion over which the average inertia could realistically be applied.

Besides the discontinuity analysis, the use of other slab input variables to model real effects was investigated, including the following:

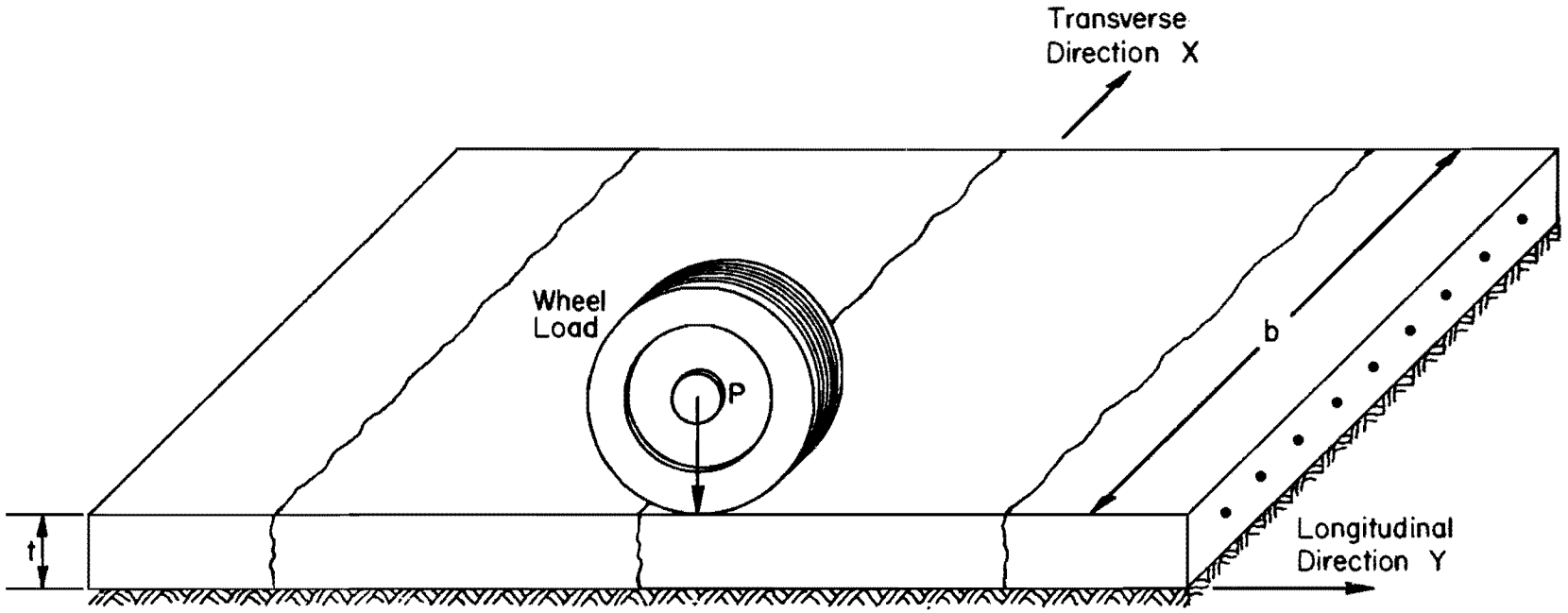

Fig 1. Continuously reinforced concrete pavement (CRCP).

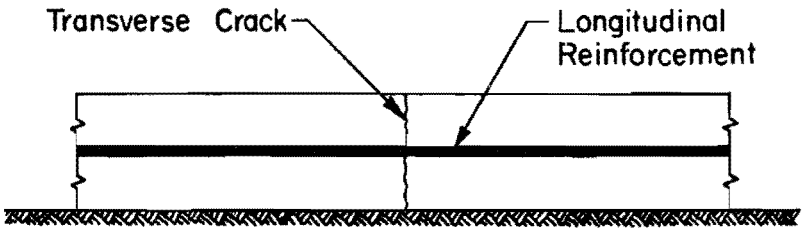

(a) Cracked portion of CRCP.

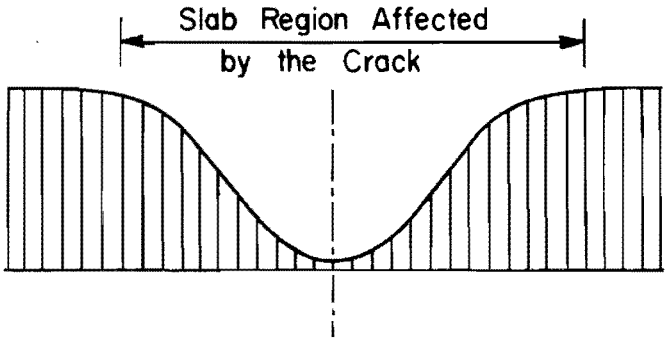

(b) Schematic variation in moment of inertia in the region of the crack.

Fig 2. Effect of a discontinuity on the bending rigidity of the slab.

(1) partitioning of the slab and use of the effect of boundary restraints to represent continuity,

(2) determination of the value of the tension in the longitudinal reinforcement and its effect on deflections and principal stresses, and

(3) determination of the value of Poisson's ratio which should be used and its sensitivity.

After the SLAB method was evaluated for its applicability to the CRCP, the second objective was approached; this was a sensitivity evaluation of the rigid pavement structural design analysis utilizing the discrete-element method.

In brief, a sensitivity analysis is a procedure to determine the change in a dependent variable due to a unit change in an independent variable. It can be used to evaluate the effect of a certain number of variables in the system and the interactions between them. In this research, the rigid pavement design variables were evaluated by means of a sensitivity analysis which determined the changes in the magnitude of deflections and principal moments or stresses due to changes in the variables. The analysis involved the levels of the variables shown in Table 1.

For this research, a full factorial of the variables listed in Table 1 was evaluated. Both deflections and principal moments were computed for variations in each variable in each block of the factorial (Table 2). Each block of the factorial involved a fixed level of three variables. Two solutions were made for each block: (1) for the loads on a crack and (2) for loads between cracks for a total of 72 different problems. Figure 3 shows the loading and crack spacing pattern for the 4 and 10-foot cases only. This work was performed for a 24 by 40-foot slab size and for two 9,000-pound wheel loads, located at 2 and 8 feet from the slab edge, respectively, which simulates an 18-kip axle load.

To cut down on the number of slab problems to be solved, the modulus of elasticity of concrete E, and the slab thickness t, were lumped together into the bending stiffness factor, namely $\frac{Et^3}{12(1 - \mu^2)}$. From the combination of the low, medium, and high levels of each of E and t, the values shown in Table 1 resulted.

The specific approach to the analysis of the cracked reinforced pavement and the sensitivity analysis by the discrete-element method are covered in the following chapters on analysis and results, Chapters 3 and 4.

TABLE 1. VARIABLES AND LEVELS IN THE DESIGN EXPERIMENT

Variable	Level		
	Low	Medium	High
Slab bending stiffness per unit length D, $(lb\text{-}in^2)/in.$	20×10^6	150×10^6	1125×10^6
Crack spacing CS, ft	4	6 and 8	10
Modulus of subgrade reaction k, $lb/in^2/in.$	40	200	1000

TABLE 2. FACTORIAL VARIABLES

Modulus of subgrade reaction, lb/in²/in.	Crack Spacing, ft	Slab bending stiffness, (lb-in²)/in. 20 x 10^6	150 x 10^6	1125 x 10^6
40	4	1	13	25
	6	2	14	26
	8	3	15	27
	10	4	16	28
200	4	5	17	29
	6	6	18	30
	8	7	19	31
	10	8	20	32
1000	4	9	21	33
	6	10	22	34
	8	11	23	35
	10	12	24	36

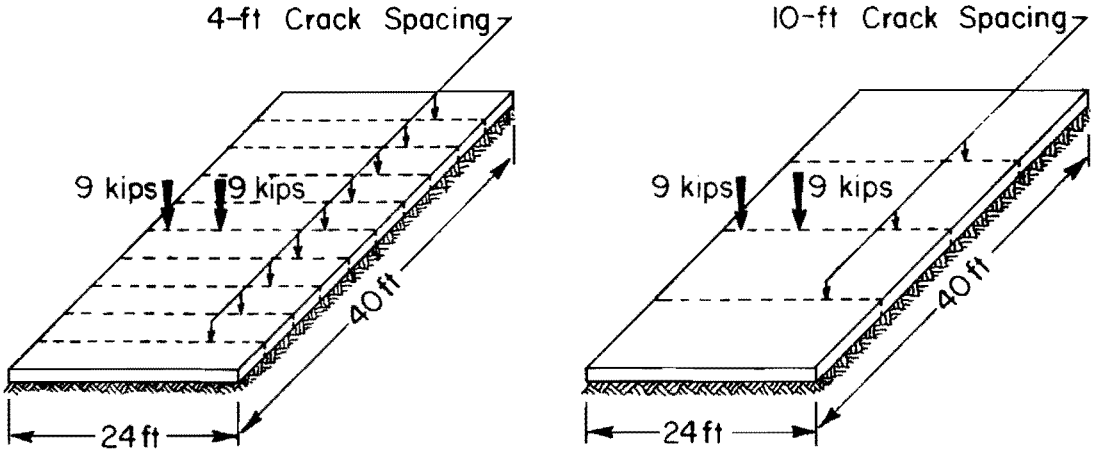

(a) Loads on the crack.

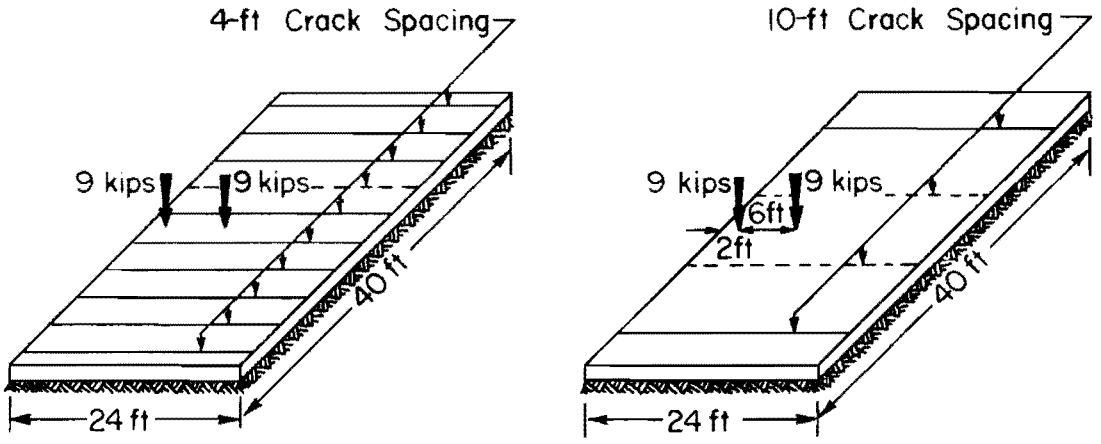

(b) Loads between cracks.

Fig 3. Pavement loading and crack spacing pattern.

CHAPTER 3. ANALYSIS AND MODELING

In this chapter, the analysis and modeling of real effects encountered in the cracked slab problem are described together with their influence on changes in deflections and stresses. These effects include slab discontinuities, boundary slab restraints, tension in the longitudinal steel, Poisson's ratio, and loading position.

Theoretical Background

Analytical solutions for two-dimensional plate problems have been discussed by Timoshenko and others (Ref 21), all of whom characterize three kinds of plate bending: (1) thin plates with small deflections, (2) thin plates with large deflections, and (3) thick plates.

For thin plates with small deflections (i.e., in which the deflection is small in comparison with thickness), a satisfactory approximate theory of bending of a plate by lateral loads can be developed by making the following assumptions:

(1) There is no deformation in the plate's middle plane.

(2) Points of the plate which initially lie normal to the middle surface of the plate remain normal to the middle surface of the plate after bending.

(3) Normal stresses in the direction transverse to the plate can be disregarded.

With these assumptions, the deflected surface of an isotropic plate is described by the biharmonic equation

$$D\left(\frac{\partial^4 w}{\partial x^4} + 2\,\frac{\partial^4 w}{\partial x^2 \partial y^2} + \frac{\partial^4 w}{\partial y^4}\right) = q \qquad (3.1)$$

where

D = the bending stiffness of the plate,

w = the deflection (with positive upward),

q = the lateral load.

A complete discussion of this equation is given in Chapter 2 of Ref 21.

For a given set of boundary conditions, solution of this differential equation gives all the information necessary for calculating stresses at any point in the plate. Closed-form solutions of this equation are available for a number of special cases, including homogeneous, isotropic plates, which generally have infinite dimensions in the x and y-directions or are round with finite radii. The loading conditions in most closed-form solutions are either uniform over the entire plate or concentrated in the center of the plate. As the problem becomes involved, with various combinations of load, support, and stiffness conditions, closed-form solutions are generally not available and a numerical method must be used to solve the problem. Such a method is the discrete-element method.

Figure 4 is a pictorial representation of the discrete-element model of the slab as suggested by Hudson and Stelzer (Ref 4). The slab or the rigid pavement structure is replaced by an analogous mechanical model representing all stiffness and support properties of the actual slab. The joints of the model are connected by rigid bars which are in turn interconnected by torsion bars representing the plate twisting stiffness C. The flexible joint models the concentrated bending stiffness D and the effects of Poisson's ratio μ. The modulus of subgrade support k is represented by independent elastic springs, i.e., the Winkler foundation (Ref 36). A problem involving almost any physical combination of loads and restraints applied to a slab, including lateral loads, in-plane forces, and applied couples or moments, can be solved. Furthermore, slab discontinuities as well as partial subgrade support can be simulated on the model.

The deflection at each joint is the unknown. The basic equilibrium equations are derived from the free-body of a slab joint with all appropriate internal and external forces and reactions. These equations include summing the vertical forces at each joint and summing the moments about each individual bar. A complete derivation of these equations and the fourth-difference equations can be found in Ref 4.

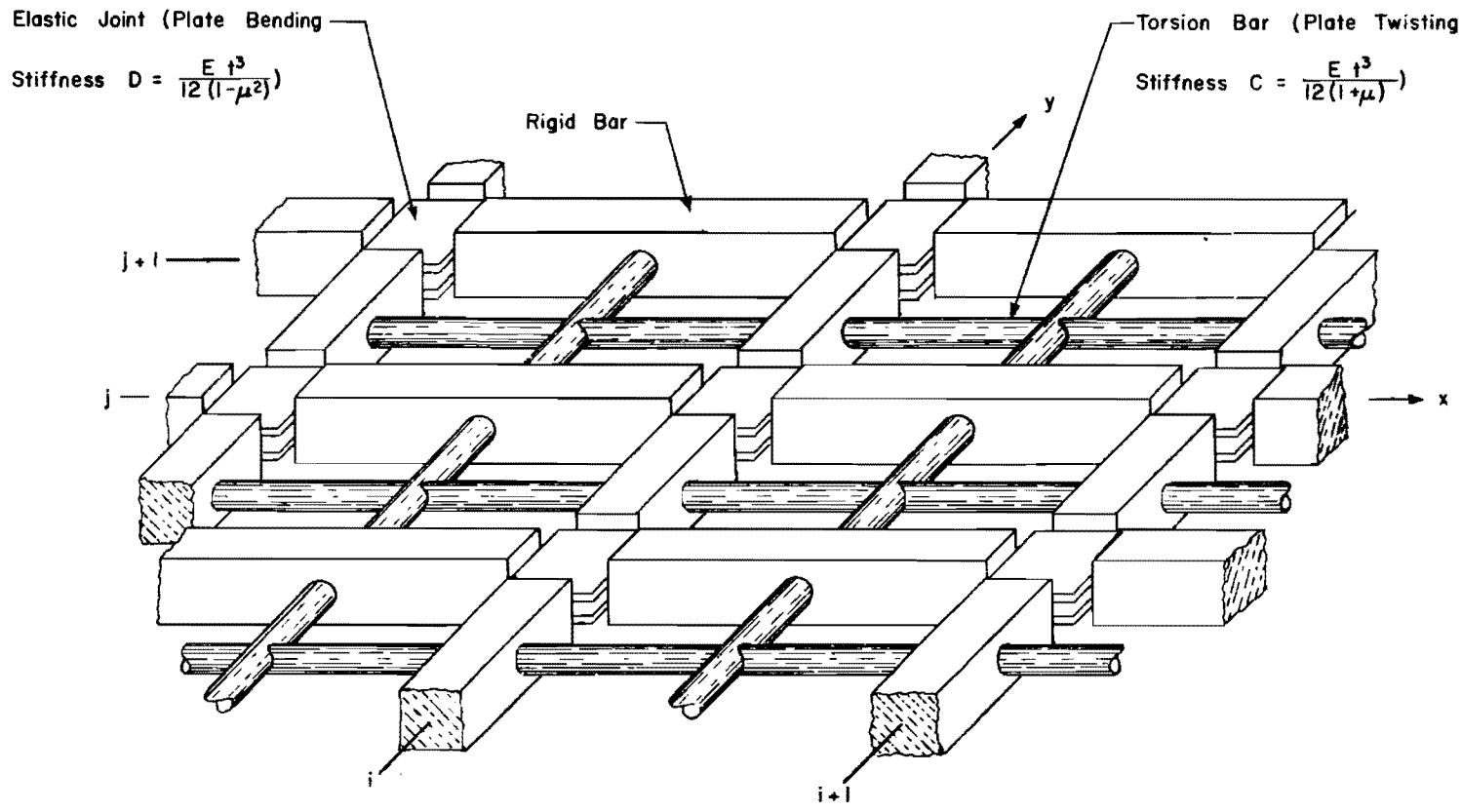

Fig 4. Discrete-element model of a plate or slab (after Ref 4).

Crack Effect and Method of Attack

Figure 5 shows a plan view of a plate segment that is divided into increments in the x and y-directions with increment lengths h_x and h_y, respectively. These "beam" increments are designated with i in the x-direction and j in the y-direction. The joint on the positive end of each increment is numbered the same as that increment. This numbering system then gives the i, j grid indicated in this plate segment. The stiffness $D_{i,j}$ for a plate is a unit value per inch of width. For use in computations, it is convenient to input average stiffness over a full increment width. $D^x_{i,j}$ represents the average stiffness in the y-direction; that is, the average bending stiffness of the plate over an area one increment wide and one increment long, centered at station i,j.

Since a discontinuity, such as a joint or crack, creates a variable distribution in the moment of inertia or stiffness (Fig 2), it can be simulated on the discrete model with one of the following methods.

The first method requires a clear determination of stiffness variation in the crack region, which is then divided into increments sufficient to define accurately the effect of the discontinuity. A disadvantage of this method is that it may not be possible to define the stiffness variation in the cracked region accurately enough to yield reasonable results. Furthermore, as the number of increments in either the x or y-direction increases, computer time increases, making the solution impractical in some cases.

The second method, which was used in this study, deals with an average value of stiffness that considers the discontinuity effect. The derivation of this average value was solely based on basic moment-curvature relationships and is independent of increment length. Hence, the whole structure can be divided into about 15 increments in each direction and reasonable results can be obtained.

Derivation of Average Moment of Inertia $\bar{I}$

For the determination of average moment of inertia $\bar{I}$, the following assumptions are made:

(1) A plane section remains plane before and after bending.

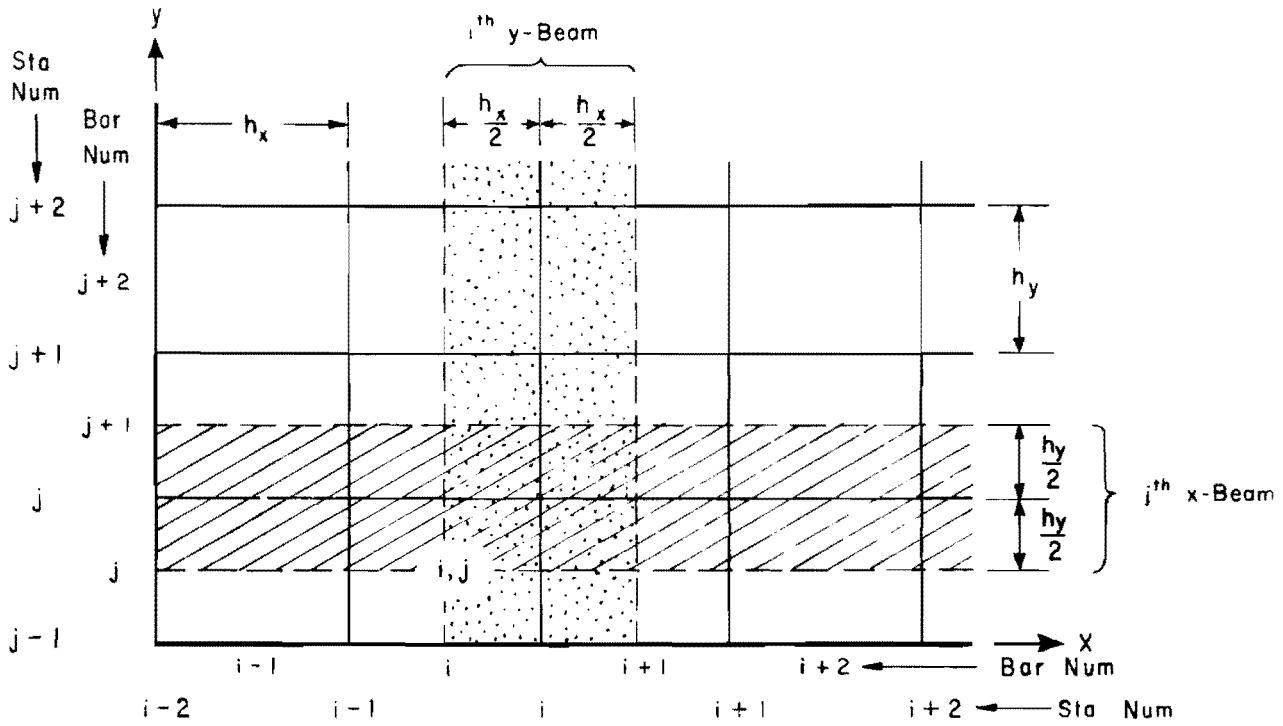

Fig 5. Plan view of plate segment divided into x and y-beams (after Ref 4).

(2) A straight line neutral axis can be assumed to represent the average of the actual variable position of the neutral axis.

(3) At the fine crack locations, any curvature will bring the two parts of the slab in touch and hence allow the transfer of bending.

With the above assumptions in mind, consider the 1-foot-wide slab shown in Fig 6. Because of the cracks, the actual rigidity of the structure is variable along its length, being largest between cracks, where the tension of the concrete contributes to the rigidity, and smallest at the cracks. Using basic moment-curvature relationships for working stress analysis,

$$\frac{1}{\bar{\rho}} = \frac{M_w}{E\bar{I}} \tag{3.2}$$

where

$\bar{\rho}$ = average radius of curvature,

M_w = working moment,

E = modulus of elasticity of concrete,

$\bar{I}$ = average moment of inertia.

Furthermore, from the strain diagram (Fig 7), the angle $\bar{\theta}$ is:

$$\frac{1}{\bar{\rho}} = \frac{\bar{e}_s}{d(1-K)} = \frac{\bar{f}_s}{E_s d(1-K)} \tag{3.3}$$

where

$\bar{e}_s$ = average strain in reinforcement,

$\bar{f}_s$ = average stress in reinforcement,

E_s = modulus of elasticity of steel,

d = distance from top compression fiber to the centroid of steel,

P = longitudinal percentage reinforcement,

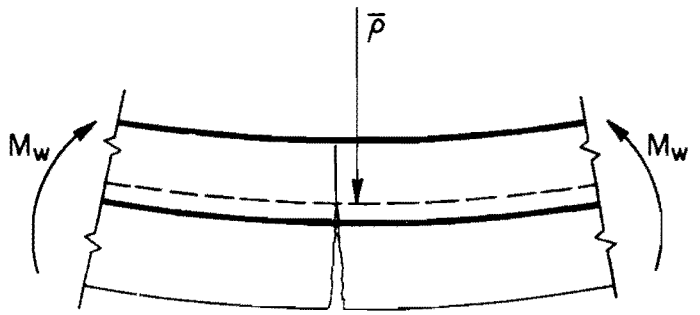

Fig 6. Cracked slab.

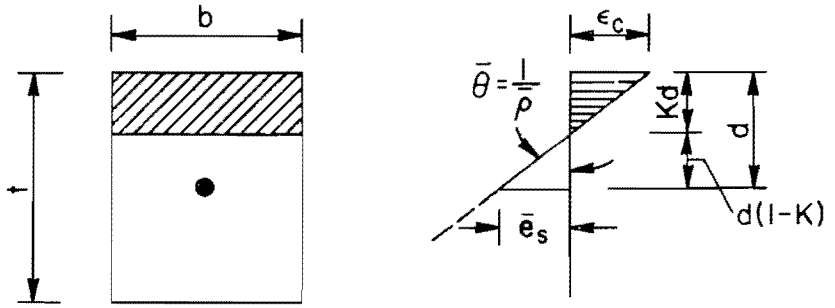

Fig 7. Strain distribution near crack location.

$$P = \frac{\text{area of steel } A_s}{\text{gross area of concrete } b \times t} \times 100 .$$

$$K = 2\left[\sqrt{Pn(1 + Pn)} - Pn\right] \qquad (3.4)$$

where

$$n = \frac{E_s}{E} .$$

In Eq 3.4, K is a fraction which when multiplied by d gives the distance to the neutral axis of the section (Appendix 1a). This is based on the cracked transformed section (Ref 35). It is worthwhile to note that the area of concrete in the percentage reinforcement term is the gross area of the section, and not, as defined in the equations for reinforced concrete, the width of the section times the distance from extreme compression fiber to the centroid of the steel. In Eq 3.4, P should be expressed as a ratio rather than a percentage.

Combining Eqs 3.2 and 3.3, and solving for $\bar{I}$, gives

$$\bar{I} = \frac{M_w nd(1-K)}{\bar{f}_s} \qquad (3.5)$$

For the determination of the average stress in the reinforcement, the contributing effect of the concrete in tension has to be considered. Let the average tensile stress of concrete between cracks be expressed as

$$\bar{f}_t = k_1 f_r \qquad (3.6)$$

where

f_r = flexural stress of concrete,

k_1 = a reduction factor based on experimental results (Appendix 1).

The part of the resisting moment corresponding to the average tensile stress of concrete $\bar{f}_t$, as shown in Fig 8 (after Ref 5), is

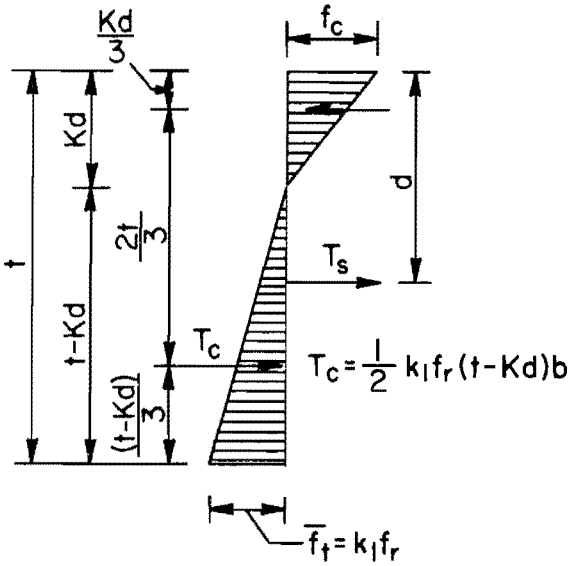

Fig 8. Stress distribution, considering average tensile concrete stress at locations away from the crack.

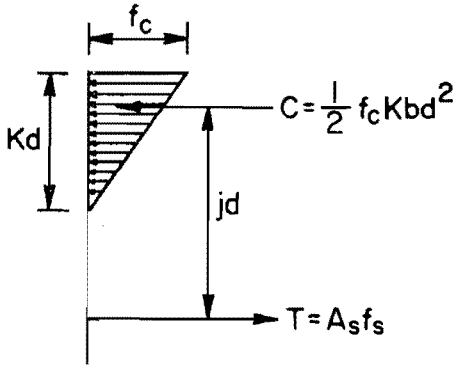

Fig 9. Stress distribution at crack location.

$$M' = T_c \left(\frac{2t}{3}\right) \tag{3.7}$$

where

T_c = the tensile force in the concrete.

Substituting the value of T_c (Fig 8) in Eq 3.7,

$$M' = \frac{k_1 f_r (t - Kd) b}{2} \left(\frac{2t}{3}\right)$$

$$= \frac{k_1 f_r bt(t - Kd)}{3} \tag{3.8}$$

Further development of the above equation is carried on in Appendix 1b, where the modulus of rupture (flexural stress at cracking f_r) is expressed in terms of the compressive strength of concrete f'_c (Ref 5). In final form

$$M' = 0.1(f'_c)^{2/3} bt(t - Kd) \tag{3.9}$$

Hence, the stress in the reinforcement f'_s corresponding to M' can be computed by

$$f'_s = \frac{M'}{A_s jd} \tag{3.10}$$

where

f'_s = tensile stress in the steel due to flexural stress in concrete at points away from crack, and

$j = 1 - \frac{K}{3}$.

But at the cracked section, the steel stress f_s is

$$f_s = \frac{M_w}{A_s jd} \tag{3.11}$$

The value of the working moment M_w depends on whether the steel or the concrete stress governs (Fig 9). If the former controls, then from Eq 3.11

$$M_w = A_s f_s jd$$

where

f_s = the allowable stress in the steel.

On the other hand, if the concrete stress governs, then

$$M_w = \frac{f_c K j b d^2}{2} \tag{3.12}$$

where

f_c = the working compressive stress in the concrete.

Substituting the controlling value of M_w in Eq 3.11, gives the value of the steel stress at the crack, and the actual average steel stress $\bar{f}_s$ at the verge of cracking is

$$\bar{f}_s = f_s - f'_s$$

Hence, the average moment of inertia is given by:

$$\bar{I} = \frac{M_w n d(1 - K)}{f_s - f'_s} \tag{3.13}$$

In the above equation, the average moment of inertia $\bar{I}$ is expressed in terms of slab geometrical characteristics and material properties. Using the preceding analysis gives the variation of the percentage reduction in bending stiffness versus the percentage reinforcement for different concrete compressive strength values, as shown in Fig 10. Bending stiffness reduction ranged from 80 to 90 percent for the change encountered in the percentage reinforcement. However, it is important to note the minor influence of the concrete compressive strength on stiffness reduction. Appendix 2 includes a sample calculation for the determination of the average moment of inertia and the corresponding stiffness reduction.

In Fig 10 it is shown that for the same percentage reinforcement, stiffness reduction (which does not include the concrete modulus) increases very slightly as f'_c increases. However, it is worth noting that the modulus of elasticity of concrete also increases with the increase in f'_c. This fact implies that the remaining stiffness (i.e., percent remaining multiplied by concrete modulus) increases with the increase in f'_c.

In the development of the above curves, the allowable concrete compressive stress was $0.45f'_c$, and the allowable tensile steel stress was 0.75 of yield, which is equivalent to a safety factor of 1.33.

Several values of the yield stress, ranging from 40 to 70 ksi, were tried. Fortunately, for the range and safety factor in the steel mentioned above, the variation of the percentage reduction in bending stiffness was independent of the yield stress. This is due to the fact that the working moment M_w, the lower of the values from Eqs 3.11 and 3.12, was governed by the latter equation where the concrete stress controls. If a lower allowable steel stress is desired, the above plot may need to be modified.

Region Affected by the Crack

Discontinuities in structural members not only cause severe localized bending stiffness reduction, but influence a certain amount of the area around them. Therefore, after determination of the average moment of inertia and the corresponding reduction in bending stiffness, one more step is required before the discrete-element model of the problem is performed. The length over which the original bending stiffness should be reduced to simulate the effect of the discontinuity must be determined.

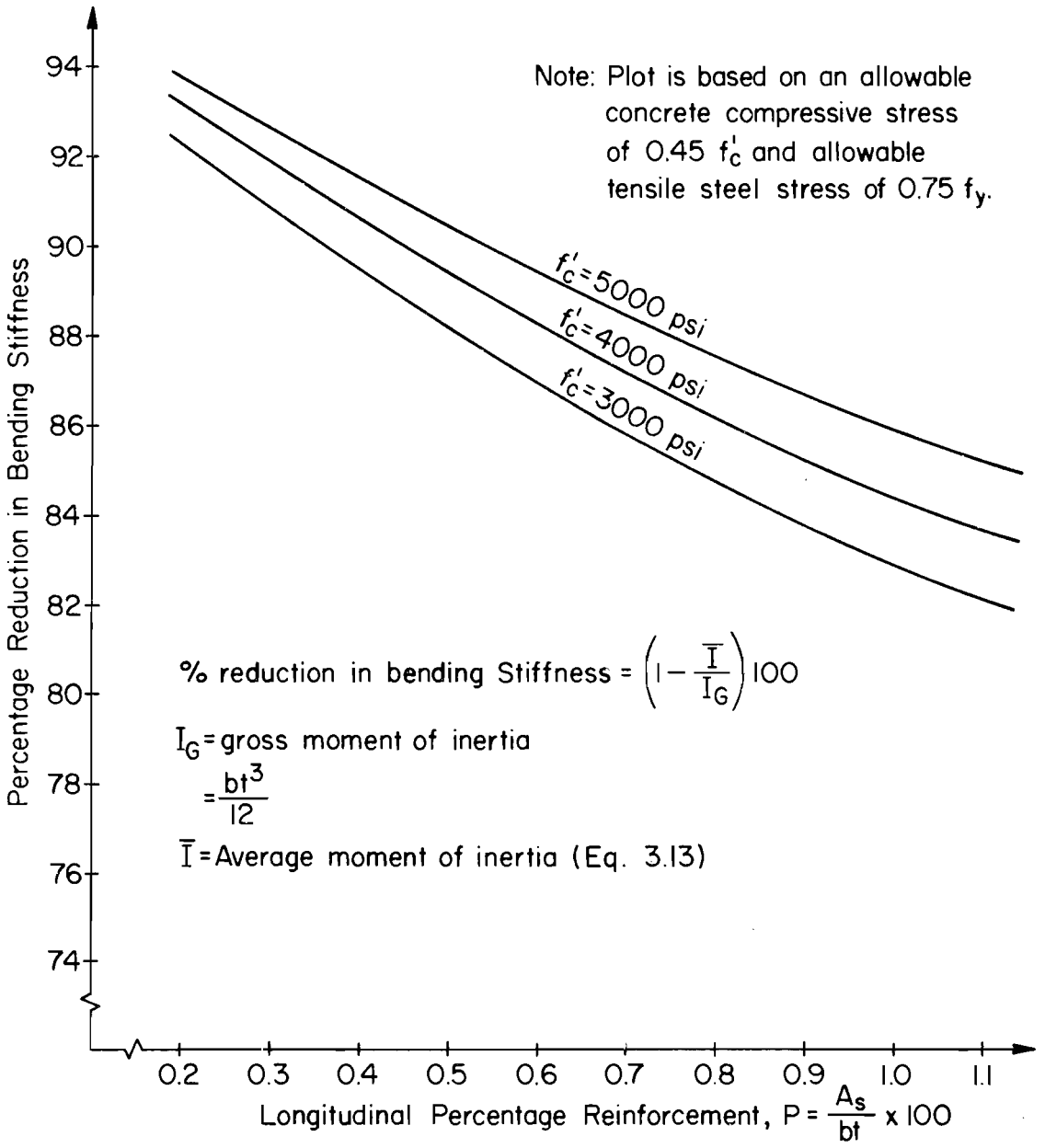

Fig 10. Variation of the percentage reduction in bending stiffness at crack location with longitudinal percentage reinforcement.

A slab portion under the effect of transverse loading (Fig 11(a)) is considered. Since the concrete does not resist any tension stresses at the crack, the compression force in the upper concrete fibers has to be balanced by a tensile steel force to maintain equilibrium at that section. In actuality, concrete fails to resist tension stresses only at a crack. Between cracks, the concrete does resist moderate amounts of tension stress; this reduces the tension force in the steel (Fig 11(b)), which creates a variable force in the bar. Since the bar must be in equilibrium, this change in bar force is resisted at the contact surface between steel and concrete by an equal and opposite force produced by the bond between steel and concrete. Figure 11(c) shows a schematic distribution of the bond stress in the cracked region; it should be remembered that the bond is nothing but the rate of change of tension. For the free-body of a bar segment shown in Fig 11(d), if U is the magnitude of the average bond force per unit length of bar, then $\Sigma F_x = 0$ yields

$$Udx + T - (T + dT) = 0$$

$$\therefore Udx = dT \tag{3.14}$$

Integrating over the required length, a

$$U \int_o^a dx = \int_{T_1}^{T_2} dT$$

where

T_1 = tension in steel at some point between cracks, and

T_2 = tension in steel at crack.

Hence:

$$Ua = T_2 - T_1 = A_s f_s - 0$$

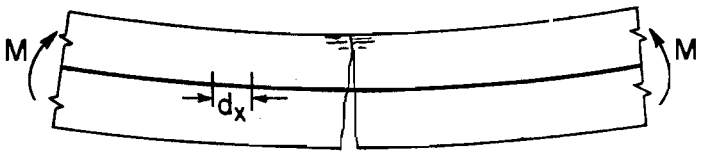

(a) Cracked slab portion.

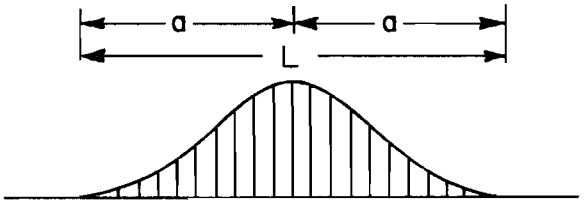

(b) Longitudinal tensile stress in the steel (schematic).

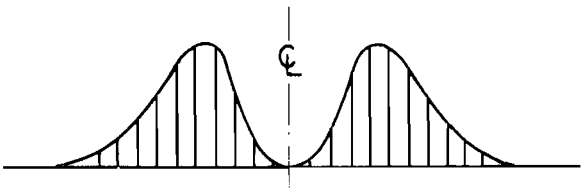

(c) Bond stress (schematic).

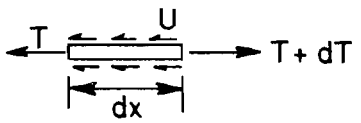

(d) Free-body of a bar segment.

Fig 11. Region affected by the discontinuity.

Therefore,

$$a = \frac{A_s f_s}{U} \tag{3.15}$$

Assuming that the bond force per unit length U is the resultant of shear type bond stresses u uniformly distributed over the contact area, then

$$U = up \tag{3.16}$$

where

p = the perimeter of the bar(s).

By substituting the value of U in Eq 3.15

$$a = \frac{A_s f_s}{up} \tag{3.17}$$

Hence, total affected length

$$L = 2a$$

$$L = 2\frac{A_s f_s}{up} \tag{3.18}$$

For the determination of the allowable bond stress u, as well as f_s, the ACI 1963 code (Section 1301) specifies the following:

(1) For tension bars, the allowable bond stress u is governed by

$$u = \frac{3.4\sqrt{f'c}}{\phi} \leq 350 \text{ psi} \tag{3.19}$$

where

ϕ = the bar diameter;

(2) The allowable stress in the steel shall not exceed 24,000 psi.

Discrete-Element Modeling of the Crack Effect

By the previous analysis, the amount of reduction in bending stiffness, as well as the length over which it should be applied, has been determined. In this section, a method for modeling the effect is discussed.

In this method there are two cases to be considered. In the first case, the region affected by the discontinuity extends over an even number of increments (Fig 12(a)). Assuming for example that this region is two increments long (L = 2h) , it is defined by three stations: two edge stations (i-1,j and i+1,j) and a middle station where the crack is located (i,j). Because the stiffness in the discrete-element model, (Fig 4) is lumped at the elastic joints or station locations, in order to simulate the effect described above, it is necessary to apply the total amount of the previously determined bending stiffness reduction at each middle station (in this case only one, i,j), and half of that amount at each of the boundary or edge stations, namely i-1,j and i+1,j . As an example, if the amount of reduction in bending stiffness is 90 percent of the original full value, 90 percent of the stiffness should be reduced at station i,j , and 45 percent at each of the edge stations, i-1,j and i+1,j .

In the second case, the area influenced by the crack extends over an odd number of increments; for example, three (L = 3h), as in Fig 12(b). The main difference between the two cases is the relative position of the ends of the reduced stiffness region and station locations. When the number of increments is even, a station is located at each of the boundaries or edges of the concerned region, which requires the half-value refinement discussed previously. When there is an odd number of increments, the edges of the reduced stiffness region lie midway between stations, and for modeling, the total reduction in bending stiffness is applied at each station (i-1,j ; i,j ; and i+1,j), with no exception.

For the case where the number of increments is even, it was mentioned that a half-value of the stiffness reduction should be applied at the edge stations. To test the sensitivity of the half reduction, several examples were studied.

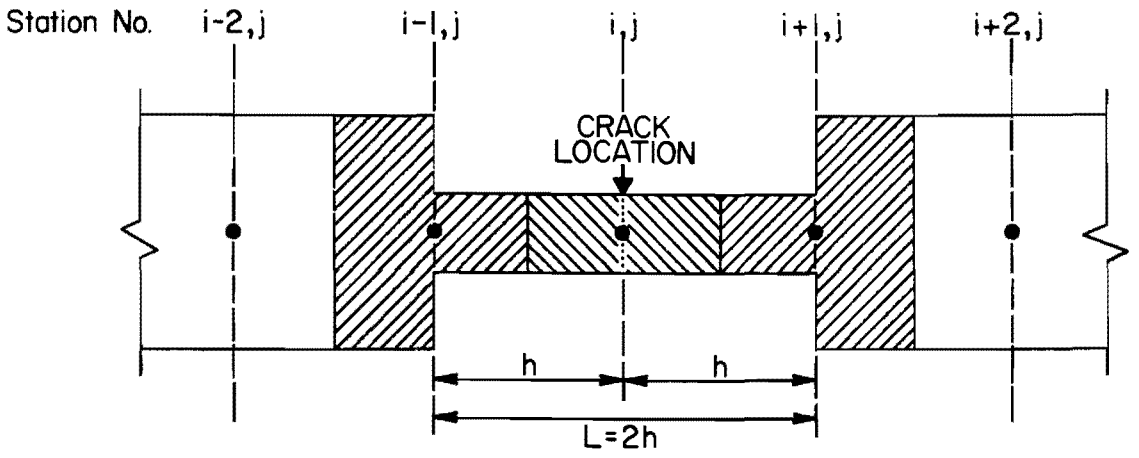

(a) Even number of increments in the region of the crack.

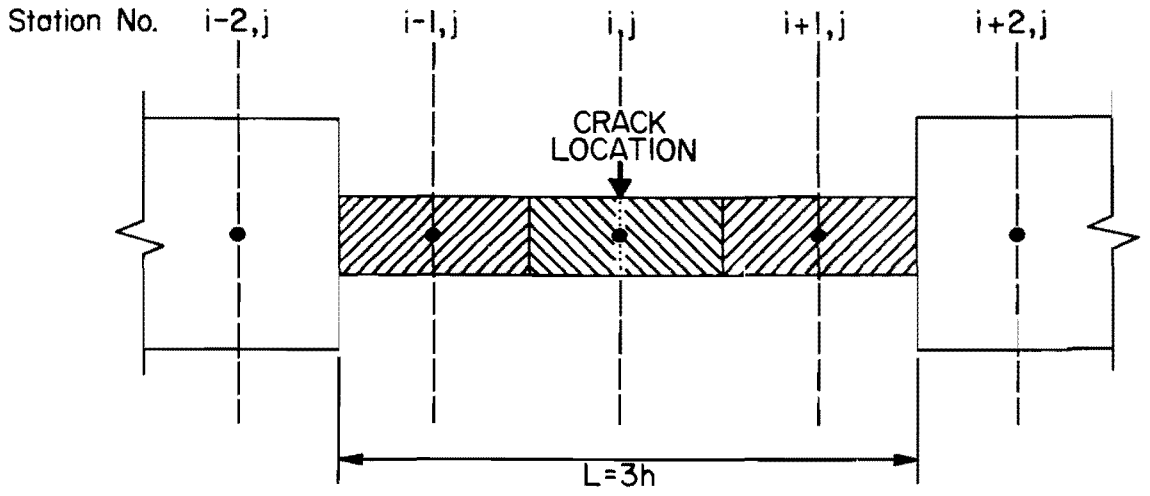

(b) Odd number of increments in the region of the crack.

Fig 12. Discrete-element modeling of crack effect.

These covered a wide range of thicknesses, moduli of elasticity, crack spacings, and moduli of subgrade reaction. Without exception, neglecting the half-value reduction at the edge stations produced only negligible changes in deflections and principal stresses.

To validate the above observation, a problem involving a 20 × 40-foot pavement loaded with a 12-kip concentrated load placed 4 feet from the edge (Fig 13) was considered. The thickness of the pavement was 8 inches, and the modulus of subgrade reaction was 100 lb/in^3. The reduction in bending stiffness was applied over a length of 12 inches at each transverse crack location. Figure 13 illustrates the change in deflection with the increase of the percent reduction in bending stiffness; as shown, the rate of change in deflection was almost negligible up to about 50 percent of the stiffness reduction, and then a significant increase was observed. Thus, applying a half value of stiffness reduction at the edge stations produced almost negligible changes in stresses and deflections.

Therefore, it is recommended that when there is an even number of increments, the subgrade is not very weak, i.e., $k \approx > 40$ lb/in^3, and there is no loss in subgrade support, the half bending stiffness reduction at the edge stations be neglected.

Suggested Method and Sample Problem

A step-by-step method has been suggested for the application of SLAB programs in the analysis of discontinuities in continuously reinforced concrete pavements.

The method consists of the following steps:

(1) Determine the physical characteristics of the concerned pavement, such as modulus of elasticity, thickness, and percentage reinforcement.

(2) Determine the percentage reduction in bending stiffness to be applied at crack locations (from Eq 3.13 or Fig 10).

(3) Determine the length affected by the discontinuity (from Eq 3.18).

(4) Decide on the increment length which best matches the slab geometry as well as the length determined from step (3).

(5) Apply the percent stiffness reduction determined in step (2) at each crack location over the length from step (3).

The use of the method on a specific problem is demonstrated in Appendix 3, with the corresponding coded data required for the program. A 24-by-40-foot slab,

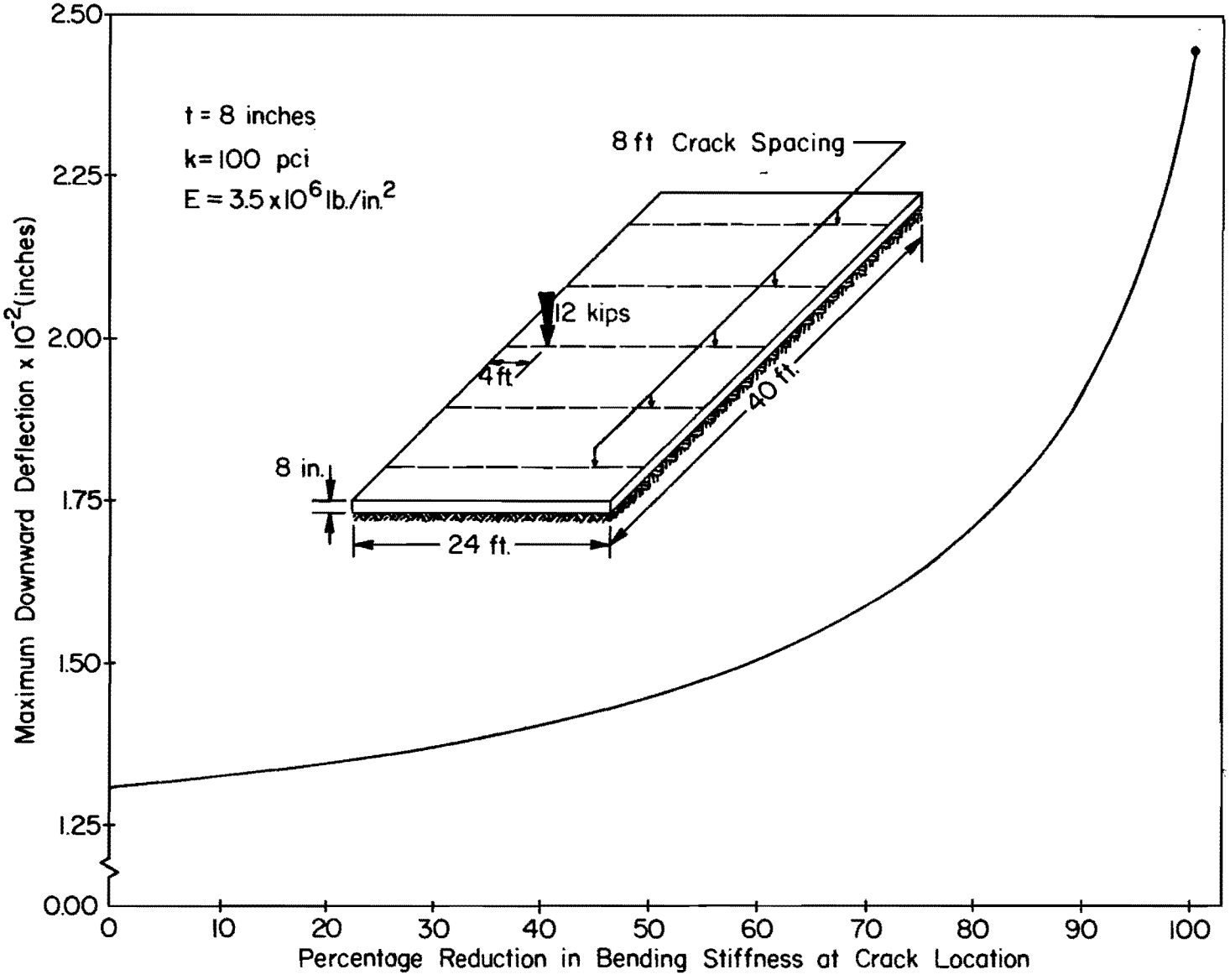

Fig 13. Effect of crack severity on deflection under a 12-kip wheel load.

loaded with two 9,000-pound wheel loads located at 2 and 8 feet from the edge was considered (Fig 14), and the percent reduction in bending stiffness determined was 90 percent over a length of 12 inches.

Besides the condition with 90 percent stiffness reduction at the crack location, two other conditions were studied: the hinged condition, where there is zero stiffness at the discontinuity, and the uncracked condition, where the full slab is treated as one piece. The variation in deflections for each of these cases is shown in Fig 14. The effect of the hairline cracks is clearly illustrated by the 30 percent increase in deflection of the 90 percent reduction case over the uncracked case. Furthermore, comparing the hinge and the uncracked cases, the percent deflection increase was doubled (60 percent). The results which also show that the percentage increase in deflections will drop for high values of stiffness and modulus of subgrade reaction, are discussed in more detail in Chapter 4.

Effect of Edge Restraints

Ideally, for discrete-element modeling of a continuously reinforced concrete pavement with no transverse joints except construction joints, as much length from the slab as possible should be considered to approximate the continuity effect. In a two-dimensional problem, such as the one encountered, isolating a certain portion of interest, for example that delineated by e-f-g-h in Fig 15(a), requires the following boundary conditions: a transverse spring S_z, and two rotational restraints R_x and R_y, in the x and y-directions, respectively (Fig 15(b)). These boundary conditions have to be applied at the end and edge stations of the slab. A rotational restraint in the discrete-element model (Fig 16) is nothing but a differential spring system which provides a force couple system that resists a change in slope but does not restrain deflections.

Practically, in most pavement problems, the most critical areas are those in the vicinity of the loads, where maximum deflections and stresses occur. From the analysis of plates on elastic supports, it can be shown that the part of the slab beyond a certain distance from the loaded area does not contribute much to the stiffness of the structure. Also, this observation is partially substantiated by field measurements (Ref 30). In other words, boundary restraints are not significant. In this section, the effect of these restraints (S_z, R_x, R_y) on different-sized portions of the pavement is studied. Results indicate

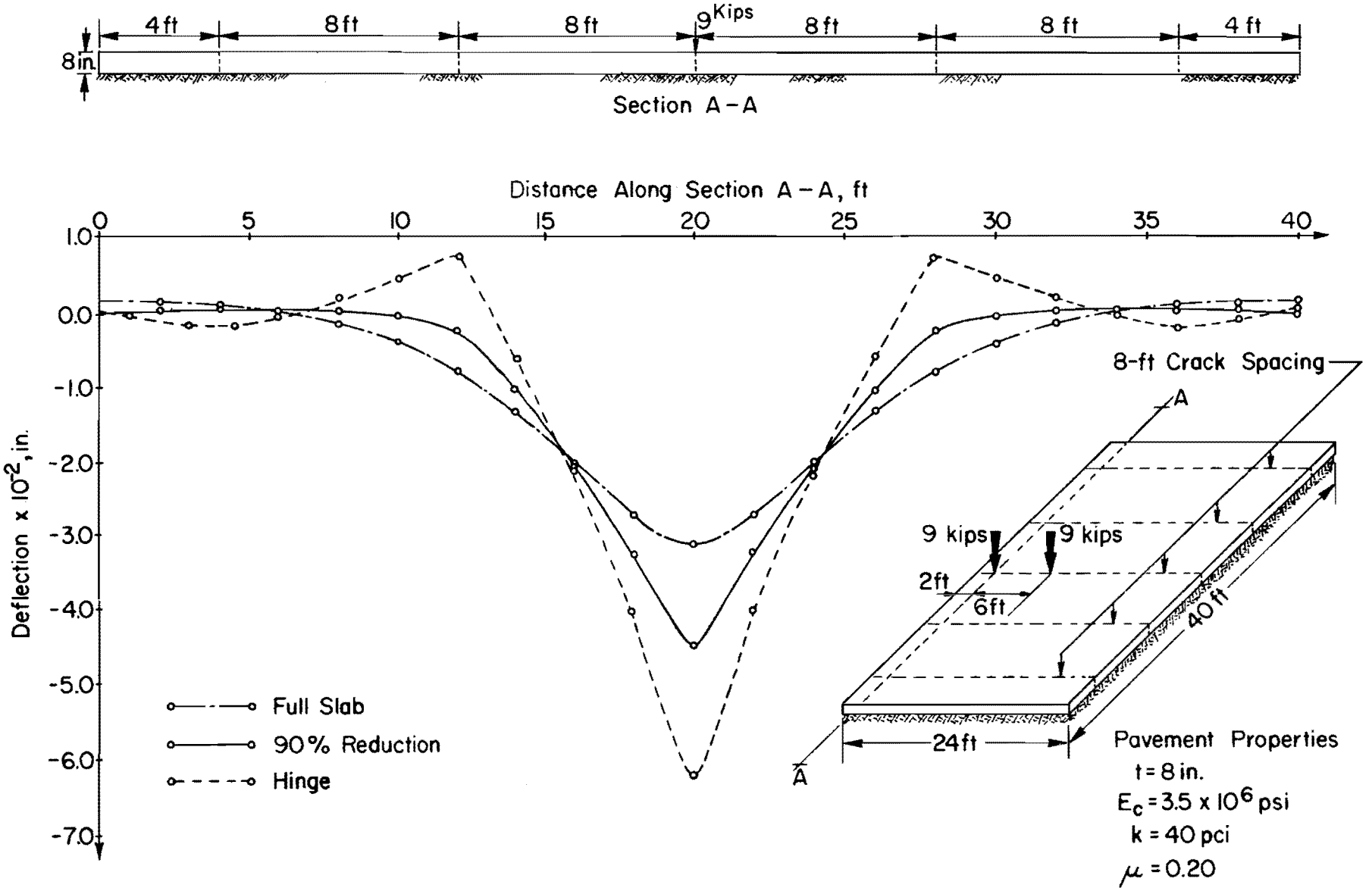

Fig 14. Influence of bending stiffness reduction at cracks on the deflection basin.

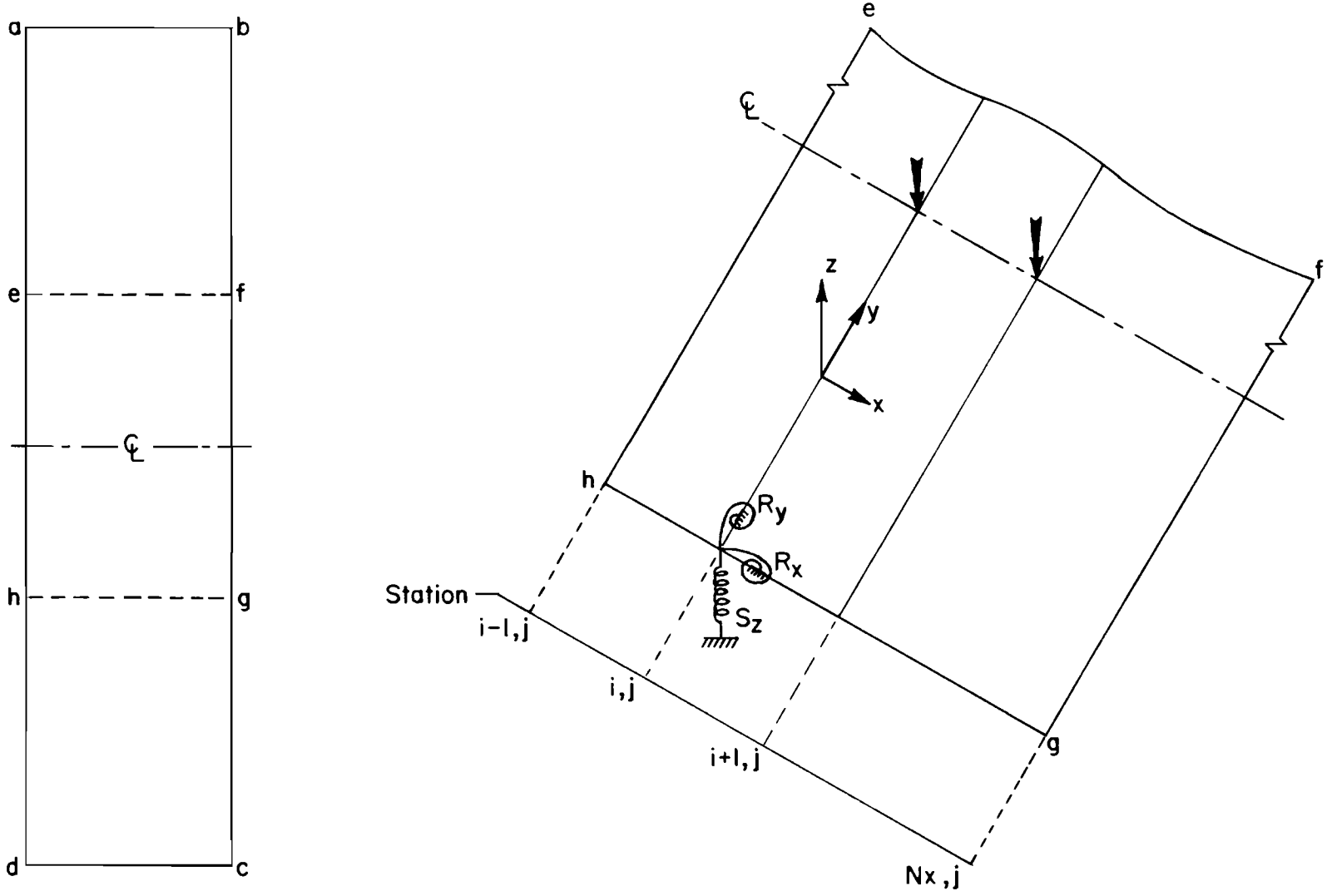

(a) Plan view of CRCP showing segment to be removed for study.

(b) Free-body segment e-f-g-h.

Fig 15. Slab partitioning with corresponding boundary restraints.

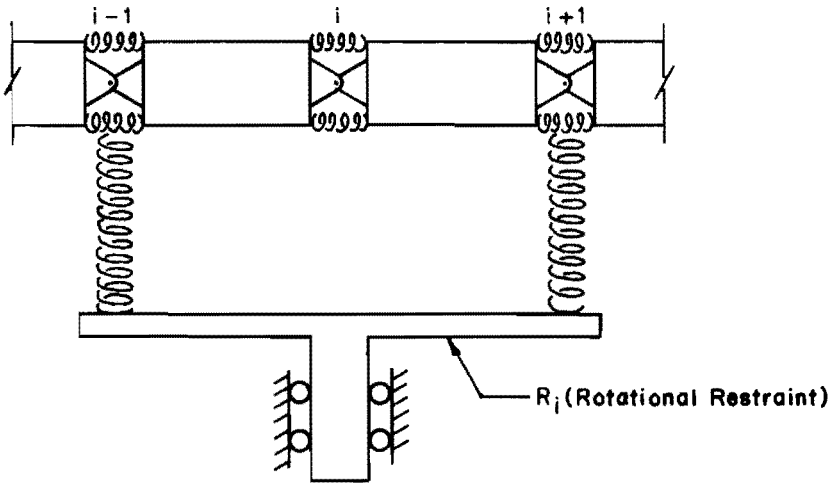

(a) Mechanical model.

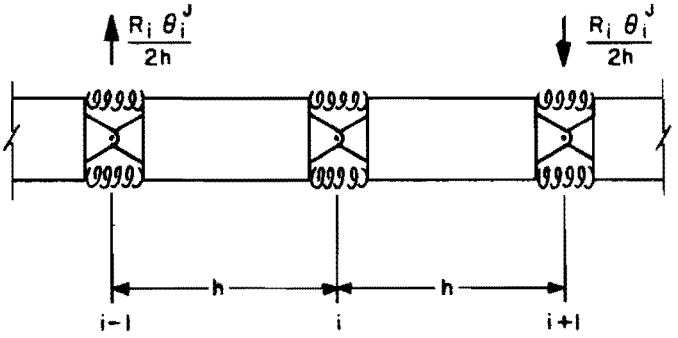

(b) Equivalent forces.

Fig 16. Rotational restraint R acting on the mechanical model (after Ref 7).

that beyond 15 to 18 feet from load locations, boundary restraints do not need to be precisely defined or even used.

This observation was investigated over a wide range of pavement characteristics, including thickness, modulus of elasticity, crack spacing, and modulus of subgrade reaction. In each combination of these factors, SLAB solutions of the following pavements were performed:

(1) a 24-by-80-foot slab with free edges (a-b-c-d in Fig 17) and

(2) a 24-by-40-foot partition (e-f-g-h) with two extreme conditions

  (a) free edge condition and

  (b) full fixity condition, where high values of S_z , R_x , and R_y (10^{30} was used) were applied at each edge station.

Table 3 shows the results for the SLAB solutions for a pavement possessing the following characteristics: thickness of 8 inches, concrete modulus of 3.5×10^6 psi, modulus of subgrade reaction of 100 lb/in^3, crack spacing of 4 feet, Poisson's ratio of 0.2, and loading arrangement as shown in Fig 17. It is obvious from the tabulated results that the percent of change in either deflection or principal moment was almost zero. Hence, whether a 24-by-80 or 24-by-40-foot slab, with or without restraints, is chosen, differences in results are quite negligible and of no practical importance. However, it should be recognized that this may vary with larger wheel loads.

Performing the same analysis on a 24-by-20-foot slab section (i-j-k-l in Fig 17) under the free edge condition resulted in an increase of 3 to 10 percent in deflections and 12 to 15 percent in principal moments, depending on the relative magnitude of the stiffness of the slab to that of the subgrade. Therefore, the 24-by-40-foot section with free edges was adopted as being more representative of the real problem.

Tension in the Longitudinal Reinforcement

Several analyses have been made for the determination of the longitudinal steel required in continuously reinforced concrete pavements (Refs 12 and 13). The purpose of this steel is to insure that the cracks in the concrete are small enough to prevent passage of surface water downward into the underlying material and to provide adequate aggregate interlock for load transfer across the crack. In contrast to the thickness of the pavement which is determined by the wheel loads, Vetter (Ref 12) showed that the amount of reinforcing steel necessary

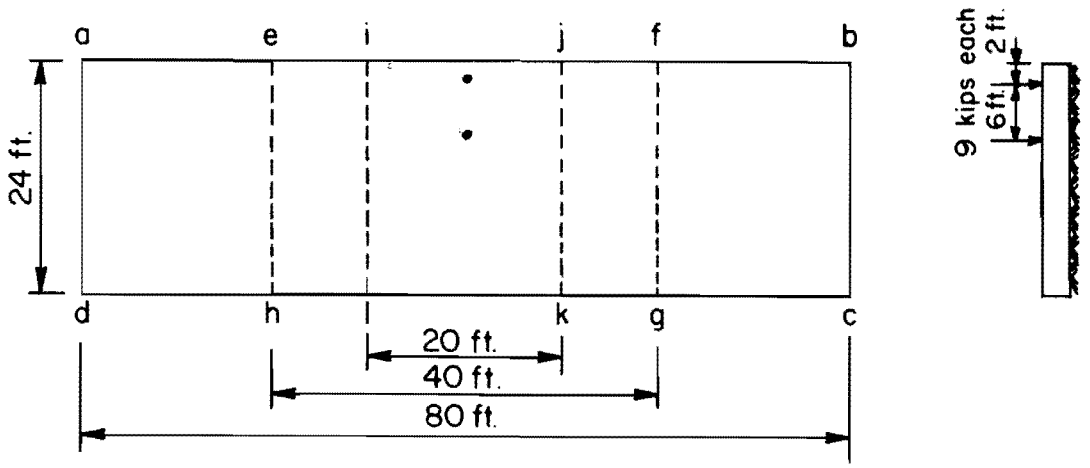

Fig 17. Slab geometric characteristics used in boundary restraint study.

TABLE 3. VALUES OF MAXIMUM DEFLECTIONS AND PRINCIPAL MOMENTS FOR DIFFERENT SLAB SIZES AND EDGE CONDITIONS

Size of Slab, feet	Condition of Edges	Maximum Deflection, inches	Maximum Principal Moment, lb-in per unit width
24 by 80	Free	0.03279	2285
24 by 40	Free	0.03279	2285
	Fixed	0.03277	2284

in pavements is based on such changes in the pavement as concrete shrinkage, moisture, and temperature induced variations.

For the determination of the longitudinal reinforcement and hence the corresponding tension, Vetter suggested the following equation:

$$P = \frac{S_t}{f_s - nS_t} \times 100 \qquad (3.20)$$

where

P = ratio of area of longitudinal steel to area of concrete, percent;

S_t = tensile strength of concrete, psi (about $0.4\ f_r$);

f_s = allowable working stress in steel, psi;

$n = \frac{E_s}{E}$;

E = modulus of elasticity of concrete;

E_s = modulus of elasticity of steel.

This formula is based on the following assumptions:

(1) that there is sufficient bond area to develop the full working stress in the steel, and

(2) that adequate load transfer is provided at transverse construction joints.

Further development of Eq 3.20 was carried on to include the coefficient of friction F between the pavement and subbase (Ref 13), and hence

$$P = (1.3 - 0.2F) \frac{S_t}{f_s - nS_t} \times 100 \qquad (3.21)$$

The frictional factor F depends on the surface smoothness of the subbase immediately beneath the rigid pavement. Recommended values of the friction factor can be obtained from Ref 2.

The formula given above will generally govern the percentage of longitudinal steel required in a continuously reinforced pavement. Under severe temperature variations or when unusual material properties are encountered, a formula which considers the thermal coefficient may be required (Ref 13), such as

$$P = (1.3 - 0.2F) \frac{S_t}{2(f_s - \Delta T \epsilon E_s)} \times 100 \tag{3.22}$$

where

ΔT = temperature range in ^{o}F;

ϵ = thermal coefficient of concrete and steel, per ^{o}F.

For the determination of tension in the steel, first solve for f_s. From Eq 3.21

$$f_s = (1.3 - 0.2F) \frac{S_t}{P} \times 100 + nS_t \tag{3.23}$$

From Eq 3.22

$$f_s = (1.3 - 0.2F) \frac{S_t}{2P} \times 100 + T\epsilon E_s \tag{3.24}$$

Therefore,

$$T_s = f_s A_s \tag{3.25}$$

$$= f_s Pbt \tag{3.26}$$

where

T_s = tension in the steel,

f_s = allowable stress in the steel calculated using Eqs 3.21 and 3.22 and taking the higher value ($f_s \leq 0.75\ f_y$) ,

t = thickness of the pavement,

b = width of the pavement.

Assuming the tension is uniform across the slab, the tension per unit width is

$$\frac{T_s}{b} = f_s P t \tag{3.27}$$

One of the important concrete properties that enters into rigid pavement design is modulus of rupture. Different values are obtained from experimental results, depending on the kind of test, but in this study, the following empirical formulas were used to determine modulus of rupture f_r .

According to the 1963 ACI Code, Section 2609(c) (Ref 23),

$$f_r = 7.5\sqrt{f'_c} \tag{3.28}$$

where

f'_c = the 28-day concrete compressive strength in psi.

From Ref 14,

$$f_r = \frac{3{,}000}{3 + \frac{12{,}000}{f'_c}} \tag{3.29}$$

The modulus of rupture can be calculated by either Eq 3.28 or 3.29. The value obtained from either of these two equations (values will be nearly identical) can be used to calculate the allowable tensile strength of concrete S_t ($S_t \approx 0.4\ f_r$).

Referring to the above equations, we find that the value of the tension varies over a fairly wide range, depending on the particular conditions studied. However, it is worthwhile to note that this tension value depends to a considerable

degree on the allowable tensile strength of concrete, which is evaluated by dividing the modulus of rupture by a factor of safety. In this study, a factor of safety of 2.5 was used. A numerical example for the determination of tension in the longitudinal steel is solved in Appendix 4.

Poisson's Ratio Effect

One of the concrete properties involved in pavement design analysis besides the modulus of elasticity and flexural strength is Poisson's ratio, μ. Previous investigations have shown that variations in μ have little effect on changes in deflections and stresses (Ref 6). This observation was also validated in this research, by discrete-element theory.

For this study, a real, typical problem was selected. Figure 18 shows a concrete slab loaded with two concentrated loads of 9,000 pounds each and with the following pavement properties: 40 feet long, 24 feet wide, 8 inches thick, concrete modulus of 5.5×10^6 psi, and modulus of subgrade reaction of 100 $lb/in^2/in$. The variation in Poisson's ratio covered the range from 0.1 to 0.3 inclusive.

Figure 19 illustrates the variation of maximum deflection and stress, which occurred directly under the edge load, with Poisson's ratio. As noticed, a change in Poisson's ratio from 0.1 to 0.3 increases the deflection by 4 percent and stress by 6 percent (Fig 19). In the factorial analysis performed, a μ value of 0.2 was chosen.

Load Position

During the service life of a pavement, many different kinds and sizes of loads are applied. These loads vary not only in magnitude, but also in number and point of application on the roadway itself. Present pavement design methods, however, usually involve the selection of one particular load position in calculating stresses. These stresses are then taken as critical and a pavement thickness is selected to give an appropriate safety factor.

Historically, particular load positions have been closely associated in design with a given type of rigid pavement. Corner loadings have been used for jointed concrete pavements and interior loads have been used for continuously reinforced concrete pavement.

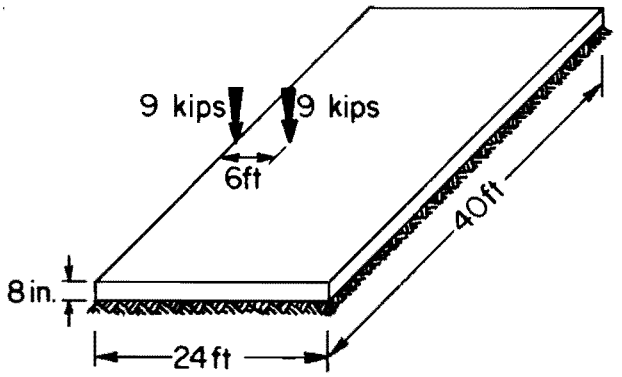

Fig 18. Example problem for the study of Poisson's ratio effect.

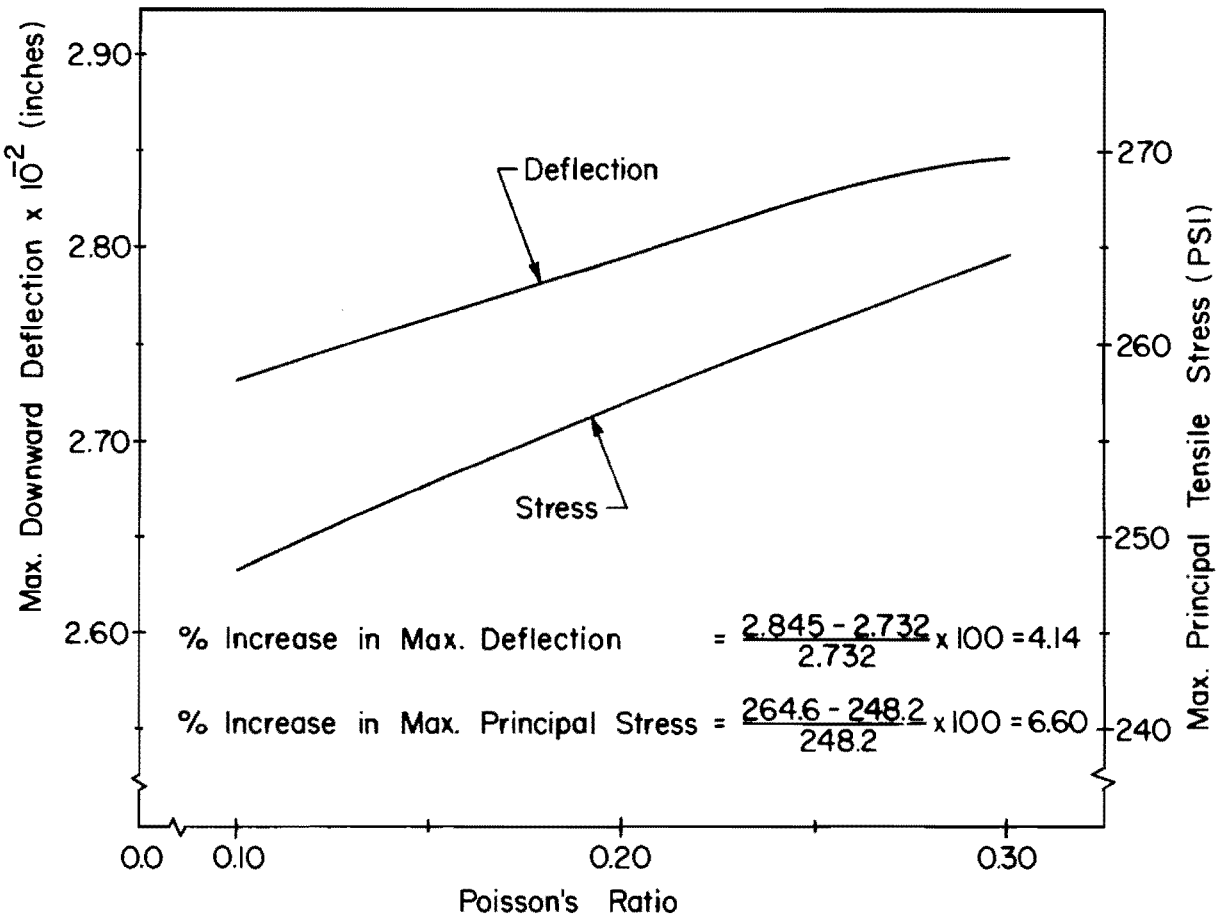

Fig 19. Influence of Poisson's ratio on maximum deflections and stresses.

Analyses have been made by Treybig, Hudson, and McCullough (Ref 22) using discrete-element theory to evaluate the relative merits of interior, corner, and edge loading conditions. The physical situation analyzed above was a 20-by-80-foot pavement loaded with 12,000 pounds concentrated at the three concerned positions (Fig 20). The influence of load placement and slab thickness on stress in pavement with different modulus subgrade values is illustrated in Fig 21. Obviously, the most critical case is the corner one. However, in the sensitivity study, two 9,000-pound wheel loads were placed at 2 and 8 feet from the edge of the slab to simulate an edge loading condition. The corner load position was not considered because the continuously reinforced pavement structure does not have any free corners which are characteristic of a true corner load condition.

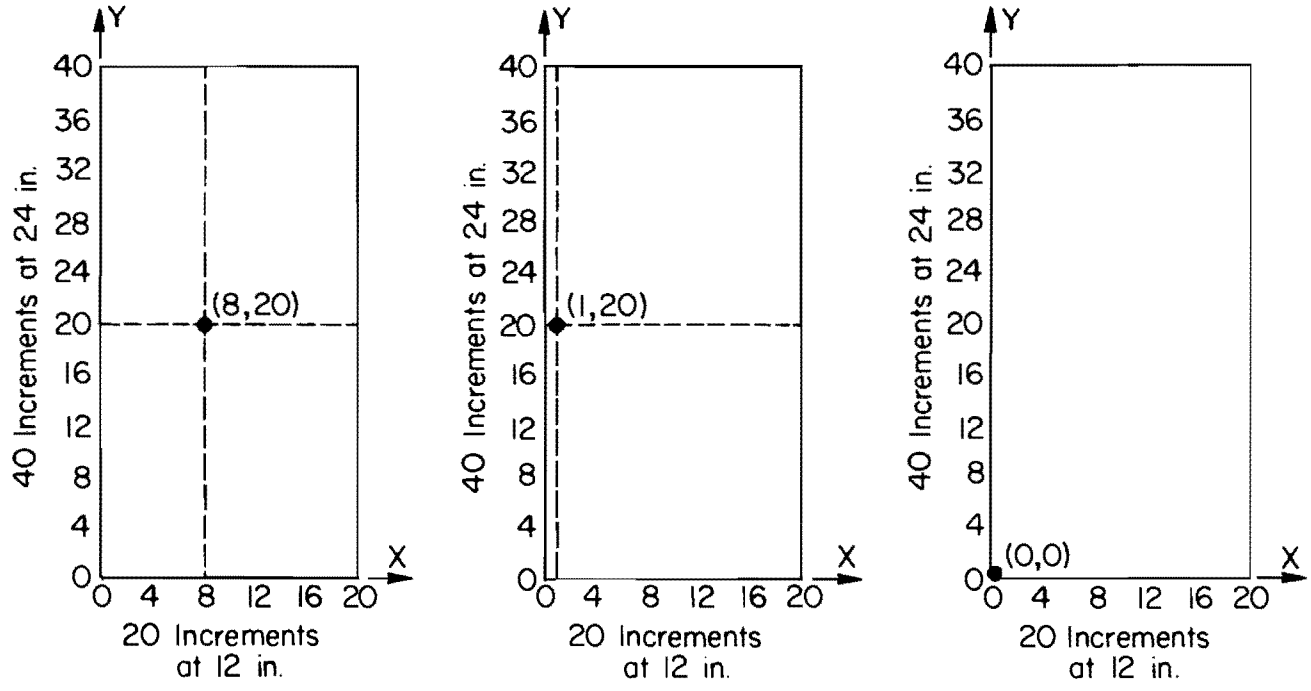

Fig 20. Interior, edge, and corner load placements on 20 x 80-foot discrete-element slab model (after Ref 22).

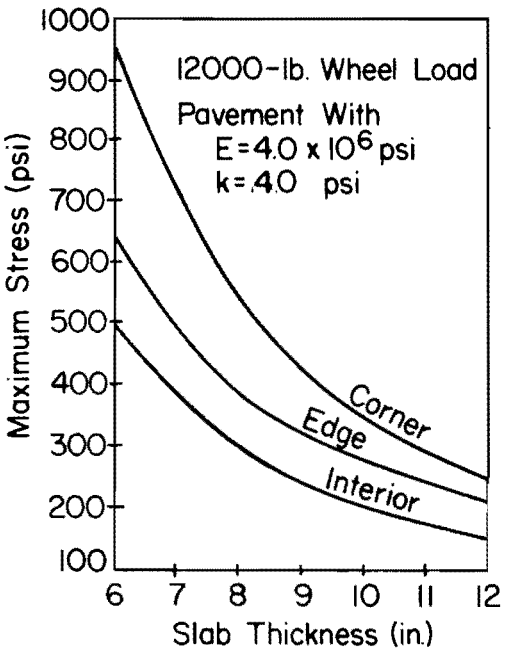

(a) k = 40 pci .

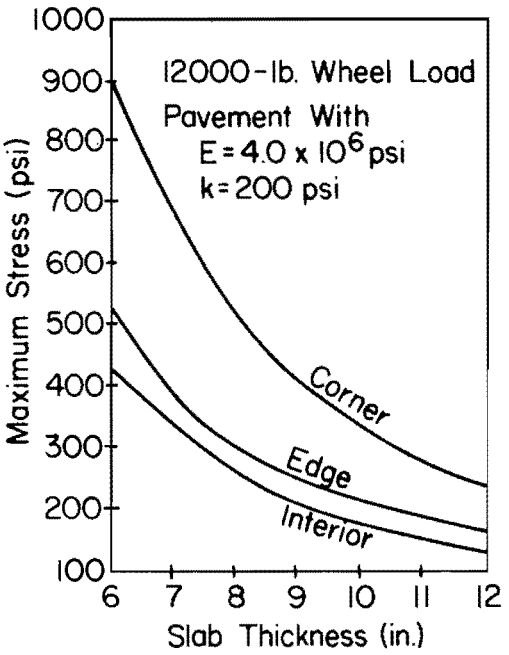

(b) k = 200 pci .

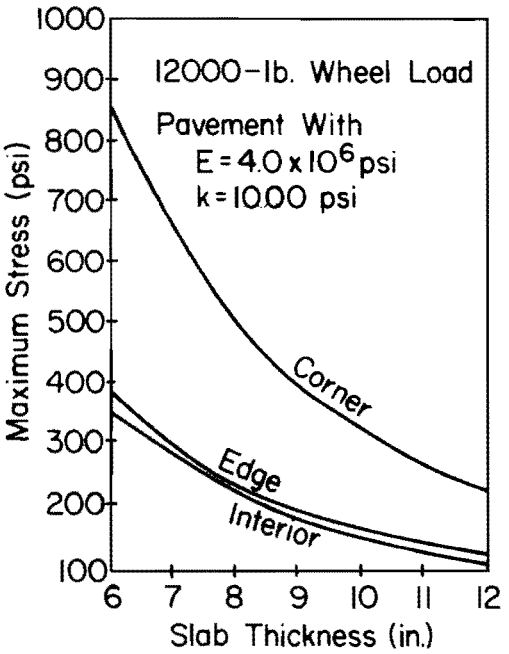

(c) k = 1000 pci .

Fig 21. Influence of load placement and slab thickness on stress for different values of modulus of subgrade reaction k (after Ref 22).

CHAPTER 4. RESULTS AND ANALYSIS

Various slab characteristics to model a real problem are presented in Chapter 3. Conclusions were drawn on their effects, based on changes in deflections and principal moments. The characteristics analyzed included reduction in the bending rigidity of the slab due to discontinuities, boundary restraints, tension in the longitudinal steel, Poisson's ratio, and load position.

The variable factors for the intended sensitivity study of CRCP design parameters and their corresponding levels are presented in Table 1. SLAB solutions were obtained for each level combination (Table 2) of these pavement parameters, namely, slab bending stiffness, modulus of subgrade reaction, and crack spacing. These solutions were repeated for two load positions: loads directly on the crack and loads midway between cracks.

SLAB Input Parameters

Percentage Reduction in Bending Stiffness. The percentage reduction in bending stiffness was determined from Fig 10. A value of 0.55 percent of longitudinal reinforcement corresponds to a 90 percent reduction in bending stiffness at each transverse crack location. The length over which this reduction was applied was 12 inches, determined from Eq 3.18 for a No. 4 bar.

Poisson's Ratio. According to Ref 6 and the analysis of the effect of Poisson's ratio of concrete, reported in Chapter 3, changes in deflections and stresses due to Poisson's ratio variations were insignificant. For this study, a value of 0.20 was used in calculating the bending and twisting stiffness slab terms.

Tension in the Longitudinal Reinforcement. Equations 3.21 and 3.22 show that the tension in the longitudinal steel depends on the compressive stress of concrete f'_c, percentage reinforcement P, range in temperature, and pavement thickness. The variation of the tension with concrete compressive stress and the percentage reinforcement were not so high when compared with

the variation due to thickness. A value of 4,000 psi was taken for f'_c, and as assumed before, 0.55 for percent of longitudinal reinforcement. From Eq 3.27 it is seen that the tension is directly proportional to the thickness of the pavement. From the three levels of the slab bending stiffness, one level of the modulus of elasticity yields three values of thickness, from which the tension values are obtained. For the 12-inch increment length in the transverse direction, the tension values were 12,000, 19,000, and 28,500 pounds per station.

Slab Plan Dimensions and the Corresponding Boundary Restraints. As previously shown (Chapter 3), no significant changes in stresses and deflections resulted, whether the 24-by-40 foot or 24-by-80 foot grid was solved with or without edge restraints. The slab size chosen for the sensitivity analysis was 24-by-40 feet with free edges.

Increment Length. A 12-inch increment length was used in both the longitudinal and transverse directions. This resulted in a 24-by-40 increment network, which was used in the analysis.

Case 1 - Loads on the Crack - SLAB Program Results

Maximum values of slab downward deflections and principal moments are shown in Tables 4 and 5, respectively.

The location of the maximum deflection was dependent on the relative magnitudes of the slab stiffness and the subgrade modulus. For the low level of stiffness, maximum deflection occurred 2 feet from the pavement edge, i.e., directly under the exterior 9,000-pound load. As stiffness increased, the maximum deflection was at the edge of the slab for low values of subgrade modulus. The effect of the subgrade was even more significant on high values of stiffness, as shown in Table 4, where the maximum deflection occurred at the pavement edge for the low and medium levels of the subgrade modulus. As far as the principal moments are concerned, the maximum value was always under the interior load, which was 8 feet from the pavement edge.

Effect of Crack Spacing. Transverse cracks in continuously reinforced concrete pavements occur randomly, and in most cases they extend the whole width of the pavement. One of the principles of the design of this pavement type is to provide sufficient reinforcement to keep the cracks tightly closed.

TABLE 4. MAXIMUM VALUES OF DOWNWARD DEFLECTION, INCHES (for 90 percent reduction in bending stiffness at cracks when loads are on the crack)

Modulus of subgrade reaction, lb/in²/in.	Crack Spacing, ft	Slab bending stiffness, (lb-in²)/in. 20×10^6	150×10^6	1125×10^6
40	4	0.0934	0.0490*	0.0248*
	6	0.0886	0.0485*	0.0246*
	8	0.0864	0.0475*	0.0245
	10	0.0859	0.0464*	0.0245*
200	4	0.0330	0.0166	0.0086*
	6	0.0321	0.0158	0.0085*
	8	0.0320	0.0153	0.0084*
	10	0.0320	0.0151	0.0083*
1000	4	0.0131	0.0057	0.0029
	6	0.0131	0.0055	0.0028
	8	0.0131	0.0054	0.0027
	10	0.0131	0.0054	0.0026

* Maximum deflection was at the pavement edge; otherwise it was under the load, 2 feet from the edge.

TABLE 5. MAXIMUM VALUES OF PRINCIPAL MOMENT,* LB-IN. PER UNIT WIDTH (for 90 percent reduction in bending stiffness at cracks when loads are on crack)

Modulus of subgrade reaction, lb/in²/in.	Crack Spacing, ft	Slab bending stiffness, (lb-in²)/in. 20×10^6	150×10^6	1125×10^6
40	4	2117	2384	2587
	6	2103	2374	2583
	8	2099	2364	2582
	10	2099	2357	2578
200	4	1839	2182	2430
	6	1835	2165	2423
	8	1835	2159	2413
	10	1835	2158	2406
1000	4	1436	1920	2240
	6	1436	1914	2223
	8	1436	1914	2215
	10	1436	1914	2213

* All values occurred 8 feet from the pavement edge.

In this work, as mentioned previously, it was assumed that a very slight curvature is needed to bring the two parts of the slab in touch and hence allow the transfer of bending.

In light of this behavior, the variation in maximum deflection with crack spacing and slab bending stiffness for a subgrade modulus of 40 pci is illustrated in Fig 22. A similar plot for maximum principal moment is shown in Fig 23. As noted, there is a slight change in both responses as the crack spacing increases over the range studied. However, it is worthwhile to note that these results were based on the same value of bending stiffness reduction at the crack location. As is demonstrated later in this study, as crack width increases, and hence the reduction in stiffness increases, the influence of crack spacing becomes more important. Similar results were obtained for the other levels of the modulus of subgrade reaction.

Effect of Modulus of Subgrade Reaction. Modulus of subgrade reaction, as defined by Westergaard and others, plays an important role in the evaluation of deflections and stresses in pavement slabs and plates resting on soils. In light of the very small effect of crack spacing, nine deflection values were determined by averaging the deflection values corresponding to the three levels of stiffness and the three levels of subgrade modulus. In other words, an average value of deflection was obtained corresponding to an average value of crack spacing.

Determining on the same basis the average values of maximum principal moment, the logarithmic influence of subgrade modulus on deflections and moments is illustrated in Figs 24 and 25. As shown, the effect of the subgrade modulus on deflection is higher than on principal moments. Slab deflection experiences an important and significant drop as subgrade modulus increases from low to medium levels. However, this deflection decrease tends to level off as the subgrade reaction exceeds the medium level and approaches the high side. This implies that for most purposes moderate values of subgrade modulus are quite satisfactory. Furthermore, there is about a 10 percent drop in the value of the principal moment as k varies from one level to another.

From this brief analysis and the variation in deflection with the radius of relative stiffness* ℓ (Fig 25), it can be shown that the contribution of

---

* Tabulated values of radius of relative stiffness ℓ for different pavement parameters are found in Appendix 5.

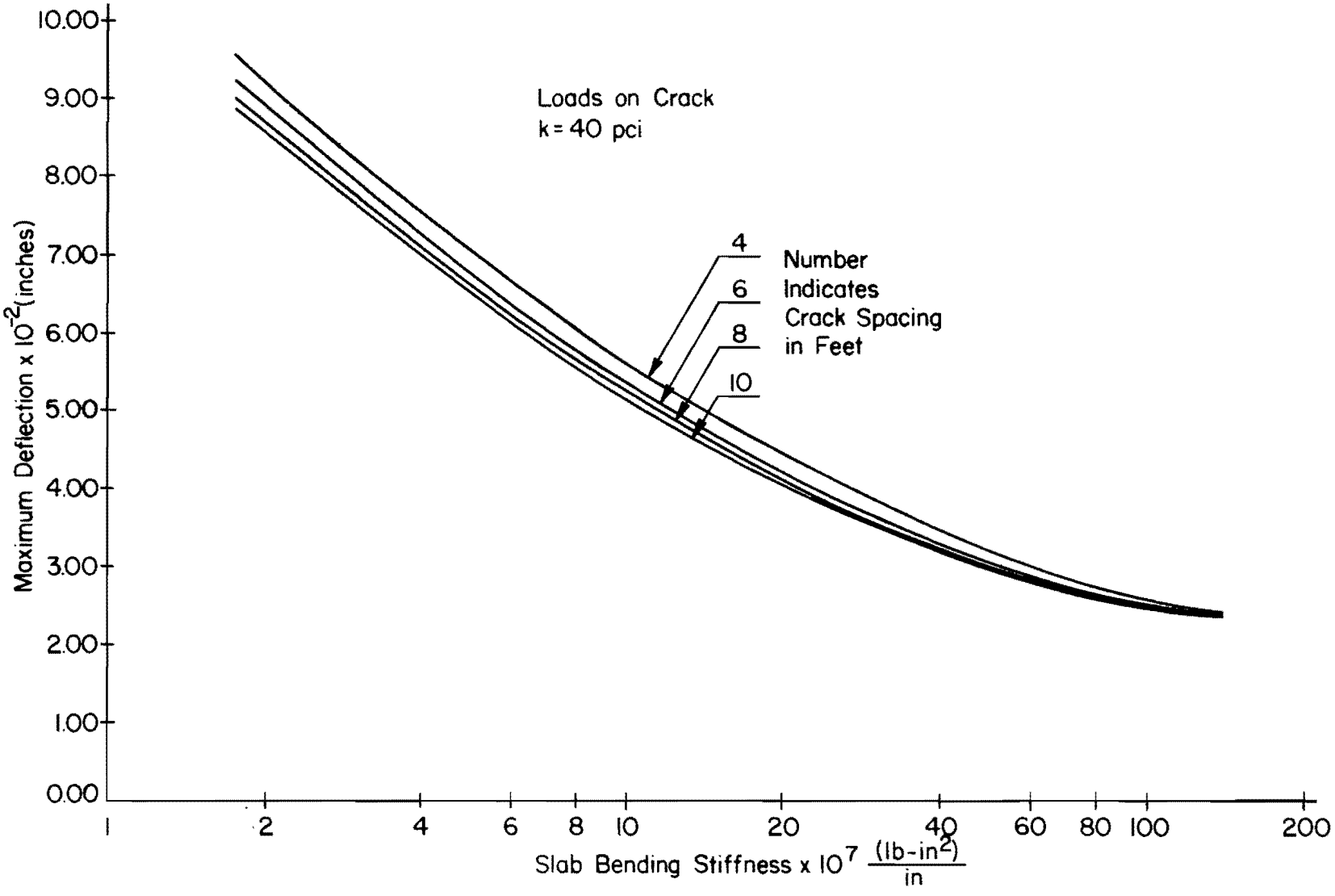

Fig 22. Effect of slab bending stiffness and crack spacing on maximum deflections for k = 40 pci.

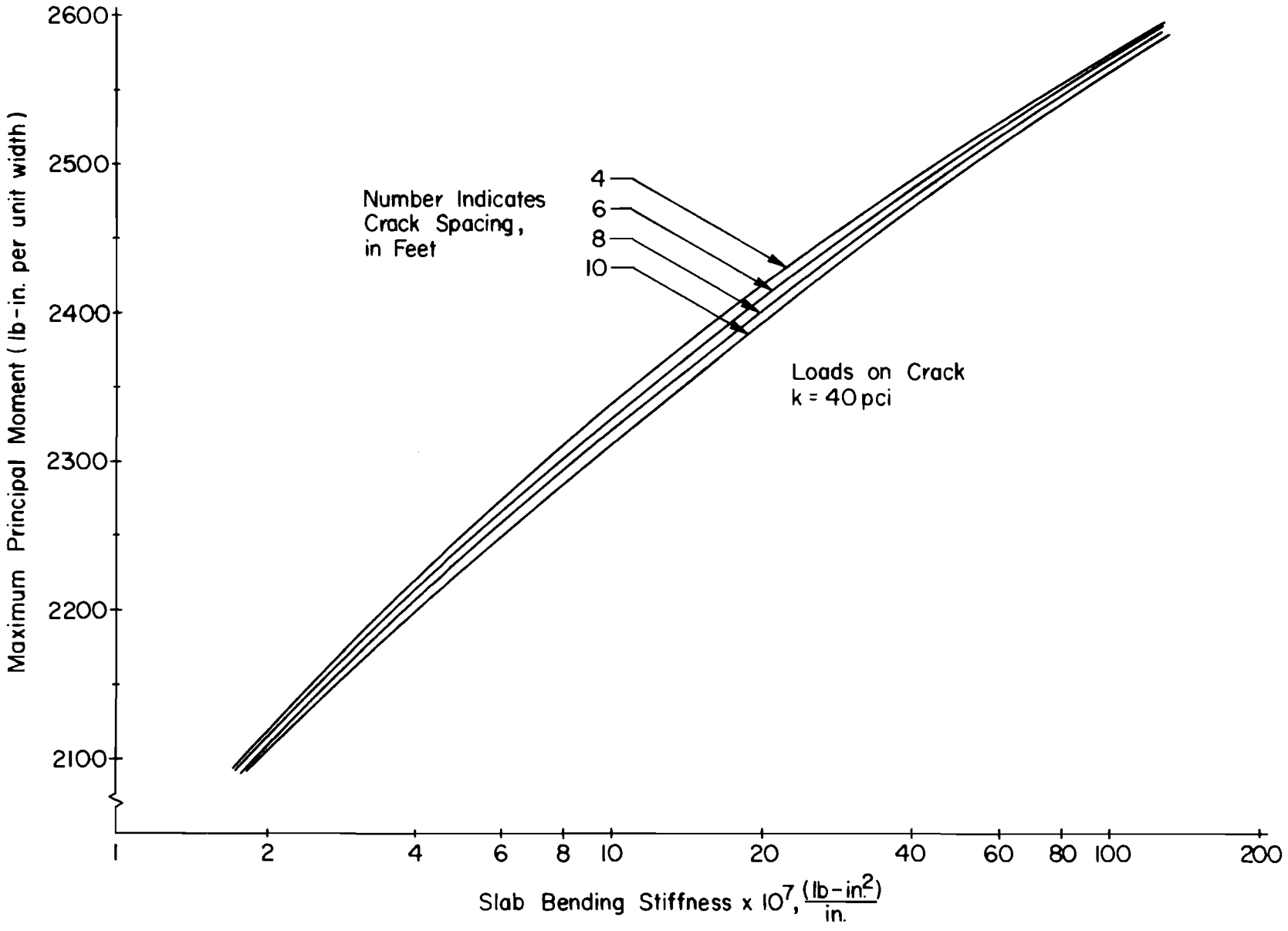

Fig 23. Effect of slab bending stiffness and crack spacing on maximum principal moment for k = 40 pci .

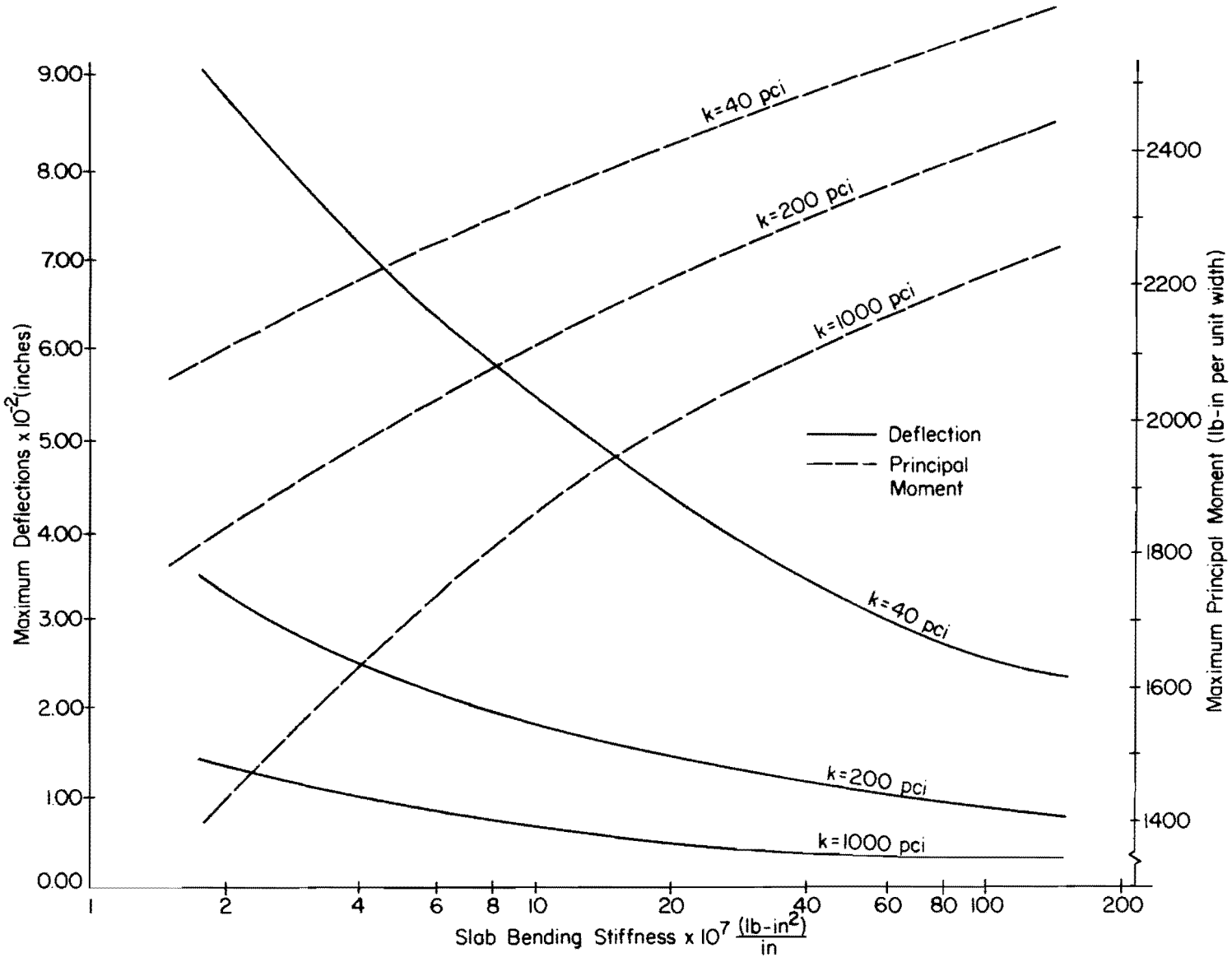

Fig 24. Influence of slab bending stiffness and subgrade modulus on maximum deflections and principal moments for the loads on the crack.

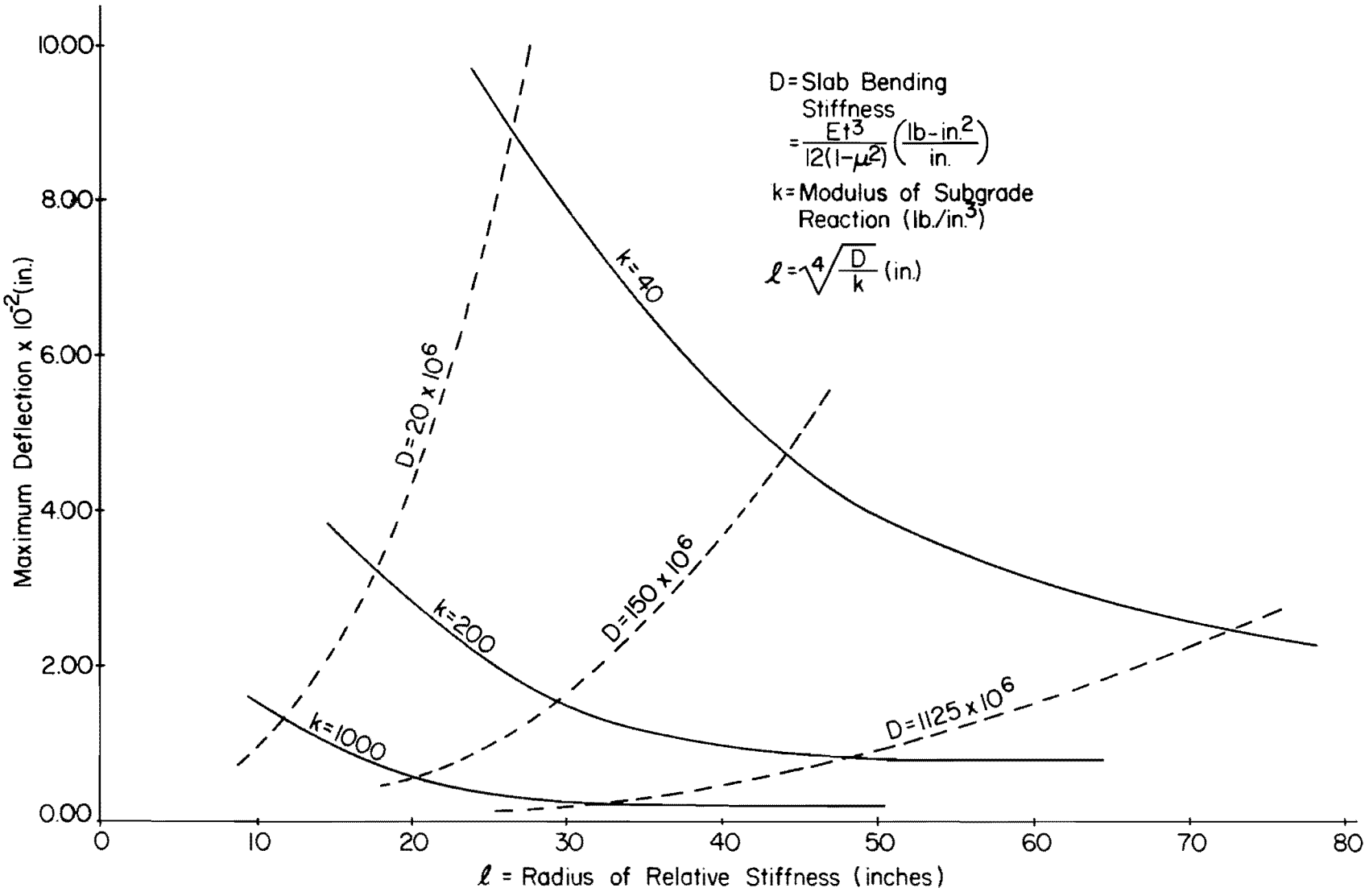

Fig 25. Variation of maximum deflection with the radius of relative stiffness for different values of D and k for loads on the crack.

subgrade modulus to changes in deflection is higher than the contribution of stiffness. This illustrates the important role that the subgrade modulus plays in the determination of slab deflection.

Effect of Slab Bending Stiffness. As mentioned previously, the slab bending stiffness per unit width is defined by $\frac{Et^3}{12(1-\mu^2)}$. Obviously the contribution of the thickness t to the magnitude of the stiffness term is more than the concrete modulus E.

The effect of bending stiffness on deflections and principal moments is illustrated in Figs 24 and 25. For the whole range of subgrade modulus, it can be seen that the influence of stiffness on principal moment is greater than on deflection. It is worthwhile to note that for low values of subgrade modulus, the decrease in deflection as stiffness increases is highly significant, and that as the subgrade modulus increases, the influence of stiffness levels off. The logarithmic effect of the stiffness term is shown in a way similar to that for subgrade modulus.

Case 2 - Loads Between Cracks - SLAB Program Results

In the case when the loads acted between cracks, the effect of crack spacing was higher than when the loads were on the crack. Except for this, results for these two load placements were quite similar. As expected, deflection values were lower for the case when the loads were between cracks, while higher values were obtained for principal moments.

Tables 6 and 7 show the maximum values of deflections and principal moments, respectively. Values of principal moment were 2 feet from the pavement edge for all ranges in the pavement design variables encountered. As was the case when the loads were on the crack, maximum deflection occurred either under the exterior load or at the pavement edge, depending on the relative values of the slab stiffness and the subgrade modulus. The effect of the subgrade modulus was more significant for the high values of stiffness.

Effect of Crack Spacing. The influence of slab stiffness and crack spacing on maximum deflections and principal moments for subgrade moduli of 40 and 200 pci is illustrated in Figs 26 and 27. The effect of crack spacing on deflections is slight or practically negligible, while changes in principal moment for the low and medium levels of k are quite considerable.

TABLE 6. MAXIMUM VALUES OF DOWNWARD DEFLECTION, INCHES (for 90 percent bending stiffness reduction at cracks when loads are between cracks)

Modulus of subgrade reaction, lb/in²/in.	Crack Spacing, ft	Slab bending stiffness, (lb-in²)/in. 20×10^6	150×10^6	1125×10^6
40	4	0.0606	0.0383*	0.0223*
	6	0.0589	0.0354*	0.0210*
	8	0.0600	0.0344*	0.0203*
	10	0.0604	0.0345*	0.0198*
200	4	0.0220	0.0109	0.0070*
	6	0.0225	0.0104	0.0064*
	8	0.0223	0.0105	0.0062*
	10	0.0220	0.0106	0.0062*
1000	4	0.0098	0.0038	0.0020*
	6	0.0097	0.0038	0.0019*
	8	0.0096	0.0038	0.0019*
	10	0.0096	0.0037	0.0019*

* Maximum deflection was at the pavement edge; otherwise it was under the load, 2 feet from the edge.

TABLE 7. MAXIMUM VALUES OF PRINCIPAL MOMENT,* LB-IN. PER UNIT WIDTH (for 90 percent bending stiffness reduction at cracks when loads are between cracks)

Modulus of subgrade reaction, lb/in²/in.	Crack Spacing, ft	Slab bending stiffness, (lb-in²)/in. 20×10^6	150×10^6	1125×10^6
40	4	2239	2791	3585
	6	2406	3049	3901
	8	2427	3226	4130
	10	2391	3320	4297
200	4	1826	2338	2940
	6	1898	2541	3206
	8	1853	2603	3398
	10	1835	2581	3518
1000	4	1444	1993	2441
	6	1401	2037	2666
	8	1395	1992	2767
	10	1396	1962	2771

* All values occurred 2 feet from pavement edge.

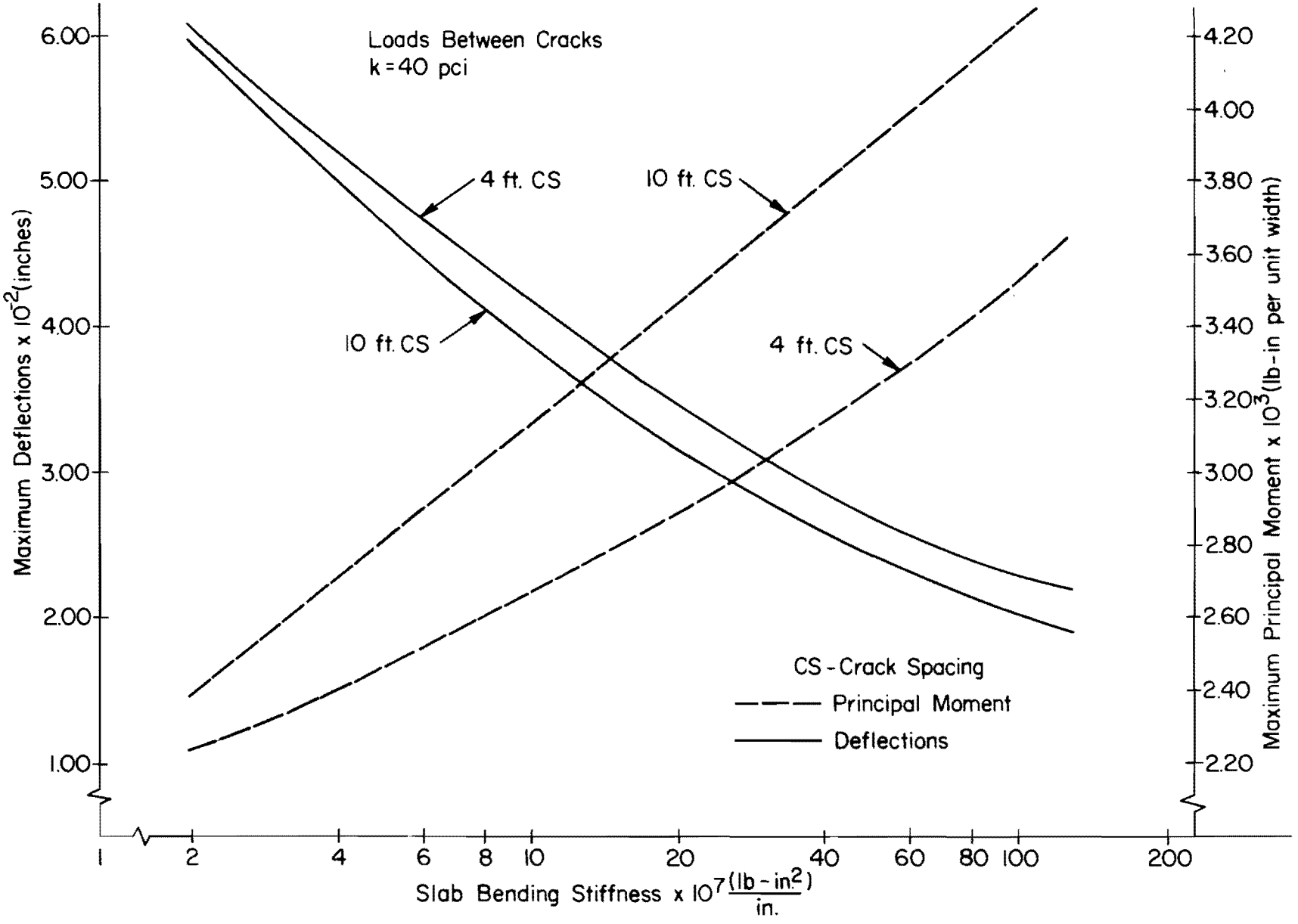

Fig 26. Effect of slab bending stiffness and crack spacing on deflections and principal moments for k = 40 pci .

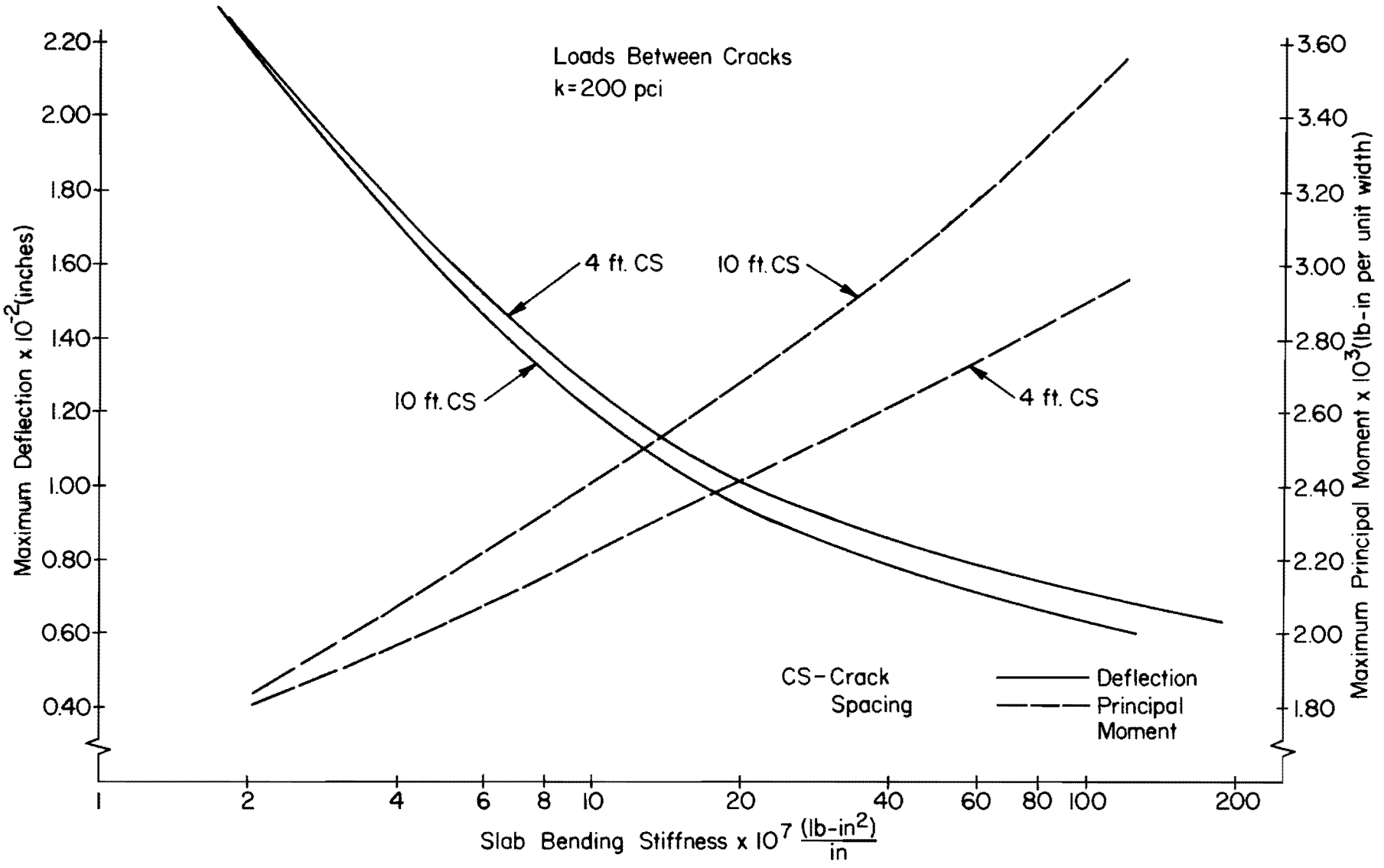

Fig 27. Effect of slab bending stiffness and crack spacing on deflections and principal moments for k = 200 pci .

Furthermore, this change in principal moment due to the spacing of the cracks increases with an increase in stiffness. The percent increase in the maximum moment between the 10 and 4-foot crack spacing (based on the 10-foot value) is about 18 percent. By comparing Figs 26 and 27, it can be seen that this percentage increase in the moment drops as k increases.

For both load placements studied (loads on and between cracks), the general trend in the magnitude of deflection is a decrease as crack spacing increases over the range studied (4 to 10 feet). This agrees fairly well with deflections measured by the Texas Highway Department. Figure 28 (after Ref 25) shows the variation of measured deflection with crack spacing. Up to the range in crack spacing investigated in this research, calculated and measured deflections agree closely. Obviously, as crack spacing increases there is a greater loss of load transfer across the discontinuities since crack width increases. This, in some cases, will cause an increase in deflection, as shown in Fig 28.

Effect of Subgrade Modulus and Bending Stiffness. For the purpose of demonstrating the effect of bending stiffness and subgrade modulus, average values of deflections and principal moments are shown in Fig 29. A similar plot (Fig 30) shows deflection variation with the radius of relative stiffness.

The essential importance of the subgrade modulus in determining the amount of slab deflection is very well illustrated. Similar to the case where the loads are on the crack, the rate of change in deflections decreases as the subgrade modulus increases. About a 20 percent drop is experienced in the magnitude of the principal moment as k increases from one level to the next.

While the subgrade modulus shows a higher contribution in the determination of deflection than principal moment, slab bending stiffness possesses a contrasting effect except for its effect on deflections for low values of subgrade modulus. Again, the logarithmic effect of stiffness as well as subgrade modulus is demonstrated.

Analysis of Variance (ANOVA)

To determine the sensitivity of the rigid pavement design variables, an analysis of variance was made on the maximum values of deflections and principal moments for both load positions. The analysis of variance considered the

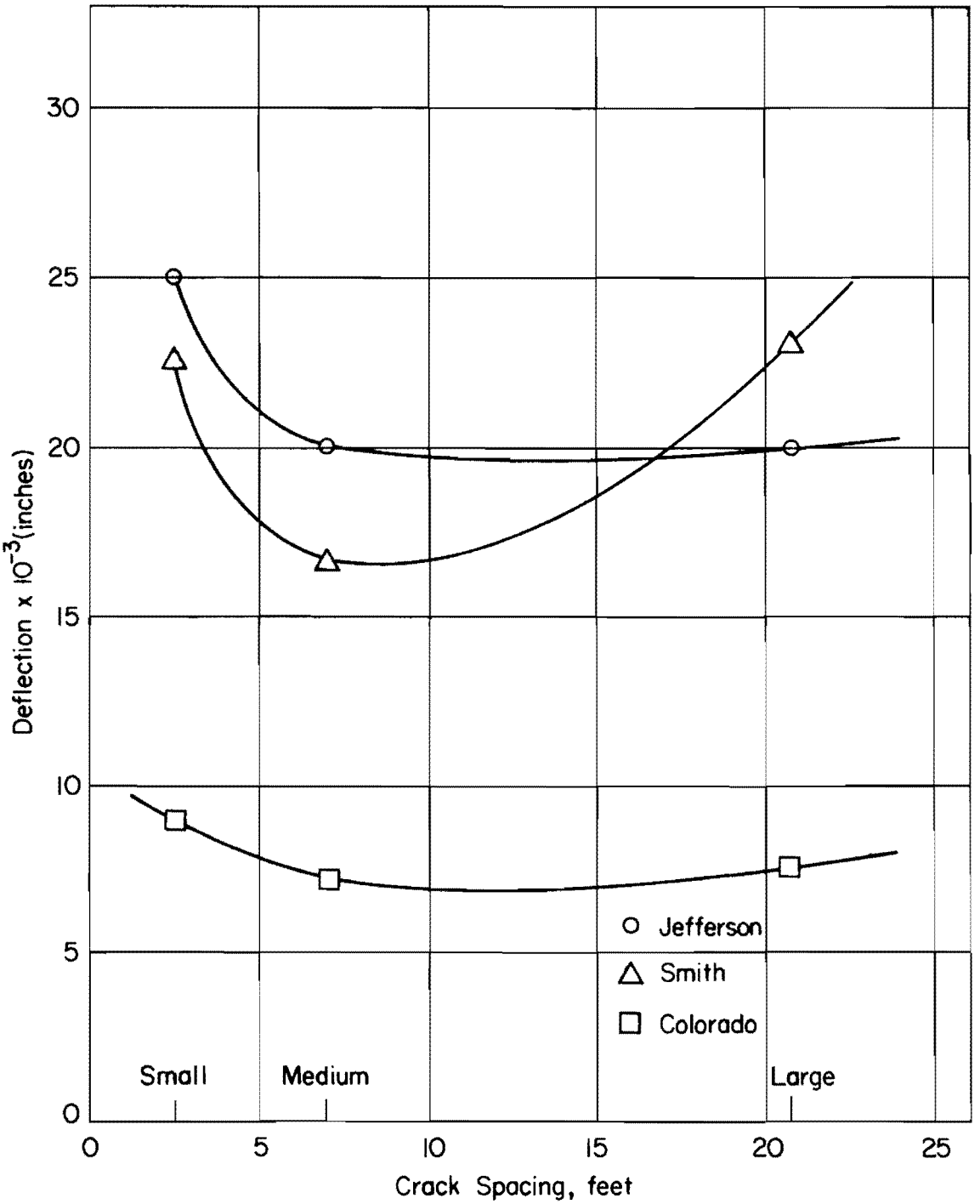

Fig 28. Variation of measured deflections with crack spacing (after Ref 25).

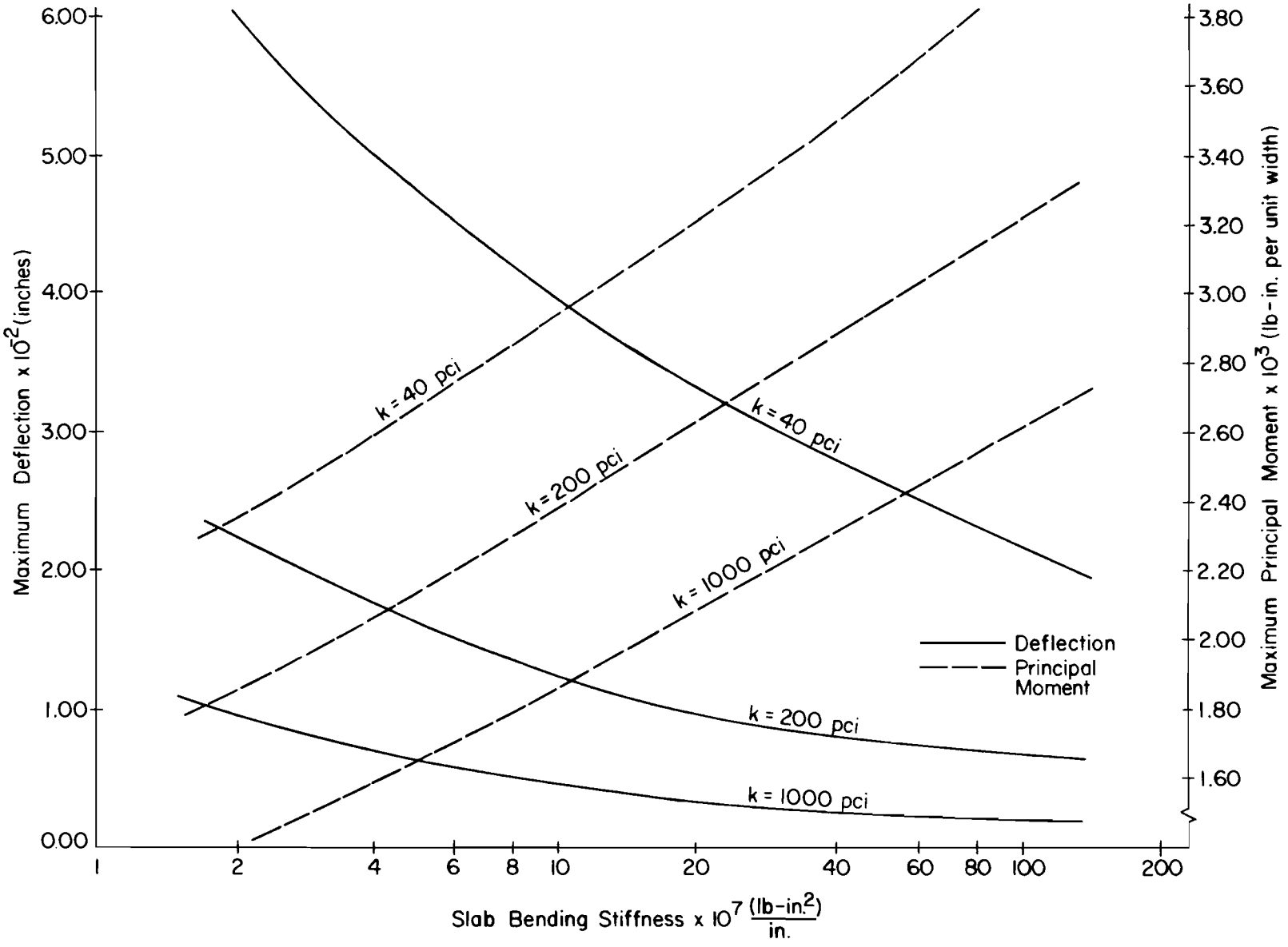

Fig 29. Influence of slab bending stiffness and subgrade modulus on maximum deflections and principal moments for the loads between cracks.

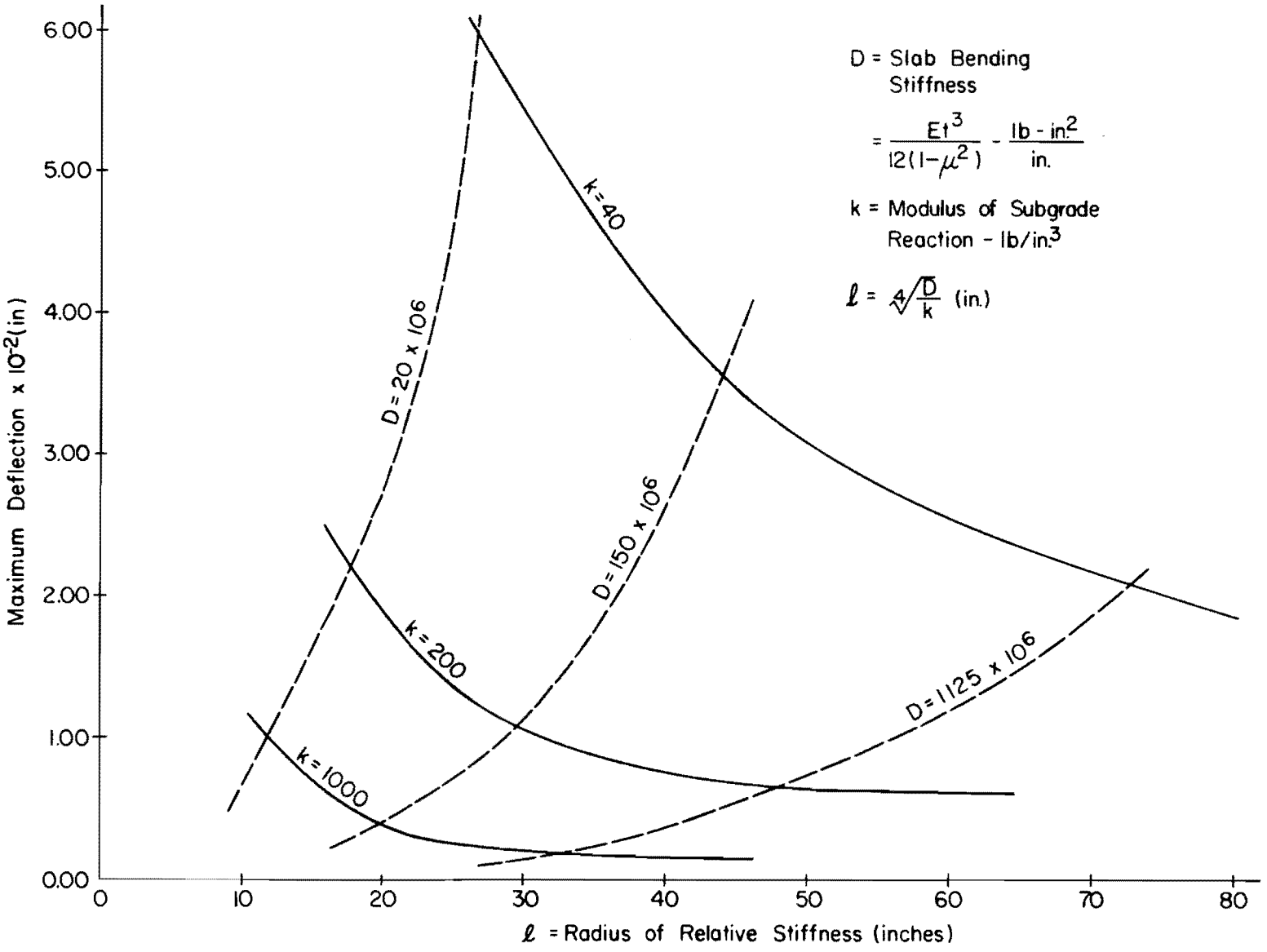

Fig 30. Variation of maximum deflection with the radius of relative stiffness for various levels of D and k for loads between cracks.

three design variables encountered, namely, slab bending stiffness, crack spacing, and subgrade modulus.

Tables 8(a) and (b) show the average contribution of the main effects of each variable and their interactions on deflections and principal moments for the loads on the crack. For the levels given to subgrade modulus, slab bending stiffness, and crack spacing, the highest average contribution in the variation in deflections (58.88 percent) was due to the main effect of the subgrade modulus. Next were bending stiffness, which accounted for 27.74 percent of the variation, and interaction of subgrade modulus and stiffness ($k \times D$), which accounted for 13.26 percent. The amount that the crack spacing contributed was negligible.

For the variation of principal moment, the main effect of slab stiffness was the largest (59.35 percent), and the main effect of the subgrade modulus was next. The effect of crack spacing was slight.

Results of the analysis of variance for the loads between cracks were similar to the case when loads were on the crack (Table 9). It is worthwhile to note that the effect of crack spacing was higher when loads were between cracks. However, over the whole range of the variables studied, neither the main effect of crack spacing nor its interaction with either k and/or D was highly significant.

ANOVA - Orthogonal Polynomial Breakdown

In a design experiment where the levels of factors are quantitative, it is often possible to extract more information on how the response variable might vary with the changing levels of the quantitative factor; e.g., how deflection varies with the modulus of subgrade reaction and whether or not there is a linear relationship between subgrade modulus and deflection.

The use of orthogonal polynomials makes the analysis rather simple, provided the experiment is designed with equispaced quantitative levels. In the design experiment studied (Table 2), the levels of slab stiffness, as well as subgrade modulus, are equispaced logarithmically. That is, each level is obtained from the preceding one by a constant multiplier, which means that the levels progress geometrically. The multiplier was 7.5 for slab stiffness, and 5.0 for subgrade modulus. The levels of crack spacing are also equispaced but constitute an arithmatic progression.

TABLE 8. GENERAL ANALYSIS OF VARIANCE FOR LOADS ON CRACK

(a) Maximum Deflections

Source of Variation	Degrees of Freedom	Sum of Squares $\times 10^3$	Mean of Squares $\times 10^3$	Average Contribution* in percent
Log (subgrade modulus), log k	2	14.089	7.045	58.88
Crack spacing, CS	3	0.012	0.004	0.05
Log (bending stiffness), log D	2	6.637	3.318	27.74
Log k × CS interaction	6	0.010	0.001	0.04
Log k × log D interaction	4	3.173	0.793	13.26
CS × log D interaction	6	0.007	0.001	0.03
Log k × CS × log D interaction	12	-	-	-
Total	35	23.930	-	100.00

(b) Maximum Principal Moments

Source of Variation	Degrees of Freedom	Sum of Squares $\times 10^{-3}$	Mean of Squares $\times 10^{-3}$	Average Contribution* in percent
Log (subgrade modulus), log k	2	1459.43	729.71	37.84
Crack spacing, CS	3	1.16	0.39	0.03
Log (bending stiffness), log D	2	2288.75	1144.38	59.35
Log k × CS interaction	6	0.20	0.03	-
Log k × log D interaction	4	105.68	26.42	2.74
CS × log D interaction	6	0.28	0.04	-
Log k × CS × log D interaction	12	0.59	0.04	-
Total	35	3856.03	-	99.96

* Based on sum of squares.

TABLE 9. GENERAL ANALYSIS OF VARIANCE FOR LOADS BETWEEN CRACKS

(a) Maximum Deflections

Source of Variation	Degrees of Freedom	Sum of Squares $\times 10^{3}$	Mean of Squares $\times 10^{3}$	Average Contribution* in percent
Log (subgrade modulus), log k	2	7.473	3.736	66.37
Crack spacing, CS	3	0.004	0.001	0.03
Log (bending stiffness), log D	2	2.705	1.352	24.04
Log k × CS interaction	6	0.006	0.001	0.05
Log k × log D interaction	4	1.069	0.267	9.50
CS × log D interaction	6	0.002	-	0.01
Log k × CS × log D interaction	12	-	-	-
Total	35	11.259	-	100.00

(b) Maximum Principal Moments

Source of Variation	Degrees of Freedom	Sum of Squares $\times 10^{-3}$	Mean of Squares $\times 10^{-3}$	Average Contribution* in percent
Log (subgrade modulus), log k	2	7599.56	3799.78	36.82
Crack spacing, CS	3	384.46	128.15	1.86
Log (bending stiffness), log D	2	12121.70	6060.87	58.73
Log k × CS interaction	6	123.98	20.66	0.60
Log k × log D interaction	4	133.45	33.36	0.65
CS × log D interaction	6	239.32	39.87	1.16
Log k × CS × log D interaction	12	36.02	3.00	0.18
Total	35	20638.52	-	100.00

* Based on sum of squares.

Loads on the Crack. Table 10(a) shows the ANOVA orthogonal breakdown for for the deflection response for loads on the crack. In tabulating the orthogonal breakdown, effects which contributed less than 1 percent in response variation were neglected.

It is worthwhile to note that the levels of subgrade modulus are equispaced in the logarithm and that the linear effect refers to the deflection variation associated with log k and not k . Likewise, the quadratic effect is associated with $(\log k)^2$. Similar statements can be made concerning the stiffness term.

General ANOVA in Table 8(a) shows that the average contribution of subgrade modulus to deflection was 58.88 percent. When this total effect is broken into its linear and quadratic log portions, it is seen that 54.40 percent of the deflection variation was due to the log linear effect and only 4.48 percent to the quadratic effect. In addition, the log linear effect of stiffness and the log linear interaction of k and D explain a substantial amount of the deflection response.

In the case of principal moments shown in Table 10(b), the logarithmic linear effects of stiffness and subgrade modulus contributed around 97 percent. None of the quadratic log effects entered into the picture, and the first order interaction of D and k was not so high as in the deflection case.

Loads Between Cracks. Similar results were obtained for the case with loads between cracks. Table 11 illustrates the orthogonal breakdown of the pavement variables for deflections and principal moments. In both deflection and principal moment responses for loads on the crack, the effect of crack spacing was less than 1 percent, but this was true only for the deflection response when the loads were between cracks; on principal moments, the linear effect of crack spacing was 1.68 percent of the total contribution, which still is not highly significant.

Comparison of Deflections for Loads at and Between Cracks

For the range of CRC pavement variables investigated in this study, deflections resulting from loads on the crack were higher than those from loads between cracks. Figures 31 and 32 show measured deflections (after Ref 16) and those calculated by the discrete-element method. In most cases, the measured value of the cracked sections was higher than that for the uncracked, which agrees fairly well with the calculated deflection. It is worthwhile to

TABLE 10. ANOVA ORTHOGONAL POLYNOMIAL BREAKDOWN FOR LOADS ON CRACK

(a) Maximum Deflections

Source of Variation	Degrees of Freedom	Sum of Squares $\times 10^3$	Mean of Squares $\times 10^3$	Contribution in percent
Log (subgrade modulus), log k	2	14.089		
Linear	1	13.016	13.016	54.40
Quadratic	1	1.073	1.073	4.48
Log (bending stiffness), log D	2	6.637		
Linear	1	6.415	6.415	26.77
Log k x log D interaction	4	3.173		
Linear x Linear	1	2.881	2.881	12.02
Linear x Quadratic	1	0.238	0.238	1.00
Residual	30	0.319	0.011	1.33
Total	35	23.942	23.634	100.00

(b) Maximum Principal Moments

Source of Variation	Degrees of Freedom	Sum of Squares $\times 10^{-3}$	Mean of Squares $\times 10^{-3}$	Contribution in percent
Log (subgrade modulus), log k	2	1459.43		
Linear	1	1448.94	1448.94	37.57
Log (bending stiffness), log D	2	2288.75		
Linear	1	2269.96	2269.96	58.87
Log k x log D interaction	4	105.68		
Linear x Linear	1	96.25	96.25	2.50
Residual	32	40.88	1.28	1.06
Total	35	3856.03	3816.43	100.00

TABLE 11. ANOVA ORTHOGONAL POLYNOMIAL BREAKDOWN FOR LOADS BETWEEN CRACKS

(a) Maximum Deflections

Source of Variation	Degrees of Freedom	Sum of Squares $\times 10^3$	Mean of Squares $\times 10^3$	Contribution in percent
Log (subgrade modulus), log k	2	7.473		
Linear	1	6.837	6.837	60.72
Quadratic	1	0.636	0.636	5.60
Log (bending stiffness), log D	2	2.705		
Linear	1	2.606	2.606	23.17
Log k × log D interaction	4	1.069		
Linear × Linear	1	0.981	0.981	8.70
Residual	31	0.203	0.006	1.81
Total	35	11.263	11.066	100.00

(b) Maximum Principal Moments

Source of Variation	Degrees of Freedom	Sum of Squares $\times 10^{-3}$	Mean of Squares $\times 10^{-3}$	Contribution in percent
Log (subgrade modulus), log k	2	7599.56		
Linear	1	7590.38	7590.38	36.77
Crack spacing, CS	4	384.46		
Linear	1	346.55	346.55	1.68
Log (bending stiffness), log D	2	12121.70		
Linear	1	12096.98	12096.98	58.62
Residual	32	604.61	18.89	2.93
Total	35	20638.52	20052.80	100.00

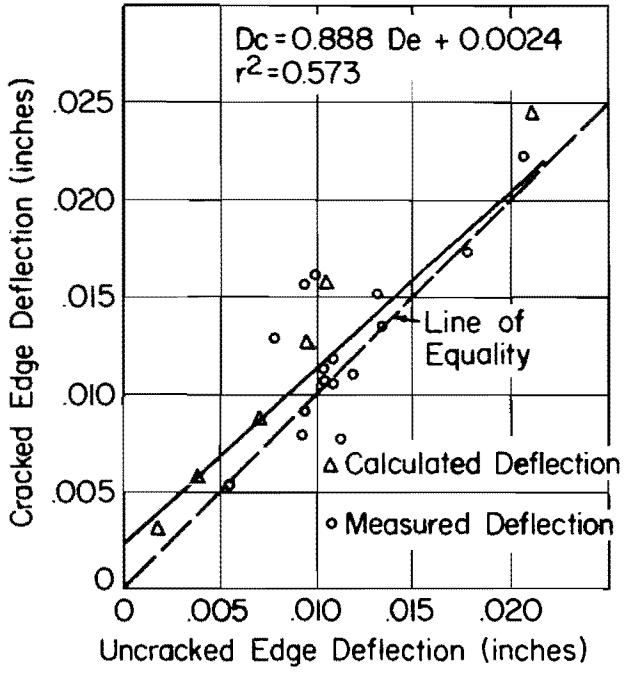

Fig 31. Cracked edge versus uncracked edge deflection - Fall (after Ref 16).

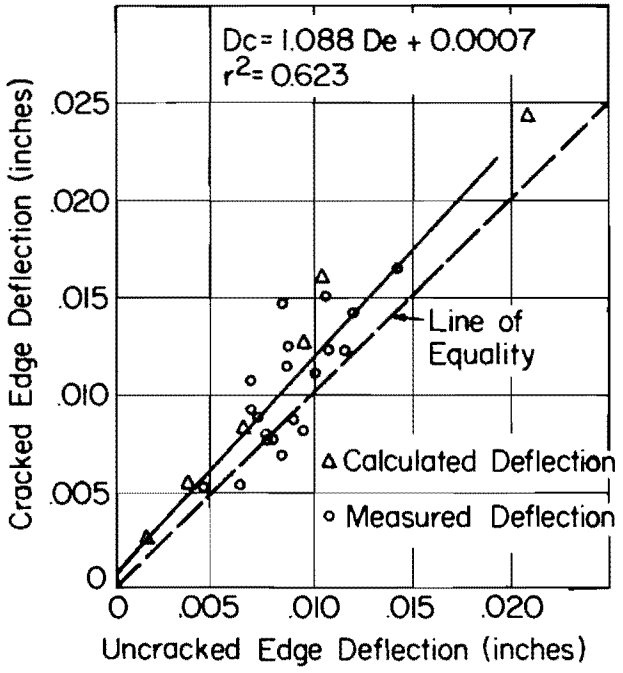

Fig 32. Cracked edge versus uncracked edge deflection - Winter (after Ref 16).

note that due to seasonal variations, load transfer across the joints varies, while the calculated values were obtained for a constant value of bending stiffness reduction at crack locations.

Comparison Between 90 Percent Stiffness Reduction and Full Slab

The effect of crack formation on structural members is an increase in the flexibility of the system. Generally this will produce an increase in deflections and a decrease in moments or stresses. Since no contraction joints are provided in continuously reinforced concrete pavements, volume-change stresses will cause random transverse cracks to develop. The influence of these transverse cracks on maximum deflection and principal moments is demonstrated in Figs 33 and 34.

Values of maximum deflections and principal moments for the full slab case are shown in Table 12. These results were compared with those of the 90 percent reduction in bending stiffness at the cracks for the two load placements. For low and medium levels of subgrade modulus, the increase in deflection when loads are on cracks is quite significant. This indicates the detrimental effect of these transverse discontinuities on the pavement slab. It is worthwhile to note that the difference in principal moments between the cracked and uncracked slab increases as the relative stiffness of the slab to that of the subgrade increases.

Comparison Between 90 and 100 Percent Reduction (Hinge) in Bending Stiffness

In this study the cracks were analyzed as if they were completely closed. Deformations in the slab are thus resisted by some degree of moment transfer across the cracks as is customary in normal structural concrete analysis (Fig 7). In practice, however, slabs have crack openings of a finite width which varies primarily due to volume changes. Considering these finite crack widths would thus involve the nonlinear relationship of no bending resistance until the crack closes at the top at which time some bending resistance would then be felt. In this section, however, comparisons of deflections and principal moments are made between the two extreme cases: partial (closed crack) and zero (open crack) bending transfer across the transverse discontinuities.

Values of deflections and principal moments for the hinge case when the loads are on the crack are shown in Tables 13 and 14, respectively. A graphic

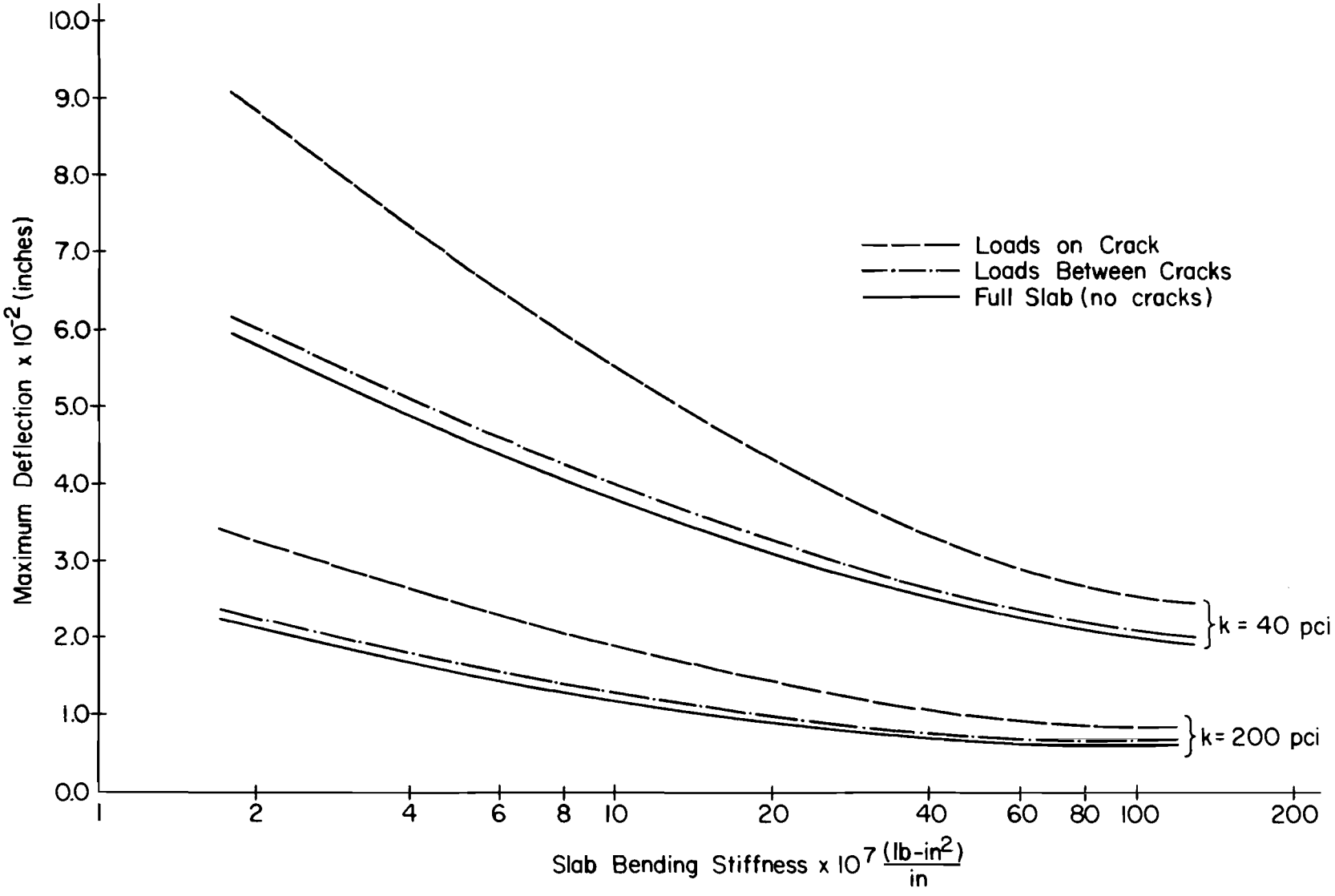

Fig 33. Influence of bending stiffness and subgrade modulus on deflection for the cracked and full (uncracked) slab.

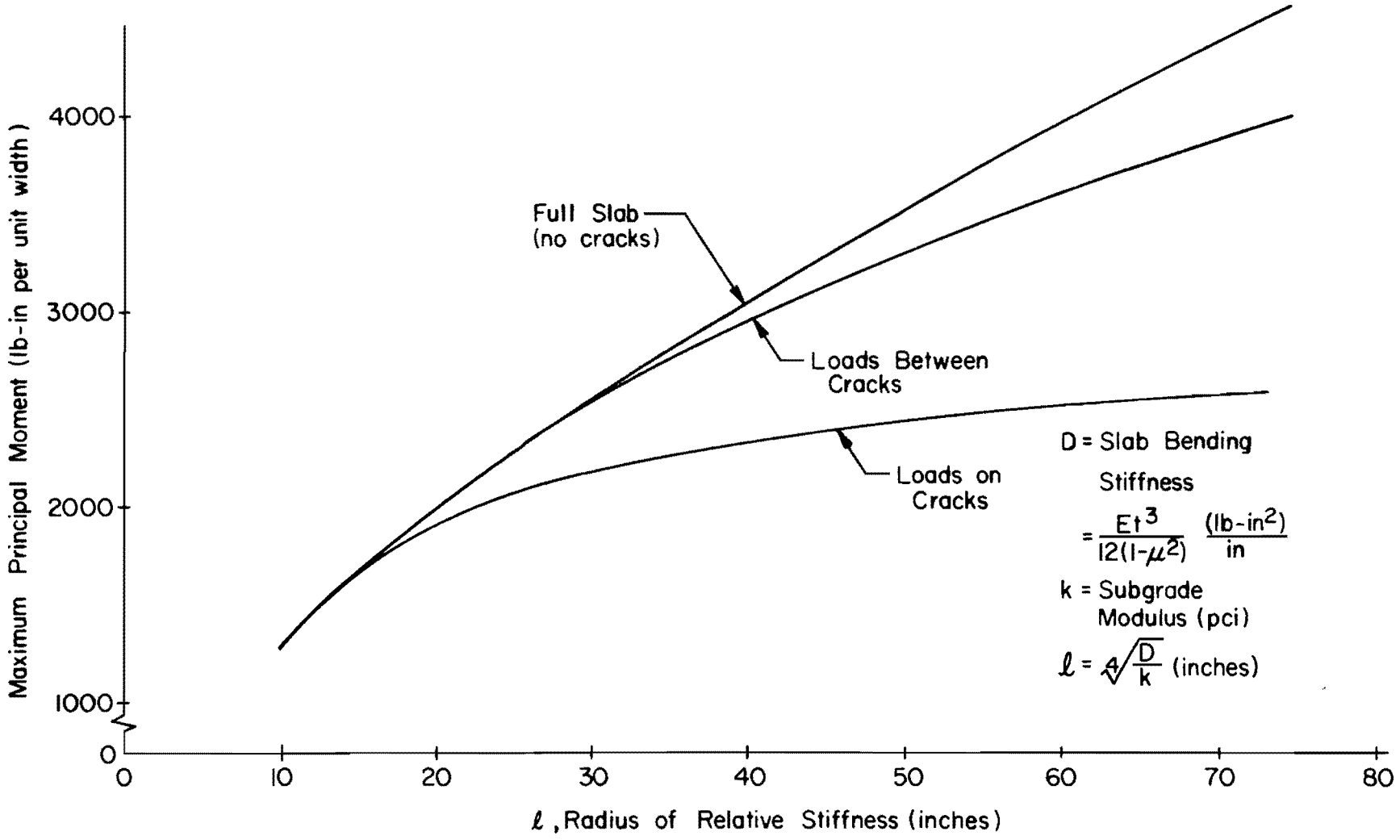

Fig 34. Influence of radius of relative stiffness on principal moments for cracked and uncracked slab for loading as shown in Fig 3.

TABLE 12. MAXIMUM VALUES OF DOWNWARD DEFLECTIONS AND PRINCIPAL MOMENTS (for the uncracked slab)

Modulus of Subgrade Reaction, lb/in²/in \ Slab Bending Stiffness, (lb-in²)/in	20×10^6	150×10^6	1125×10^6
40	0.0582*	0.0340	0.0196
	2336**	3233	4491
200	0.0217	0.0103	0.0612
	1836	2501	3462
1000	0.0096	0.0036	0.0018
	1397	1956	2671

* Deflection, inches

** Principal moments, lb-in per unit width

TABLE 13. VALUES OF MAXIMUM DEFLECTION, INCHES (for 100 percent bending stiffness reduction at cracks when loads are on the crack)

Modulus of subgrade reaction, lb/in²/in.	Crack Spacing, ft	Slab bending stiffness, (lb-in²)/in. 20×10^6	150×10^6	1125×10^6
40	4	0.1277	0.0905*	0.0643*
	6	0.1087	0.0741*	0.0515*
	8	0.1036	0.0671*	0.0438*
	10	0.1030	0.0598*	0.0388*
200	4	0.0380	0.0246	0.0176*
	6	0.0362	0.0202	0.0141*
	8	0.0362	0.0188	0.0121*
	10	0.0362	0.0185	0.0111*
1000	4	0.0139	0.0068	0.0046
	6	0.0139	0.0063	0.0037
	8	0.0139	0.0063	0.0034
	10	0.0139	0.0063	0.0033

* Maximum deflection was at the pavement edge; otherwise it was under the load, 2 feet from the edge.

TABLE 14. VALUES OF MAXIMUM PRINCIPAL MOMENT,* LB-IN PER UNIT WIDTH (for 100 percent bending stiffness reduction at cracks when loads are on the crack)

Modulus of subgrade reaction, lb/in²/in.	Crack Spacing, ft	Slab bending stiffness, (lb-in²)/in. 20×10^6	150×10^6	1125×10^6
40	4	2096	2354	2554
	6	2083	2331	2543
	8	2079	2318	2535
	10	2078	2312	2532
200	4	1838	2156	2402
	6	1834	2138	2380
	8	1834	2132	2365
	10	1834	2131	2358
1000	4	1438	1916	2211
	6	1438	1909	2190
	8	1438	1909	2182
	10	1438	1909	2180

* All values occurred 8 feet from pavement edge.

representation is used to compare the ratios of deflections and principal moments in the hinge case with those in the 90 percent reduction case.

Figure 35 demonstrates the change in deflections (expressed as a ratio of the values for the 100 to the 90 percent reductions) with the change in radius of relative stiffness for different crack spacing patterns for loads on the crack. It is seen that for high values of the radius of relative stiffness, as crack spacing decreases, changes in maximum deflections are highly significant. Obviously, this will emphasize the effect of the width of the crack on the behavior of the pavement structure. Deflections increase at a significant rate as the crack width increases. Hence, crack width should be given special consideration and narrow cracks are indeed the desirable objective for successful performance of a continuously reinforced concrete pavement.

No significant difference in principal moments was evident between the 100 and 90 percent reductions when the loads were acting on the cracks. The same thing applies to deflections when loads were acting between cracks (Tables 6 and 15). Comparing the values of principal moment for the loads between cracks (Tables 7 and 16), certain differences resulted for high values of radius of relative stiffness (Fig 36). The ratio of the two moment values approaches unity as crack spacing increases, and practically no difference is encountered in the range of 8 to 10 feet.

Therefore, the structural behavior of CRC pavement shows that crack width has a very important effect on the performance of such pavement. Due to the volume changes in the concrete mix, there is a direct relationship between the crack width and crack spacing. As crack spacing increases, crack width increases, and in turn causes significant changes in the pavement structure. Deflections increase at a high rate as crack width increases, causing several modes of distress. Furthermore, as illustrated in Fig 36, no significant drop is encountered in the principal moments between the partial and hinge cases for the 8 and 10-foot crack spacing.

Discussion of Results

Transverse cracks are characteristic of continuously reinforced concrete pavements and significantly influence the behavior and performance of this pavement type. Comparison between the cracked and uncracked slab (Figs 33 and 34) indicates that when loads were on the crack, there was a substantial increase in slab deflections, while the drop in principal moment that occurred

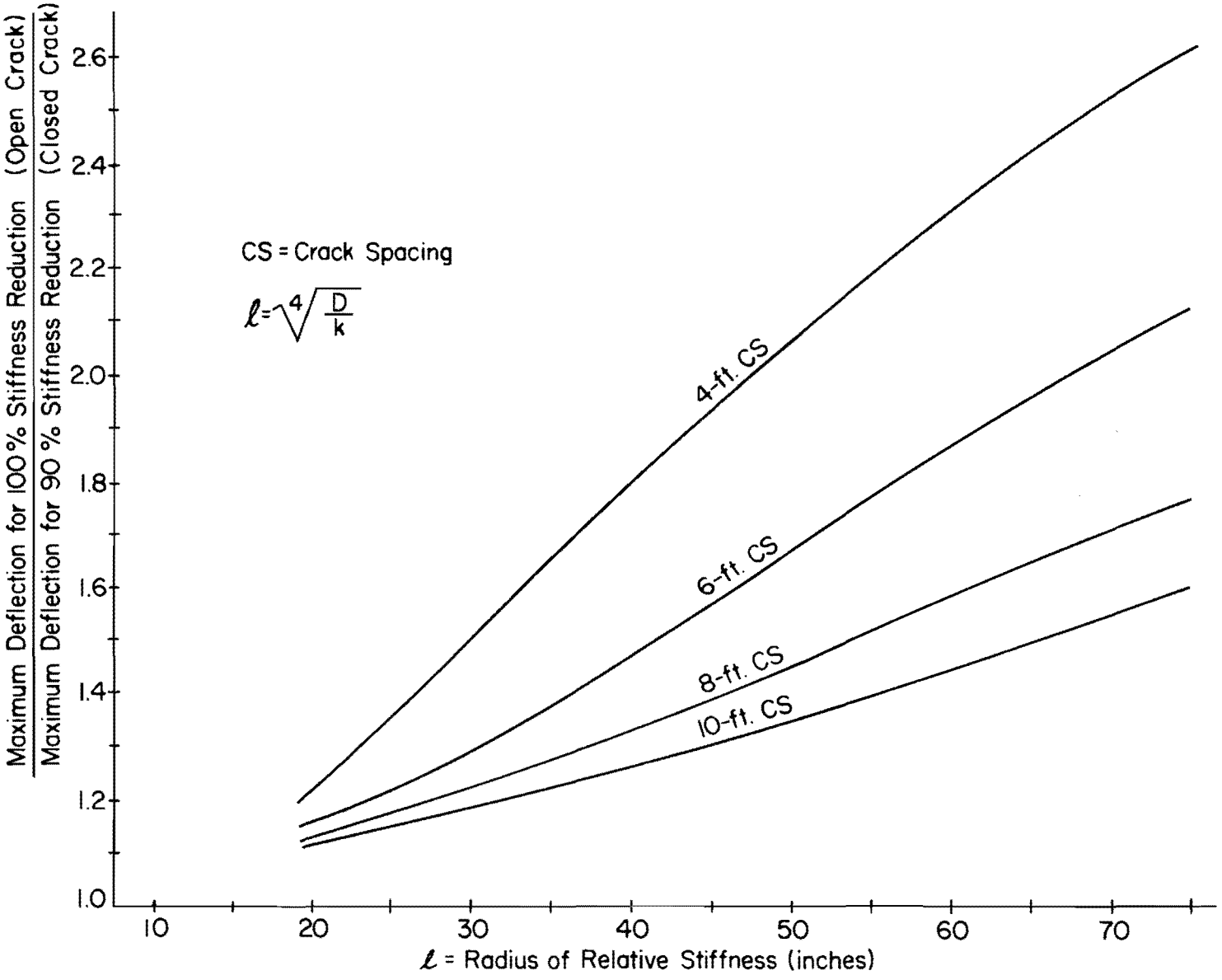

Fig 35. Comparison of maximum deflection between the 100 and 90 percent reduction in bending stiffness at crack locations for loads on the crack.

TABLE 15. VALUES OF MAXIMUM DEFLECTION, INCHES (for 100 percent bending stiffness reduction at cracks when loads are between cracks)

Modulus of subgrade reaction, lb/in²/in.	Crack Spacing, ft	Slab bending stiffness, (lb-in²)/in. 20 x 10^6	150 x 10^6	1125 x 10^6
40	4	0.0626	0.0457*	0.0330*
	6	0.0594	0.0375*	0.0261*
	8	0.0613	0.0349*	0.0225*
	10	0.0619	0.0350*	0.0207*
200	4	0.0221	0.0116	0.0087*
	6	0.0228	0.0105	0.0070*
	8	0.0226	0.0107	0.0064*
	10	0.0221	0.0109	0.0063*
1000	4	0.0099	0.0037	0.0022*
	6	0.0097	0.0038	0.0019*
	8	0.0096	0.0038	0.0019*
	10	0.0096	0.0038	0.0020*

* Maximum deflection was at the pavement edge; otherwise it was under the load, 2 feet from the edge.

TABLE 16. VALUES OF MAXIMUM PRINCIPAL MOMENT,* LB-IN PER UNIT WIDTH (for 100 percent bending stiffness reduction at cracks when loads are between cracks)

Modulus of subgrade reaction, lb/in²/in.	Crack Spacing, ft	Slab bending stiffness, (lb-in²)/in. 20 x 10^6	150 x 10^6	1125 x 10^6
40	4	2159	2311	2430
	6	2446	2828	3042
	8	2487	3198	3558
	10	2427	3398	3971
200	4	1919	2196	2332
	6	1925	2561	2876
	8	1861	2676	3294
	10	1834	2641	3560
1000	4	1458	2005	2226
	6	1402	2077	2647
	8	1394	2010	2840
	10	1396	1964	2852

* All values occurred 2 feet from the pavement edge.

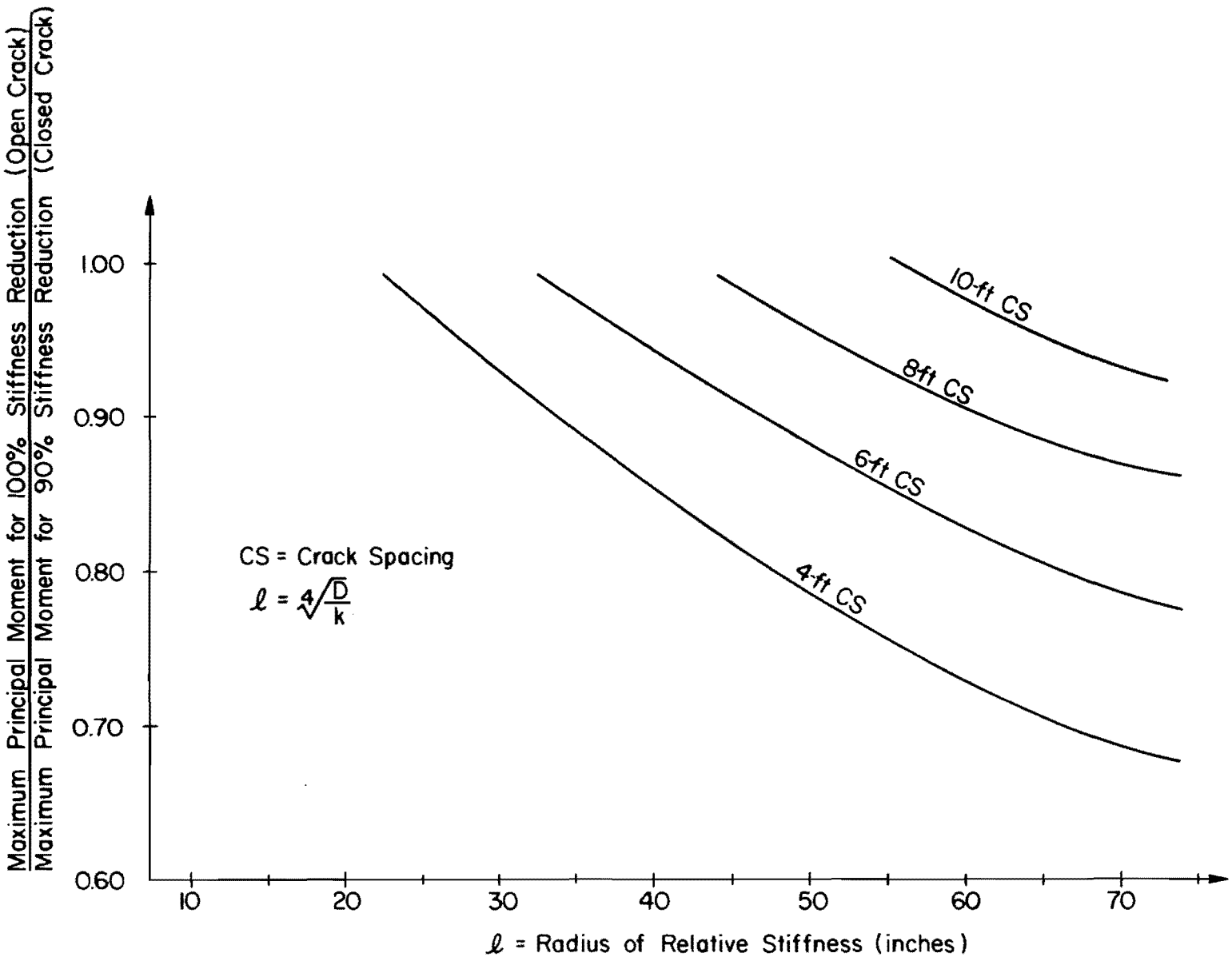

Fig 36. Comparison of maximum principal moment between the 100 and 90 percent reduction in bending stiffness at crack locations for loads between cracks.

for loads between cracks was not highly significant. This illustrates the detrimental effects of these transverse discontinuities on the pavement structure.

According to SLAB program results, the modulus of subgrade reaction, as defined by Westergaard and others, plays an important role in the determination of deflections and principal moments (Figs 24 through 30). Pavement deflections decrease at a significant rate as subgrade modulus increases. Furthermore, there is about a 10 percent decrease in the value of principal moment as k varies from one level to the next when loads are on the crack, and about a 20 percent decrease for the case when loads are between cracks.

While the subgrade modulus showed a higher contribution in the determination of deflections than principal moments, slab bending stiffness possessed a contrasting effect (Figs 24, 26, 27, and 29). Hence, if the most important design criteria are pavement stresses, the thickness of the slab is the factor which requires the greatest consideration, and it is followed in importance by the modulus of subgrade reaction.

For the case when loads were on the crack, as crack spacing varied over the range studied (4 to 10 feet) a small change was encountered in deflections and principal moments (Figs 22 and 23). For the second load placement investigated (i.e., loads between cracks), the effect of crack spacing on deflections was also slight or practically negligible, while changes in principal moments for the low and medium levels of k were significant (Figs 26 and 27).

The analysis of variance performed on the SLAB results has indicated that the main effects of slab bending stiffness and subgrade modulus contributed around 90 percent to the variation in each of the deflection and principal moment responses (Tables 8 and 9). It also showed the minor effect of crack spacing on the pavement behavior.

The polynomial orthogonal breakdown yielded similar results for the two load placements. The logarithmic linear effect of subgrade modulus and bending stiffness was highly significant, and explained most of the variations in the pavement responses, deflections, and principal moments.

The comparison between the 90 percent (closed crack) and 100 percent (open crack) reduction in bending stiffness at the crack location indicated the importance of crack width on the behavior of continuously reinforced concrete pavements. Slab deflections increase at a high rate as crack width increases

(Fig 35), while no significant drop is encountered in the principal moments (Fig 36).

Use of Results

In the previous discussion, the graphical representation of results and the analysis of variance results were used to explain the behavior of continuously reinforced concrete pavements under transverse static loading. Other important uses of these results can be in the design and analysis of such pavements. Figure 34 gives the maximum principal moment, based on average values of crack spacing, for different combinations of slab stiffness and subgrade modulus. If a particular crack spacing pattern is of interest, tabulated values of principal moments (Tables 4 through 7) or Figs 26 and 27 can be used. Besides principal moments, maximum slab deflection can be obtained, depending on the load position and pavement characteristics (Figs 24 through 30).

It is worthwhile to note that the reported deflections and moments are due to two 9,000-pound wheel loads located 2 and 8 feet from the edge of the pavement. Pavement responses for the same loading pattern and different load magnitudes can be calculated from those presented in this study, simply by linear interpolation.

Since the range of pavement design variables considered in this study is likely to exist in design practice, another use of these results can be in developing regression equations to predict the maximum deflections and principal moments or stresses for both loading arrangements. These equations may be used in the development of design charts or nomographs, or they may be a part of a pavement systems analysis model that requires stress or deflection values for certain pavement design parameters.

CHAPTER 5. CONCLUSIONS, RECOMMENDATIONS, AND IMPLEMENTATION

Conclusions

The problem of transverse cracking in continuously reinforced concrete pavement (CRCP) and its influence on the bending rigidity of the slab in the longitudinal direction have been studied using basic moment-curvature relationships. A procedure to simulate this effect using the discrete-element methods is outlined. Besides the crack effect, other slab characteristics have been investigated for use in modeling the real problem. These included slab partitioning with the corresponding boundary conditions and tension in the longitudinal reinforcement.

This investigation was conducted to determine by use of the discrete-element slab model, the sensitivity of pavement deflection and principal moment (or stress) to changes in design parameters. The conclusions are limited to the range of variables studied in this experiment. These findings however, can provide reasonable information to use in design, for selecting those variables which require the most intensive consideration and those which will yield the best results.

Based on changes in deflections and principal moments, the following conclusions have been drawn.

(1) The effect of transverse cracks in CRCP on the longitudinal bending rigidity of the slab is highly important.

(2) The effect of variations in Poisson's ratio is negligible.

(3) When a CRC pavement is analyzed (considering no loss in subgrade support), it is reasonable to consider only the partition or area extending 15 to 20 feet on each side of the loaded area. No boundary restraints are needed at the edges of the partition of this size.

(4) Higher principal moments or stresses are produced when loads are located between cracks than when loads are at the cracks. The reverse is true for the deflection response.

(5) The effect of crack spacing on deflections and principal moments was greater for the case of 100 percent reduction in bending stiffness at crack location that it was for the 90 percent case.

(6) As crack spacing increases, principal moment values for the loads placed between cracks approach those of the full slab case.

(7) The modulus of subgrade reaction is important in determining the amount of deflection.

(8) Principal moments or stresses are mainly dependent on, first, the stiffness of the slab and, second, the subgrade modulus.

(9) The width of the crack has a big influence on the performance of continuously reinforced concrete pavements. The reduction of the bending rigidity of the slab and the consequent increase in the slab deflection as a result of an increase in crack width are important. Perhaps the requirement most necessary to the success of continuously reinforced concrete pavement is that the steel reinforcement hold transverse cracks as tight as possible.

(10) For the increments given to subgrade modulus, slab bending stiffness, and crack spacing, the analysis of variance and its orthogonal polynomial breakdown showed that:

(a) a definite logarithmic linear trend of subgrade modulus with deflection is observed, as well as a tendency toward a logarithmic quadratic relationship;

(b) the linear effect of the log of bending stiffness on principal moments and deflections is quite significant; and

(c) interactions do occur between design variables indicating the effect of any one design variable on deflections and principal moments is dependent on levels of the other two design variables.

Recommendations

Based on this investigation, it is recommended that

(1) Pavement design procedures include greater consideration of the modulus of subgrade reaction, because of its influence on deflections and stresses.

(2) Stress criteria in present design procedures be coupled with deflection criteria which will enable the designer to insure a pavement deflection less than the desired maximum.

(3) Transverse cracks be maintained very narrow in order to:

(a) prevent progressive infiltration of incompressible materials, such as soil, which eventually might cause excessive compressive stress to develop in the pavement and thus produce blow-ups;

(b) prevent appreciable amounts of surface water from reaching the subgrade and, by the same token, if the pavement happens to be built directly on soils which are of the potentially pumping types, the cracks must be maintained tightly closed so that pumpable material cannot be ejected through them; and

(c) maintain effective aggregate interlock between the crack interfaces.

Implementation

The research study reported herein was an analytical look at the parameters affecting the structural behavior of continuously reinforced concrete pavements. The results of the study can be made even more useful by correlating them with work from Research Project 1-8-69-123, entitled "A System Analysis of Pavement Design and Research Implementation." The findings of the study are quite useful for evaluating the importance of CRC pavement parameters and should ultimately lead to improved pavement design methods.

REFERENCES

1. Hudson, W. Ronald, and Hudson Matlock, "Discontinuous Orthotropic Plates and Slabs," Research Report No. 56-6, Center for Highway Research, The University of Texas, Austin, May 1966.

2. McCullough, B. F., "Design Manual for Continuously Reinforced Concrete Pavement," United States Steel Corporation, Pittsburgh, Pennsylvania, January 1970.

3. Treybig, H. J., W. R. Hudson, and B. F. McCullough, "Sensitivity Analysis of the Extended AASHO Rigid Pavement Design Equation," Highway Research Record No. 239, Highway Research Board, 1970.

4. Stelzer, C. Fred, Jr., and W. Ronald Hudson, "A Direct Computer Solution for Plates and Pavement Slabs," (DSLAB 5), Research Report No. 56-9, Center for Highway Research, The University of Texas at Austin, October 1967.

5. Wei-Wen Yu, and George Winter, "Instantaneous and Long-Time Deflections of Reinforced Concrete Beams Under Working Loads," Journal of the American Concrete Institute, July 1960.

6. "Design of Concrete Airport Pavement," Portland Cement Association, 1955.

7. Panak, John J., and Hudson Matlock, "A Discrete-Element Method of Multiple-Loading Analysis for Two-Way Bridge Floor Slabs," (SLAB 30), Research Report No. 56-13, Center for Highway Research, The University of Texas at Austin, January 1970.

8. Guralnick, S. A., "Some Basic Concepts of the Problem of Shear Strength of Reinforced Concrete Beams," Ph.D. Dissertation, Cornell University, February 1958.

9. Sachnowski, K. W., "Stahlbeton-Konstruktionen," VEB Verlag Technik, Berlin, 1956.

10. Nawy, Edward G., "Crack Control in Reinforced Concrete Structures," Journal of the American Concrete Institute, October 1968.

11. Agarwal, Sohan L., and W. Ronald Hudson, "Experimental Verification of Discrete-Element Solutions for Plates and Pavement Slabs," Research Report No. 56-15, Center for Highway Research, The University of Texas at Austin, April 1970.

12. Vetter, C. P., "Stresses in Reinforced Concrete Due to Volume Changes," Transactions, Vol 98, Proceedings of the American Society of Civil Engineers, 1933.

13. "AASHO Interim Guide for the Design of Rigid Pavement Structures," AASHO Committee on Design, April 1962.

14. Lin, T. Y., Design of Prestressed Concrete Structures, Wiley, Second Edition, New York, 1963.

15. Kher, Ramesh, W. Ronald Hudson, and B. Frank McCullough, "A Systems Analysis of Rigid Pavement Design," Research Report 123-5, Center for Highway Research, The University of Texas at Austin, November 1970.

16. McCullough, B. F., and Harvey J. Treybig, "A Statewide Deflection Study of Continuously Reinforced Concrete Pavement in Texas," Texas Highway Department, Research Report 46-5, August 1966.

17. Herrmann, Leonard R., "Finite-Element Bending Analysis for Plates," Journal of the Engineering Mechanics Division, Vol 93, No. EM5, Proceedings of the American Society of Civil Engineers, 1967.

18. "Continuously Steel Reinforced for Experimental Concrete Pavements," Highway Research Board, Bulletin No. 214, 1959.

19. Westergaard, H. M., "Analytical Tools for Judging Results of Structural Tests of Concrete Pavements," Public Roads, Vol 14, No. 10, 1933.

20. Westergaard, H. M., "Computation of Stresses in Concrete Roads," Proceedings, Fifth Annual Meeting of the Highway Research Board, 1926.

21. Timoshenko, S., and S. Woinowsky-Krieger, Theory of Plates and Shells, Second Edition, McGraw-Hill, New York, Cleveland, 1967.

22. Treybig, H. J., W. R. Hudson, and B. F. McCullough, "Effect of Load Placement on Rigid Pavement Behavior," to be published in Proceedings, ASCE National Meeting on Transportation Engineering, July 1970.

23. American Concrete Institute Standards, 1966.

24. McCullough, B. F., and H. J. Treybig, "Determining the Relationship of Variables in Deflection of Continuously Reinforced Concrete Pavement," Texas Highway Department, Research Report 46-4, August 1965.

25. McCullough, B. F., and Ivan K. Mays, "A Laboratory Study of the Variables That Affect Pavement Deflection," Texas Highway Department, Research Report 46-6, August 1966.

26. Richmond, B. Samuel, Statistical Analysis, Second Edition, The Ronald Press Company, New York, 1957.

27. Hicks, R. Charles, Fundamental Concepts in the Design of Experiments, Holt, Rinehart, and Winston, Inc., New York, 1964.

28. Siddiqi, Qaiser S., and W. Ronald Hudson, "Experimental Evaluation of Subgrade Modulus and Its Application in Model Slab Studies," Research Report No. 56-16, Center for Highway Research, The University of Texas at Austin, April 1970.

29. Treybig, Harvey J., "Performance of Continuously Reinforced Concrete Pavement in Texas," Texas Highway Department, Research Report 46-8(F), August 1968.

30. McCullough, B. F., "Development of Equipment and Techniques for a Statewide Rigid Pavement Deflection Study," Texas Highway Department, Research Report 46-1, January 1965.

31. Treybig, Harvey J., "Observation and Analysis of Continuously Reinforced Concrete Pavement," Texas Highway Department, Research Report 46-7, April 1968.

32. Shelby, M. D., and B. F. McCullough, "Determining and Evaluating the Stresses in an In-Service Continuously Reinforced Concrete Pavement," Highway Research Record No. 5, National Academy of Sciences, Washington, D. C., January 1963.

33. Shelby, M. D., and B. F. McCullough, "Experience in Texas with Continuously Reinforced Concrete Pavements," Bulletin 274, Highway Research Board, National Academy of Sciences, Washington, D. C., January 1960.

34. Hveem, F. N., "Pavement Deflections and Fatigue Failures," Bulletin 114, Highway Research Board, National Academy of Sciences, Washington, D. C., 1955.

35. Winter, G., L. C. Urquhart, C. E. O'Rouke, and A. H. Nilson, Design of Concrete Structures, Seventh Edition, McGraw-Hill Book Company, New York, 1964.

36. Winkler, E., "Die Lehre von Elasticitaet and Festigkeit," (on elasticity and fixity), Prague, 1867.

APPENDIX 1

DETERMINATION OF THE LOCATION OF THE NEUTRAL AXIS OF THE CRACKED TRANSFORMED SECTION

AND

DERIVATION OF RESISTING MOMENT M' DUE TO THE TENSILE STRESS OF CONCRETE

APPENDIX 1a. DETERMINATION OF THE LOCATION OF THE NEUTRAL AXIS OF THE CRACKED TRANSFORMED SECTION

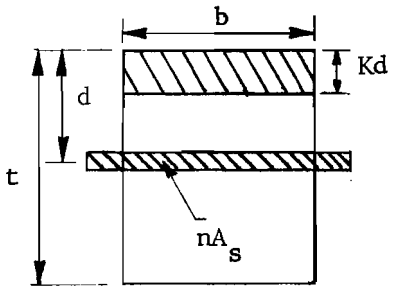

Fig A1. Cracked transformed section.

To determine the location of the neutral axis, the moment of the compression area about the axis is set equal to the moment of the tension area, which gives

$$b\frac{(Kd)^2}{2} - nA_s(d - Kd) = 0 \qquad \text{(A1a.1)}$$

Substituting $p = \frac{A_s}{bt}$, and $d = \frac{t}{2}$ in the above equation, one gets:

$$b\frac{(Kt)^2}{8} - npbt(\frac{t}{2} - K\frac{t}{2}) = 0 \qquad \text{(A1a.2)}$$

Dividing through by $\frac{bt^2}{2}$

$$\frac{K^2}{4} - pn(1 - K) = 0 \qquad \text{(A1a.3)}$$

from which

$$K = 2[\sqrt{pn(1+Pn)} - Pn] \qquad \text{(A1a.4)}$$

APPENDIX 1b. DERIVATION OF RESISTING MOMENT M' DUE TO THE TENSILE STRESS OF CONCRETE (After Ref 5)

Determination of Resisting Moment M'

From Eq 3.8

$$M' = \frac{k_1 f_r bt(t - Kd)}{3} \qquad \text{(A1b.1)}$$

where M' is the part of the resisting moment corresponding to the average tensile stress of concrete $\bar{f}_t$ $(k_1 f_r)$. Many attempts have been made to express the modulus of rupture of concrete as a simple fraction of f'_c . An equation

$$f_r = k_2 (f'_c)^{2/3} \qquad \text{(A1b.2)}$$

has been suggested as a better function by Guralnick (Ref 8) and also in a Russian text (Ref 9) (k_2 is a constant which depends on aggregate type, cement, etc.). Thus,

$$M' = \frac{k_1 k_2 (f'_c)^{2/3} bt(t - Kd)}{3} \qquad \text{(A1b.3)}$$

or

$$M' = k_3 (f'_c)^{2/3} bt(t - Kd) \qquad \text{(A1b.4)}$$

where

$$k_3 = \frac{(k_1 k_2)}{3} \qquad \text{(A1b.5)}$$

Sixty-eight short-time load beam tests were evaluated to determine k_3, and the average value was found to be 0.097 (Ref 5), but for simplicity $k_3 = 0.1$ can be used without noticeable error. Thus,

$$M' = 0.1(f_c')^{2/3}bt(t - Kd) \qquad \text{(A1b.6)}$$

APPENDIX 2

SAMPLE CALCULATION FOR THE DETERMINATION OF THE AVERAGE MOMENT OF INERTIA AND THE CORRESPONDING REDUCTION IN BENDING STIFFNESS

APPENDIX 2. SAMPLE CALCULATION FOR THE DETERMINATION OF THE AVERAGE MOMENT OF INERTIA AND THE CORRESPONDING REDUCTION IN BENDING STIFFNESS

Given

Material properties.

Concrete compressive strength f'_c = 4,000 psi

Yield stress of steel f_y = 60,000 psi

Ratio of the modulus of elasticity of steel to that of concrete n = 8.0

Slab section properties.

Total thickness t = 8.00 inches

Width (1-foot strip) b = 12.00 inches

Longitudinal percentage reinforcement P = 0.60

Calculations

From Eq 3.13,

$$\bar{I} = \frac{M_w nd(1-K)}{f_s - f'_s} \tag{A2.1}$$

For this particular problem,

$$n = 8 \tag{A2.2}$$

$$d = \frac{t}{2} = \frac{8.0}{2} = 4.0 \tag{A2.3}$$

From Eq 3.4,

$$K = 2\left[\sqrt{Pn(1 + Pn)} - Pn\right] \tag{A2.4}$$

for

$$Pn = \frac{0.6}{100} \times 8 = 0.048 \tag{A2.5}$$

$$K = 0.353 \tag{A2.6}$$

Determine f_s'

$$f_s' = \frac{M'}{A_s jd} = \frac{0.1(f_c')^{2/3} bt(t-Kd)}{A_s jd} \tag{A2.7}$$

where

$$A_s = P \times bt = \frac{0.6}{100} \times 12 \times 8 = 0.576 \text{ in}^2 \tag{A2.8}$$

$$j = 1 - \frac{K}{3} = 1 - \frac{0.353}{3} = 0.882 \tag{A2.9}$$

$$f_s' = \frac{0.1(4,000)^{2/3} 12 \times 8(8 - 0.353 \times 4)}{0.576 \times 0.882 \times 4} = 7,850 \text{ psi} \tag{A2.10}$$

To determine M_w, two cases should be considered:

(1) Assuming steel stress controls,

$$M_w = A_s f_s jd$$

$$= 0.576(0.75 \times 60,000)0.882 \times 4$$

$$= 91,500 \text{ inch-pounds} \tag{A2.11}$$

(2) Assuming concrete stress controls,

$$M_w = \frac{1}{2} f_c Kjbd^2$$

$$= \frac{1}{2}(0.45 \times 4{,}000)0.353 \times 0.882 \times 12(4)^2$$

$$= 53{,}800 \text{ inch-pounds} \qquad \text{(A2.12)}$$

Here, the second case governs, and $M_w = 53{,}800$ inch-pounds.

Determine f_s by

$$f_s = \frac{M_w}{A_s jd} = \frac{53{,}800}{0.576 \times 0.882 \times 4} = 26{,}450 \text{ psi} \qquad \text{(A2.13)}$$

Then

$$\bar{I} = \frac{53{,}800 \times 8 \times 4(1 - 0.353)}{26{,}450 - 7{,}850}$$

$$= 59.9 \text{ in}^4 \qquad \text{(A2.14)}$$

and gross moment of inertia

$$I_G = \frac{1}{12} bt^3$$

$$= \frac{1}{12} \times 12(8)^3$$

$$= 512 \text{ in}^4 \qquad \text{(A2.15)}$$

Therefore

$$\text{Percent stiffness reduction} = \left(1 - \frac{\bar{I}}{I_G}\right)100 = \left(1 - \frac{59.9}{512}\right)$$

$$= 88.3 \qquad \text{(A2.16)}$$

APPENDIX 3

EXAMPLE PROBLEM AND CODED DATA INPUT

APPENDIX 3. EXAMPLE PROBLEM AND CODED DATA INPUT

Modeling Crack Effect

(1) Pavement physical characteristics:

Length of slab 40 feet

Width of slab 24 feet

Pavement thickness $t = 8.0$ inches

Longitudinal percentage reinforcement $P = 0.50$

Compressive strength of concrete $f'_c = 4{,}000$ psi

Modulus of elasticity of concrete $E = 3.5 \times 10^6$ psi

Modulus of subgrade reaction $k = 40$ lb/in^2/in

Poisson's ratio = 0.20

(2) Percentage reduction in bending stiffness:

Assume that the allowable concrete compressive strength is $0.45\ f'_c$. The plot in Fig 10 is used, and with $P = 0.50$ percent, the percentage reduction in bending stiffness is 89.5 (use 90.0).

(3) Length along which to apply the stiffness reduction:

From Eq 3.18

$$L = 2\frac{A_s f_s}{up}$$

For most practical cases, No. 4 or 5 bars are generally used. For a No. 4 bar

$\phi = 0.50$ inch

$A_s = 0.20$ in^2

$p = 1.57$ inch

$$u = \frac{3.4\ \sqrt{f'c}}{D} \leq 350 \text{ psi}$$

$$u = \frac{3.4\ \sqrt{4,000}}{0.50} = 430, \text{ hence}$$

$$u = 350 \text{ psi}$$

$$L = 2\,\frac{0.20 \times 20,000}{1.57 \times 350}$$

$$= 14.5 \text{ inches}$$

(4) Increment length h :

A 12-inch increment length is taken in each direction. The bending stiffness in the y-direction was reduced by 90 percent (since cracks ran transversely) over one increment length, which is quite satisfactory.

Computations for Coded Data Input

$$h_x = h_y = 12 \text{ inches}$$

Slab bending stiffness per unit length $D = \frac{Et^3}{12(1 - \mu^2)}$

$$\therefore D^x = D^y = \frac{(3.5 \times 10^6)(8)^3}{12[1 - (0.2)^2]}$$

$$= 1.60 \times 10^8 \text{ inch-pounds}$$

$$\frac{D^x}{4} = \frac{D^y}{4} = 4.0 \times 10^7 \text{ inch-pounds}$$

Since the cracks are in the x-direction, D^y should be reduced.

$\therefore$ Reduction in $D^y = 0.9\ D^y$

$$= 0.9\ (1.60 \times 10^8) = (1.44 \times 10^8) \text{ inch-pounds}$$

Elastic spring constant $S = kh_x h_y$

$= 40 \times 12 \times 12$

$= 5.76 \times 10^3$

$\therefore \frac{S}{4} = 1.44 \times 10^3$ pounds per inch

Twisting stiffness $C = \frac{Et^3}{12(1 + \mu)}$

$= \frac{(3.5 \times 10^6)(8)^3}{12(1 + 0.2)}$

$= 1.280 \times 10^8$ in-pounds

IDENTIFICATION SAMPLE PROBLEM CODED BY A.A.A. DATE 24-6-71 PAGE 1 OF 2

```
APPLICATION OF DISCRETE-ELEMENT SLAB PROGRAMS
ANALYSIS OF CRACKS IN CONTINUOUSLY REINFORCED CONCRETE PAVEMENTS. WRH-AAA.
01    24X40 FT, D=160E+06, CRACK SPACING=8 FT, K=40 PCI, LOADS ON CRACK
                                                1   16    0    1
24  40                    1.200E+01 1.200E+01 2.000E-01
 0   0  24  40 4.000E+07 4.000E+07                                1.440E+03
 0   1  24  39 4.000E+07 4.000E+07                                1.440E+03
 1   0  23  40 4.000E+07 4.000E+07                                1.440E+03
 1   1  23  39 4.000E+07 4.000E+07                                1.440E+03
 0   4  24   4           -7.200E+07
 1   4  23   4           -7.200E+07
 0  12  24  12           -7.200E+07
 1  12  23  12           -7.200E+07
 0  20  24  20           -7.200E+07
 1  20  23  20           -7.200E+07
 0  28  24  28           -7.200E+07
```

IDENTIFICATION _____ CODED BY _____ DATE _____ PAGE ____ OF ____

1	28	23	28		-7.200E+07	
0	36	24	36		-7.200E+07	
1	36	23	36		-7.200E+07	
2	20	2	20			-9.000E+03
8	20	8	20			-9.000E+03
1	1	24	40	1.280E+08		

APPENDIX 4

SAMPLE CALCULATION FOR DETERMINATION OF TENSION IN THE LONGITUDINAL STEEL

APPENDIX 4. SAMPLE CALCULATION FOR DETERMINATION OF TENSION IN THE LONGITUDINAL STEEL

Given

Concrete compressive strength $f'_c = 5{,}000$ psi

Modulus ratio $n = \frac{E_s}{E} = 7.00$

Yield stress of steel $f_y = 60{,}000$ psi

Longitudinal percentage reinforcement $P = 0.60$

Pavement thickness $t = 8$ in

Temperature range $\Delta T = 30^{o}$ F

Thermal coefficient of concrete and steel $\epsilon = 5 \times 10^{-6}$ per ^{o}F

Calculations

Modulus of rupture f_r

From Eq 3.28

$$f_r = 7.5\sqrt{f'_c}$$

$$= 7.5\sqrt{5{,}000} = 530 \text{ psi}$$

From Eq 3.29

$$f_r = \frac{3{,}000}{3 + \frac{12{,}000}{5{,}000}} = 555 \text{ psi}$$

$\therefore$ the allowable tensile strength

$$S_t = 0.4\, f_r$$

$$= 0.4(530) = 212 \text{ psi}$$

Stress in the steel f_s

Neglecting temperature effects (Eq 3.23)

$$f_s = (1.3 - 0.2 \times 1.5) \frac{212}{0.60} \times 100 + (7 \times 212)$$

$$= 36{,}840 \text{ psi} < 0.75 f_y$$

Considering the temperature range encountered (Eq 3.24)

$$f_s = (1.3 - 0.2 \times 1.5) \frac{212}{2 \times 0.60} \times 100 + (30 \times 5 \times 10^{-6} \times 29 \times 10^{6})$$

$$= 22{,}027 \text{ psi} < 0.75 f_y$$

Hence, allowable steel stress = 36,840 psi.

Tension per inch width

$$\frac{T_s}{b} = f_s Pt$$

$$= 36{,}840 \times 0.006 \times 8$$

$$= 1768 \text{ lb/in}$$

Assuming that the increment length in the longitudinal direction is 12 inches, then

$$T_s = 1768 \times 12$$

$$= 21{,}200 \text{ lb/station}$$

Actually, this is the lumped value over one increment length.

APPENDIX 5

TABULATED VALUES OF RADIUS OF RELATIVE STIFFNESS ℓ

TABLE A5.1. VALUES OF RADIUS OF RELATIVE STIFFNESS ℓ , INCHES

(Poisson's Ratio $\mu = 0.15$)

Modulus of Elasticity of Concrete E, lb/sq in.	Modulus of Subgrade Reaction k, lb/cu in.	Pavement Thickness t, inches								
		t=5	t=6	t=7	t=8	t=9	t=10	t=11	t=12	t=13
3×10^6	50	28.3	32.4	36.4	40.2	43.9	47.6	51.1	54.5	57.9
	100	23.8	27.3	30.6	33.8	37.0	40.0	43.0	45.9	48.7
	200	20.0	22.9	25.7	28.4	31.1	33.6	36.1	38.6	40.9
	300	18.1	20.7	23.3	25.7	28.1	30.4	32.6	34.8	37.0
	500	15.9	18.2	20.5	22.6	24.7	26.7	28.7	30.7	32.6
	700	14.6	16.8	18.8	20.8	22.7	24.6	26.4	28.2	29.9
	1000	13.4	15.3	17.2	19.0	20.8	22.5	24.2	25.8	27.4
4×10^6	50	30.4	34.8	39.1	43.2	47.2	51.1	54.9	58.6	62.2
	100	25.6	29.3	32.9	36.4	39.7	43.0	46.2	49.3	52.3
	200	21.5	24.6	27.7	30.6	33.4	36.1	38.8	41.4	44.0
	300	19.4	22.3	25.0	27.6	30.2	32.7	35.1	37.4	39.8
	500	17.1	19.6	22.0	24.3	26.6	28.7	30.9	32.9	35.0
	700	15.7	18.0	20.2	22.3	24.4	26.4	28.4	30.3	32.2
	1000	14.4	16.5	18.5	20.4	22.3	24.2	26.0	27.7	29.4

(Continued)

TABLE A5.1. (Continued)

Modulus of Elasticity of Concrete E, lb/sq in.	Modulus of Subgrade Reaction k, lb/cu in.	Pavement Thickness t, inches								
		t=5	t=6	t=7	t=8	t=9	t=10	t=11	t=12	t=13
5×10^6	50	32.1	36.8	41.4	45.7	49.9	54.0	58.0	62.0	65.8
	100	27.0	31.0	34.8	38.4	42.0	45.4	48.8	52.1	55.3
	200	22.7	26.0	29.2	32.3	35.3	38.2	41.0	43.8	46.5
	300	20.5	23.5	26.4	29.2	31.9	34.5	37.1	39.6	42.0
	500	18.1	20.7	23.3	25.7	28.1	30.4	32.6	34.8	37.0
	700	16.6	19.0	21.4	23.6	25.8	27.9	30.0	32.0	34.0
	1000	15.2	17.4	19.6	21.6	23.6	25.6	27.4	29.3	31.1
6×10^6	50	33.6	38.6	43.3	47.8	52.3	56.6	60.7	64.8	68.9
	100	28.3	32.4	36.4	40.2	43.9	47.6	51.1	54.5	57.9
	200	23.8	27.3	30.6	33.8	37.0	40.0	43.0	45.9	48.7
	300	21.5	24.6	27.7	30.6	33.4	36.1	38.8	4.14	44.0
	500	18.9	21.7	24.3	26.9	29.4	31.8	34.2	36.5	38.7
	700	17.4	19.9	22.4	24.7	27.0	29.2	31.4	33.5	35.6
	1000	15.9	18.2	20.5	22.6	24.7	26.7	28.7	30.7	32.6

TABLE A5.2. VALUES OF RADIUS OF RELATIVE STIFFNESS ℓ, INCHES

(Poisson's Ratio $\mu = 0.20$)

Modulus of Elasticity of Concrete E, lb/sq in.	Modulus of Subgrade Reaction k, lb/cu in.	Pavement Thickness t, inches								
		t=5	t=6	t=7	t=8	t=9	t=10	t=11	t=12	t=13
3×10^6	50	28.4	32.6	36.6	40.4	44.1	47.8	51.3	54.8	58.2
	100	23.9	27.4	30.7	34.0	37.1	40.2	43.1	46.1	48.9
	200	20.1	23.0	25.9	28.6	31.2	33.8	36.3	38.7	41.1
	300	18.1	20.8	23.4	25.8	28.2	30.5	32.8	35.0	37.2
	500	16.0	18.3	20.6	22.7	24.8	26.9	28.9	30.8	32.7
	700	14.7	16.8	18.9	20.9	22.8	24.7	26.5	28.3	30.1
	1000	13.4	15.4	17.3	19.1	20.9	22.6	24.3	25.9	27.5
4×10^6	50	30.5	35.0	39.3	43.4	47.4	51.3	55.1	58.9	62.5
	100	25.7	29.4	33.0	36.5	39.9	43.2	46.4	49.5	52.6
	200	21.6	24.7	27.8	30.7	33.5	36.3	39.0	41.6	44.2
	300	19.5	22.4	25.1	27.7	30.3	32.8	35.2	37.6	39.9
	500	17.2	19.7	22.1	24.4	26.7	28.9	31.0	33.1	35.1
	700	15.8	18.1	20.3	22.4	24.5	26.5	28.5	30.4	32.3
	1000	14.4	16.5	18.6	20.5	22.4	24.3	26.1	27.8	29.6

(Continued)

TABLE A5.2. (Continued)

Modulus of Elasticity of Concrete E, lb/sq in.	Modulus of Subgrade Reaction k, lb/cu in.	Pavement Thickness t, inches								
		t=5	t=6	t=7	t=8	t=9	t=10	t=11	t=12	t=13
5×10^6	50	32.3	37.0	41.5	45.9	50.2	54.3	58.3	62.2	66.1
	100	27.1	31.1	34.9	38.6	42.2	45.6	49.0	52.3	55.6
	200	22.8	26.2	29.4	32.5	35.5	38.4	41.2	44.0	46.7
	300	20.6	23.6	26.5	29.3	32.0	34.7	37.3	39.8	42.2
	500	18.1	20.8	23.4	25.8	28.2	30.5	32.8	35.0	37.2
	700	16.7	19.1	21.5	23.7	25.9	28.1	30.1	32.2	34.2
	1000	15.3	17.5	19.6	21.7	23.7	25.7	27.6	29.4	31.2
6×10^6	50	33.8	38.7	43.5	48.1	52.5	56.8	61.0	65.1	69.2
	100	28.4	32.6	36.6	40.4	44.1	47.8	51.3	54.8	58.2
	200	23.9	27.4	30.7	34.0	37.1	40.2	43.1	46.1	48.9
	300	21.6	24.7	27.8	30.7	33.5	36.3	39.0	41.6	44.2
	500	19.0	21.8	24.4	27.0	29.5	31.9	34.3	36.6	38.9
	700	17.5	20.0	22.5	24.8	27.1	29.4	31.5	33.7	35.8
	1000	16.0	18.3	20.6	22.7	24.8	26.9	28.9	30.8	32.7

TABLE A5.3. VALUES OF RADIUS OF RELATIVE STIFFNESS ℓ , INCHES

(Poisson's Ratio $\mu = 0.25$)

Modulus of Elasticity of Concrete E, lb/sq in.	Modulus of Subgrade Reaction k, lb/cu in.	Pavement Thickness t, inches								
		t=5	t=6	t=7	t=8	t=9	t=10	t=11	t=12	t=13
3×10^6	50	28.6	32.8	36.8	40.7	44.4	48.1	51.6	55.1	58.5
	100	24.0	27.5	30.9	34.2	37.3	40.4	43.4	46.3	49.2
	200	20.2	23.2	26.0	28.7	31.4	34.0	36.5	39.0	41.4
	300	18.3	20.9	23.5	26.0	28.4	30.7	33.0	35.2	37.4
	500	16.1	18.4	20.7	22.9	25.0	27.0	29.0	31.0	32.9
	700	14.8	16.9	19.0	21.0	23.0	24.8	26.7	28.5	30.2
	1000	13.5	15.5	17.4	19.2	21.0	22.7	24.4	26.1	27.7
4×10^6	50	30.7	35.2	39.5	43.7	47.7	51.6	55.5	59.2	62.9
	100	25.8	29.6	33.2	36.7	40.1	43.4	46.6	49.8	52.9
	200	21.7	24.9	27.9	30.9	33.7	36.5	39.2	41.9	44.5
	300	19.6	22.5	25.3	27.9	30.5	33.0	35.4	37.8	40.2
	500	17.3	19.8	22.2	24.6	26.8	29.0	31.2	33.3	35.4
	700	15.9	18.2	20.4	22.6	24.7	26.7	28.7	30.6	32.5
	1000	14.5	16.6	18.7	20.7	22.6	24.4	26.2	28.0	29.7

(Continued)

TABLE A5.3. (Continued)

Modulus of Elasticity of Concrete E, lb/sq in.	Modulus of Subgrade Reaction k, lb/cu in.	Pavement Thickness t, inches								
		t=5	t=6	t=7	t=8	t=9	t=10	t=11	t=12	t=13
5×10^6	50	32.5	37.2	41.8	46.2	50.5	54.6	58.6	62.6	66.5
	100	27.3	31.3	35.1	38.8	42.4	45.9	49.3	52.6	55.9
	200	23.0	26.3	29.5	32.7	35.7	38.6	41.5	44.3	47.0
	300	20.7	23.8	26.7	29.5	32.2	34.9	37.5	40.0	42.5
	500	18.3	20.9	23.5	26.0	28.4	30.7	33.0	35.2	37.4
	700	16.8	19.2	21.6	23.9	26.1	28.2	30.3	32.4	34.4
	1000	15.4	17.6	19.8	21.8	23.9	25.8	27.7	29.6	31.4
6×10^6	50	34.0	39.0	43.7	48.3	52.8	57.1	61.4	65.5	69.6
	100	28.6	32.8	36.8	40.7	44.4	48.1	51.6	55.1	58.5
	200	24.0	27.5	30.9	34.2	37.3	40.4	43.4	46.3	49.2
	300	21.7	24.9	27.9	30.9	33.7	36.5	39.2	41.9	44.5
	500	19.1	21.9	24.6	27.2	29.7	32.1	34.5	36.8	39.1
	700	17.6	20.1	22.6	25.0	27.3	29.5	31.7	33.9	36.0
	1000	16.1	18.4	20.7	22.9	25.0	27.0	29.0	31.0	32.9

THE AUTHORS

Adnan Abou-Ayyash was a graduate research assistant with the Center for Highway Research at The University of Texas at Austin. A native of Lebanon, his previous experience includes field construction in that country. His research interest is primarily in the area of pavement systems.

W. Ronald Hudson is an Associate Professor of Civil Engineering and Associate Dean of the College of Engineering at The University of Texas at Austin. He has had a wide variety of experience as a research engineer with the Texas Highway Department and the Center for Highway Research at The University of Texas at Austin and was Assistant Chief of the Rigid Pavement Research Branch of the AASHO Road Test. He is the author of numerous publications and was the recipient of the 1967 ASCE J. James R. Croes Medal. He is presently concerned with research in the areas of (1) analysis and design of pavement management systems, (2) measurement of pavement roughness performance, (3) slab analysis and design, and (4) tensile strength of stabilized subbase materials.